Title
Evolution of Marine Fish Biodiversity: Phylogenomics and Ecological Processes Shaping Diversification

Author
Sorenson, Laura

Publication Date
2014

Peer reviewed|Thesis/dissertation

UNIVERSITY OF CALIFORNIA

Los Angeles

Evolution of Marine Fish Biodiversity: Phylogenomics and Ecological Processes Shaping Diversification

A dissertation submitted in partial satisfaction of the

requirements for the degree Doctor of Philosophy

in Biology

by

Laura Sorenson

2014

ABSTRACT OF THE DISSERTATION

Evolution of Marine Fish Biodiversity: Phylogenomics and Ecological Processes Shaping Diversification

by

Laura Sorenson

Doctor of Philosophy in Biology

University of California, Los Angeles, 2014

Professor Michael E. Alfaro, Chair

Understanding the evolutionary factors underlying the disparity in species richness across groups is a fundamental challenge in fish evolutionary biology. A difficulty in investigating this field lies in the paucity of robust, well-sampled phylogenies that act as a necessary framework to test hypotheses about the affects of ecology on fish evolution. In chapter one I use molecular sequence data to generate a time-calibrated hypothesis of surgeonfish (Family: Acanthuridae) relationships. I found strong support that the gizzard-like stomach, an important morphological trait for benthic grazing species including some *Acanthurus* and all *Ctenochaetus*, evolved only once, contrary to a previous hypothesis of multiple, independent origins. The timetree also shows that the subfamily Nasinae (genus *Naso*) experienced high turnover since originating in the Miocene, and that the extant species arose much more recently (~17 Ma) than previous

hypotheses. To abet creating robust phylogenies across a diverse set of species and at multiple phylogenetic levels, I developed a new genomic method capturing ultraconserved elements (UCEs). UCEs are highly conserved regions of the genome that are flanked by more variable regions, making them ideal for target enrichment. I created custom probes targeting 500 loci across fishes and used massively parallel sequencing to obtain a phylogenomic dataset both efficiently and economically. I validate this method by resolving the higher-level relationships among ray-finned fishes. The well-supported topology reveals monophyly of *Amia* and *Lepisosteus* (Holostei), and suggests that elopomorphs, then osteoglossomorphs were the first teleost lineages to diverge. The results show that sequence capture of UCE loci and their flanking regions provides an excellent approach to resolve the fish Tree of Life. In chapter three, I use molecular data to generate the most comprehensive, time-calibrated phylogeny for the sharks. This framework is then used to understand the influence of ecology (e.g. habitat preference) on the diversification of these fishes. My results show that deepwater radiations and transitions to coral reefs have played an important role in generating extant biodiversity. Coral reefs, therefore, have greatly influenced species richness across multiple fish trophic levels, from algivores to top predators like sharks.

The dissertation of Laura Sorenson is approved.

David K. Jacobs

Peter C. Wainwright

Michael E. Alfaro, Committee Chair

University of California, Los Angeles

2014

For Rick, Mary, Melissa, Rick,

Mildred, Margaret,

Ruth, Cindy, Bob, John,

Keith, and Caitlynn

TABLE OF CONTENTS

LIST OF FIGURES

CHAPTER 1

CHAPTER 2

CHAPTER 3

LIST OF TABLES

CHAPTER 1

CHAPTER 2

CHAPTER 3

ACKNOWLEDGMENTS

I thank Dr. Michael Alfaro for guidance, patience, and financial support to conduct this research. I am grateful to Dr. Francesco Santini for his mentorship, intellectual conversations, and research assistance. I would like to thank my committee, Drs. David Jacobs, Blaire Van Valkenburgh, Peter Wainwright, and Robert Wayne for their guidance and advice along the way.

Many additional people have provided me research opportunities and/or contributed to my achievements these past few years. I would like to thank all of my co-authors and collaborators for their support, especially Drs. Bruno Frédérich, Jessica Lynch Alfaro, Paul Barber, Shang-Yin Vanson Liu, and Rosalía Aguilar Medrano. Many thanks to Jocelyn Yamadera and Winnie Fong for their patience and willingness to provide logistical support.

I am deeply grateful to the network of people that provided me samples and/or allowed me to poke around in the fish collection. My research could not have been completed without your assistance. I would especially like to thank HJ Walker (Scripps), Jeff Siegel and Rick Feeney (Natural History Museum of Los Angeles), Mark Erdmann, and Mark McGrouther (Australian Museum).

I thank my family, especially my parents and siblings, for support and understanding when I have to work all the time, and for the endless supply of Caribou coffee that fueled the writing of this dissertation. Thank you to the Oakdalians for ice cream trips and a plan D (if this science thing doesn't work out, we can still open the Caribou).

Chapters one and two of this dissertation are reprinted in accordance with reserved rights granted to authors. Chapter one is a reprint of Sorenson L, Santini F, Carnevale G, Alfaro ME (2013) A multi-locus timetree of surgeonfishes (Acanthuridae, Percomorpha), with revised family taxonomy, Molecular Phylogenetics and Evolution 68: 150-160. Chapter two is a reprint of Faircloth B, Sorenson L, Santini F, Alfaro ME (2013) A phylogenomic perspective on the radiation of ray-finned fishes based upon targeted sequencing of ultraconserved elements (UCEs), PLOS ONE 8: e65923. Chapter three is the manuscript version of Sorenson L, Santini F, Alfaro ME (*in press*) The influence of shallow and deepwater habitats on the radiation of modern sharks, Journal of Evolutionary Biology. I acknowledge Molecular Phylogenetics and Evolution, Elsevier, Journal of Evolutionary Biology, Blackwell Publishing, and the European Society for Evolutionary Biology for publishing these works. I would like to thank all of my co-authors on these papers, Francesco Santini, Giorgio Carnevale, Brant Faircloth, and the PI of these studies, Michael Alfaro, for their contributions.

VITA

Graduated with a Bachelor of Science degree from Hawai'i Pacific University in 2005 with *magna cum laude* honors. Worked at the Hawai'i Institute of Marine Biology before attending the Virginia Institute of Marine Science. Earned a Master of Science degree in marine science from the College of William & Mary, Virginia Institute of Marine Science in 2011.

CHAPTER 1:

A multi-locus timetree of surgeonfishes (Acanthuridae, Percomorpha), with revised family taxonomy

Molecular Phylogenetics and Evolution 68 (2013) 150–160

Contents lists available at SciVerse ScienceDirect

Molecular Phylogenetics and Evolution

journal homepage: www.elsevier.com/locate/ympev

A multi-locus timetree of surgeonfishes (Acanthuridae, Percomorpha), with revised family taxonomy

Laurie Sorenson [a,*], Francesco Santini [a,b], Giorgio Carnevale [b], Michael E. Alfaro [a]

[a] University of California Los Angeles, Department of Ecology and Evolutionary Biology, 610 Charles E Young Drive South, Los Angeles, CA 90095, USA
[b] Università degli Studi di Torino, Dipartimento di Scienze della Terra, Via valperga Caluso, 35 10125 Torino, Italy

ARTICLE INFO

Article history:
Received 30 November 2012
Revised 2 March 2013
Accepted 2 March 2013
Available online 28 March 2013

Keywords:
Acanthuroidei
Phylogeny
Divergence times
Fossils
Coral reefs

ABSTRACT

We present the most comprehensive time-calibrated, species-level hypothesis of the timing of Acanthuridae (surgeonfishes and allies) evolution based on 76% of the extant diversity and nine genes. We recover two major acanthurid clades, Nasinae and Acanthurinae, and infer a much more recent Nasinae crown age (17 Ma) compared to a previous dating study for *Naso*. The Acanthurinae represent an older group that originated ~42 Ma, with most diversification occurring since the Early Miocene (beginning ~21 Ma). Our results strongly support a paraphyletic *Acanthurus* and *Ctenochaetus*, with multiple analyses recovering a clade grouping *Ctenochaetus, A. nubilus* and *A. pyroferus*. Contrary to previous studies, we also provide strong evidence that thick-walled, gizzard-like stomachs evolved only once within *Acanthurus* and that this morphology has a common origin in *Acanthurus* and *Ctenochaetus*. Based on our molecular analyses, in conjunction with the large body of morphological evidence, we recommend dissolving the genus *Ctenochaetus* into the genus *Acanthurus*.

1. Introduction

Surgeonfishes (Family: Acanthuridae) are charismatic members of subtropical and tropical ecosystems, and are especially prominent on and around coral reefs. The 83 described acanthurid species (Bernal and Rocha, 2011; Froese and Pauly, 2012; Randall et al., 2011) are distributed into six genera (Randall, 1955): *Acanthurus* (surgeonfishes), *Ctenochaetus* (bristletooths), *Prionurus* (sawtails), *Zebrasoma* (tangs), the monotypic *Paracanthurus* (the palette tang), and *Naso* (unicornfishes). The common name of the group derives from the presence of a scalpel-like modified scale on the caudal peduncle (Winterbottom, 1993), which may be used for inter- and intra-specific aggressive behaviors (Randall, 2001). The forms of this feature vary by genera; the scalpel is a single, modified, moveable scale in *Acanthurus*, *Ctenochaetus*, *Zebrasoma* and *Paracanthurus*, but present as variable numbers (1–10) of fixed plates in *Naso* and *Prionurus*, which tend to have keels or large spines (Winterbottom, 1993).

Acanthurids are primarily herbivores but consume a relatively wide variety of dietary resources, including planktonic animal matter, organic detritus (Choat et al., 2002), and invertebrates (Klanten et al., 2004). Dentition can vary dramatically within and across genera, and is strongly related to diet (Tyler, 1970a). Algal grazers or browsers (e.g. *Acanthurus*, *Zebrasoma*) tend to have spatulate tooth morphologies, while zooplanktivorous *Naso* species have pointy, serrated teeth (e.g. Tyler, 1970a). Many species form feeding aggregations (e.g. Randall, 2001), but others may defend territories (e.g. Nursall, 1974; Randall, 2001). Ecological diversity has been well-examined in this group, and is most evident in the genera *Naso* and *Acanthurus* (Winterbottom and McLennan, 1993; Klanten et al., 2004). Foraging diversity and strong association with coral reefs make the acanthurids an interesting and important group to study the tempo of evolution leading to extant reef fish biodiversity, and investigate the importance of ecological factors in driving diversification on the reef.

Morphological evolution of the Acanthuridae has been relatively well-explored from both osteological (Tyler, 1970a, 1970b; Guiasu and Winterbottom, 1993) and myological (e.g. Borden, 1998; Winterbottom, 1993) perspectives (Fig. 1). Morphological (e.g. Gosline, 1968; Mok, 1977; Greenwood et al., 1966; Tyler et al., 1989) and larval characters (Johnson and Washington, 1987) have also been examined in several higher-level phylogenetic studies including other Acanthuroidei taxa. Johnson and Washington (1987) proposed three postlarval forms: one form suggesting a *Paracanthurus* + *Zebrasoma* relationship, another grouping *Naso*, and a third common to *Acanthurus*, *Ctenochaetus*, and *Prionurus*. Two subfamily designations based on several autapomorphies were proposed by Tyler et al. (1989) that grouped *Naso* into the Nasinae, and the remaining genera into the Acanthurinae (Fig. 1a). Subsequently, Winterbottom (1993) split the Acanthurinae into three tribes based on myological characters: Acanthurini,

* Corresponding author.
E-mail address: lsorenson@ucla.edu (L. Sorenson).

1055-7903/$ - see front matter © 2013 Elsevier Inc. All rights reserved.
http://dx.doi.org/10.1016/j.ympev.2013.03.014

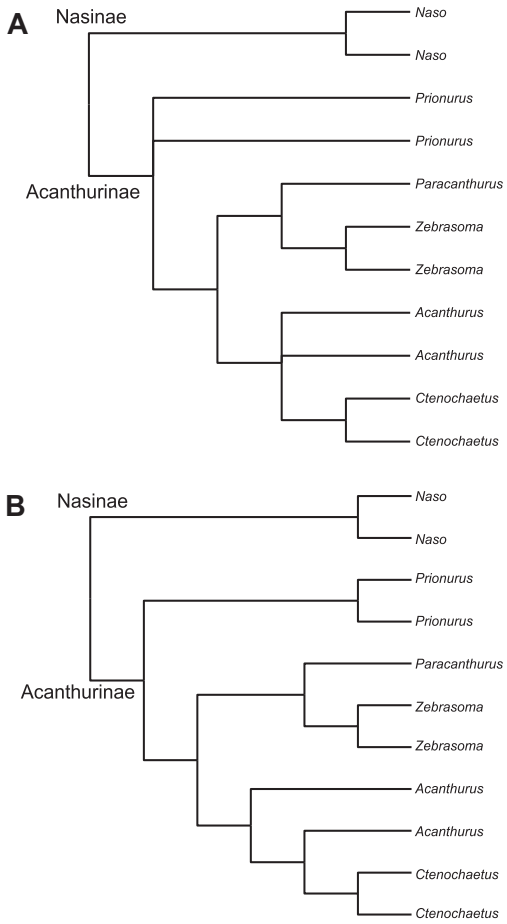

Fig. 1. Previous hypotheses of Acanthuridae relationships based on morphological (A) and molecular (B) data. Osteological and myological studies (Guiasu and Winterbottom, 1993; Winterbottom, 1993) could not recover monophyly of *Acanthurus*, and osteological studies did not support monophyly of *Prionurus*. Molecular studies (Clements et al., 2003; Klanten et al., 2004) suggested monophyly of *Prionurus*, but paraphyly of *Acanthurus*.

made up of *Acanthurus* + *Ctenochaetus*; Prionurini (*Prionurus*); and Zebrasomini (*Zebrasoma* + *Paracanthurus*). Guiasu and Winterbottom's (1993) analysis of 42 osteological characters supported Winterbottom's (1993) hypothesis that *Naso* is the sister group to all other acanthurids, with *Paracanthurus* + *Zebrasoma* being the sister group to *Acanthurus* + *Ctenochaetus*, and *Prionurus* being sister to this larger clade (Fig. 1). While both studies inferred strong support for *Ctenochaetus* monophyly (e.g. 14 osteological synapomorphies in Guiasu and Winterbottom, 1993), *Acanthurus* showed great variation, and no myological or osteological synapomorphies could be described for the species examined (Guiasu and Winterbottom, 1993). This led Winterbottom (1993) to conclude that *Acanthurus* may not be a monophyletic group. This conclusion was also supported by other morphological traits shared between some *Acanthurus* and *Ctenochaetus* species that had been described in non-explicitly phylogenetic studies, including the presence of thick-walled, gizzard-like stomachs in benthic grazers (Jones, 1968). *Acanthurus* species have either thick or thin-walled stomach types, whereas thick-walled, gizzard-like stomachs are present in all *Ctenochaetus* (Randall, 1956; Jones, 1968; Hiatt and Strasburg, 1960; Randall and Clements, 2001). *Acanthurus* species with this stomach morphology include the following 18 species: *A. auranticavus*, *A. bahianus*, *A. bariene*, *A. blochii*, *A. chirurgus*, *A. chronixis*, *A. dussumieri*, *A. fowleri*, *A. gahhm*, *A. grammoptilus*, *A. maculiceps*, *A. mata*, *A. monroviae*, *A. nigricauda*, *A. olivaceus*, *A. pyroferus*, *A. tennentii*, and *A. xanthopterus* (the newly resurrected *A. tractus*, which is the result of the splitting of *A. bahianus* into two species (Bernal and Rocha, 2011), is likely to possess this feature as well, bringing the total to 19). The evolution of acanthurid stomach morphologies is not well-understood, and it is uncertain whether gizzard-like stomachs evolved multiple times independently within *Acanthurus*, as suggested by Clements et al. (2003).

Most acanthurid molecular phylogenetic studies to date have suffered from limited taxonomic coverage within the family, and/or few genetic loci. Some phylogenies investigating higher-level relationships within the suborder Acanthuroidei (Tang et al., 1999; Holcroft and Wiley, 2008), which includes the Acanthuridae, have supported major groups hypothesized by more recent morphological trees (e.g. Guiasu and Winterbottom, 1993; Tyler et al., 1989; Winterbottom, 1993) (Fig. 1b). Tang et al. (1999) and Holcroft and Wiley (2008), however, tested only genus-level relationships using two mitochondrial or five nuclear loci, respectively. Neither study was able to resolve the relationships among the *Acanthurus* and *Ctenochaetus* taxa with confidence. Clements et al. (2003) sequenced short fragments of the mitochondrial loci *12S*, *16S*, t-Pro, and control region for 21 acanthurid taxa and four outgroups. Their parsimony and maximum likelihood analyses inferred very different topologies, but both recovered a paraphyletic *Acanthurus*. Their maximum likelihood tree and one parsimony tree suggested a paraphyletic *Ctenochaetus* as well (albeit with very low statistical support) and both the parsimony and maximum likelihood trees also failed to recover a monophyletic Acanthuridae (the outgroups *Luvarus* and *Zanclus* appear as sister taxa, and together form the sister clade to either *Naso* in the maximum likelihood tree, or *Paracanthurus* + *Zebrasoma* in the parsimony trees). Finally Klanten et al. (2004) generated a time-calibrated species-level phylogeny for the genus *Naso*, with additional sampling within Acanthuridae (36 total surgeonfish taxa), and recovered similar results. Klanten et al. (2004) used two mitochondrial loci (a short *Cytb* fragment and *16S*) and the nuclear *ETS2* locus to infer relationships using parsimony, maximum likelihood, and Bayesian inference, and used a penalized likelihood method and an estimation of rates of molecular evolution derived from other fish groups to date a tree containing only *Naso* species. Despite efforts along morphological and molecular fronts, we still do not have a densely sampled, time-calibrated hypothesis of acanthurid relationships and timing of evolution for this important reef fish group. Greater taxonomic coverage in molecular studies is clearly necessary to understand the evolutionary relationships among acanthurid genera and species.

In this paper we present a time-calibrated molecular hypothesis of Acanthuridae species relationships using data from two mitochondrial and seven nuclear loci. Our tree contains all six genera and 76% of the species diversity, representing the most complete taxonomic sampling effort and molecular dataset to date for this group. We provide a timescale for the evolution of Acanthuridae, and test the hypothesis that the thick-walled, gizzard-like stomach morphology evolved multiple times in *Acanthurus*.

2. Materials and methods

2.1. Taxonomic sampling

We obtained tissue samples for 41 acanthurid species and two outgroup taxa through museum and personal collections, and pur-

chases from fish wholesalers. We selected *Zanclus cornutus* and *Luvarus imperialis* as outgroups based on previously published morphological and molecular work supporting Acanthuroidei monophyly and the relationships among the acanthurids, Zanclidae, and Luvaridae (e.g. Mok, 1977; Johnson and Washington, 1987; Tyler et al., 1989; Holcroft and Wiley, 2008). We also obtained GenBank sequence data for all available acanthurid species to increase our taxonomic coverage. Twenty-two species in our phylogeny are represented only by data obtained from GenBank. In total, our dataset includes 63 of 83 acanthurid species (Table 1).

2.2. Molecular methods

Genomic DNA was extracted using the Qiagen DNeasy Blood and Tissue Kit (Qiagen, Valencia, California). We amplified and sequenced two mitochondrial genes, *cox1* and *Cytb*, and the following six nuclear genes: *ENC1*, *myh6*, *plagl2*, *Rag1*, *Rh*, *zic1*. Sequence data for an additional nuclear locus, *ETS2*, and genes in our sampling already available for species for which we did not possess tissues were obtained from GenBank.

Gene amplifications were conducted using the polymerase chain reaction (PCR) in 25-μl reactions containing the following reagents (Promega): 5.0 μl 5 × Green GoTaq Flexi PCR buffer; 2.0 μl $MgCl_2$ (25 mM); 0.5 μl dNTP mix (2.5 mM each); 2.5 μl forward + reverse primer mix (10 μM each); 0.125 μl GoTaq DNA polymerase (5 U/μl); with 1–10 ng of template. Cycling conditions and primer sequences were obtained from the primary literature (Chen et al., 2003; Ward et al., 2005; Sevilla et al., 2007; Holcroft and Wiley, 2008). PCR products were cleaned using ExoSap (Amersham Biosciences) and cycle sequenced using the BigDye Terminator v.3.1 cycle sequencing kit (Applied Biosystems). Bi-directional sequencing was conducted on an ABI 3730xl DNA Analyzer (Applied Biosystems) by the Life Sciences Core Laboratories Center at Cornell University.

2.3. Phylogenetic analyses

Raw sequences were examined and contigs were generated using Geneious 5.4 (Biomatters Inc.). We aligned contig consensus sequences and GenBank sequences using MUSCLE (Edgar, 2004), and gene alignments were adjusted by eye in Geneious. We trimmed all alignments to minimize missing characters. Final gene alignments contained 651 bp for *cox1*, 1093 bp for *Cytb*, 807 bp for *ENC1*, 421 bp for *ETS2*, 769 bp for *myh6*, 680 for *plagl2*, 1556 for *Rag1*, 799 for *Rh*, and 822 bp for *zic1*. We ran maximum likelihood (ML) analyses on individual gene alignments in RAxML (Stamatakis, 2006) to check for gene history incongruence and identify potentially misidentified sequences (results not presented). We used the GTR + G substitution model and 100 fast bootstrap replicates.

We concatenated all the gene alignments using Mesquite 2.75 (Maddison and Maddison, 2011), resulting in a 7598 bp full data matrix. We also produced a reduced data matrix including only the 44 acanthurids for which we possessed complete or almost complete gene sampling to assess whether missing data significantly affected our results. We removed two taxa that were represented only by *cox1* sequences (*Ctenochaetus flavicauda* and *Zebrasoma rostratum*), as well as 17 taxa with only *ETS2* gene and short fragment *Cytb* sequences (derived from Klanten et al., 2004).

We selected the best fitting substitution model using jModelTest (Posada, 2008) for each locus using the corrected Akaike Information Criterion (AICc; Akaike, 1973). We chose from models that can be applied in MrBayes 3.2 (Ronquist et al., 2012). The GTR + G model was selected for *cox1*, *Cytb*, *myh6*, *plagl2*, and *Rag1*; SYM + G was selected for *ENC1*; and HKY + G was selected for *ETS2*, *Rh*, and *zic1*. Because the proportion of invariant sites is accounted for by the gamma parameter (Yang, 2006), we did not consider the *I* parameter in our candidate pool of models.

We reconstructed phylogenetic relationships using the reduced and full data matrices in RAxML (Stamatakis, 2006). The concatenated alignments were partitioned by gene and assigned the GTR + G substitution model – the most similar model to the jModelTest results available in RAxML – to run a maximum likelihood search for the best tree. We then used the GTR + CAT model to run 1000 fast bootstrap replicates on both datasets.

Acanthurid phylogenetic relationships were also reconstructed using a Bayesian framework using MrBayes 3.2 (Ronquist et al., 2012). The alignments were partitioned by gene and assigned the substitution models selected by jModelTest. The reduced and full datasets were each run with four chains for 20 million generations, sampling every 1000 generations. Trace files were inspected in Tracer 1.5 (Drummond and Rambaut, 2007) to ensure chain convergence. The first 25% of trees were discarded as burnin, and the remaining trees were combined to obtain a 50% majority rule consensus tree.

We also estimated a species tree based on eight loci utilizing a reduced taxonomic set in *BEAST (Heled and Drummond, 2010) using the program BEAST 1.7.4 (Drummond et al., 2012). We removed the *ETS2* locus and the taxa from Klanten et al. (2004) for which we did not sequence additional genes to minimize the effect of missing data. Each gene was partitioned individually and assigned the substitution model selected by jModelTest with the exception of *ENC1*; SYM + G was not an available model in *BEAST so the GTR + G model was used. We linked the *cox1* and *Cytb* loci and applied a local molecular clock model and a birth–death prior. The analysis was run for 200 million generations, sampling every 5000 generations. Chain mixing and convergence was ensured by inspecting trace files in Tracer 1.5 (Drummond and Rambaut, 2007). The first 10% of trees were removed as burnin, and we generated the species tree using TreeAnnotator (Drummond and Rambaut, 2007).

We tested the monophyly of *Ctenochaetus*, which does not appear to be monophyletic in molecular phylogenies (Clements et al., 2003; Klanten et al., 2004), using the approximately unbiased (AU) test (Shimodaira, 2002). The ML tree topologies and per-site log likelihoods were obtained in RAxML (Stamatakis, 2006) for the unconstrained and constrained (*Ctenochaetus* monophyly enforced) trees. The per-site log likelihoods were used in Consel 0.20 (Shimodaira and Hasegawa, 2001) to conduct the AU test using multiscale bootstrap resampling in ten sets of 10,000 replicates. Consel calculates *p*-values based on the bootstrap replicates for each of the candidate topologies, and provides the Bayesian posterior probabilities of each topology calculated from the log likelihood values.

2.4. Divergence time estimation and comparative methods

We used the program BEAST 1.7.4 (Drummond et al., 2012) to infer divergence times using the full dataset. The dataset was partitioned and the substitution models were assigned as described above for the *BEAST analysis. Uncorrelated exponential priors were used and a birth–death prior was selected for rates of cladogenesis.

We used two fossil calibration points to date our tree. The Middle Eocene *Sorbinithurus sorbinii* from Monte Bolca (Italy), which was identified by Tyler (2000) as a stem Nasinae on the basis of six characters (short non-protruding first dorsal-fin spine; three or fewer pelvic-fin rays; presence of a dorsal pterygial shield; a small uroneural; fusion of hypurals one through four; a shallow caudal peduncle), was used to assign a minimum age of 50 My (Papazzoni and Trevisani, 2006) to the crown Acanthuridae. The basal Eocene *Kushlukia permira* from the lowermost layers of the mid-

Table 1
List of taxa and GenBank accession numbers used in this study. *Zanclus cornutus* and *Luvarus imperialis* were used as outgroups.

	Taxon name	*cox1*	*Cytb*	*ENC1*	*ETS2*	*myh6*	*plagl2*	*Rag1*	*Rh*	*zic1*
Zanclidae										
	Zanclus cornutus	KC623652	AP009162	EF539247	AY264679	EF536300	EF536262	EF530100		EF533923
Luvaridae										
	Luvarus imperialis	KC623653	AP009161	EF539246	AY264678	EF536299	EF536261	EF530099	EU637975	EF533971
Acanthuridae										
	Acanthurus achilles	KC623654	KC623692	KC623730		KC623763	KC623798	KC623828	KC623863	KC623902
	Acanthurus auranticavus	KC623655	KC623693	KC623731		KC623764	KC623799	KC623829	KC623864	KC623903
	Acanthurus bariene	KC623657	KC623695	KC623733		KC623766	KC623801	KC623831	KC623866	KC623905
	Acanthurus blochii	HM034180	AY264632	KC623734	AY264685	KC623767	KC623802	KC623832	KC623867	KC623906
	Acanthurus chirurgus	KC623658	KC623696	KC623735		KC623768	KC623803	KC623833	KC623868	KC623907
	Acanthurus coeruleus	KC623659	KC623697	KC623736		KC623769	KC623804	KC623834	KC623869	KC623908
	Acanthurus dussumieri		AY264633		AY264686					
	Acanthurus guttatus	KC623660	KC623698	EF539241		EF536294	EF536256	EF530094	KC623870	EF533917
	Acanthurus japonicus	KC623661	KC623699	KC623737		KC623770	KC623805	KC623835	KC623871	KC623909
	Acanthurus leucocheilus	KC623662	KC623700				KC623806	KC623836	KC623872	KC623910
	Acanthurus leucosternon	KC623663	EU136032	KC623738		KC623771	KC623807	KC623837	KC623873	KC623911
	Acanthurus lineatus	KC623664	EU273284	KC623739		KC623772	KC623808	KC623838	KC623874	KC623912
	Acanthurus mata	KC623665	KC623701	KC623740		KC623773	KC623809	KC623839	KC623875	KC623913
	Acanthurus monroviae	KC623666	KC623702	KC623741		KC623774	KC623810	KC623840	KC623876	KC623914
	Acanthurus nigricans	KC623667	KC623703	KC623742		KC623775	KC623811	KC623841	KC623877	KC623915
	Acanthurus nigricauda	HM034189	KC623704	KC623743		KC623776	KC623812	KC623842	KC623878	KC623916
	Acanthurus nigrofuscus	KC623668	KC623705	KC623744	AY264688	KC623777	KC623813	KC623843	KC623879	KC623917
	Acanthurus nigroris		HM242385							
	Acanthurus nubilus	HM034193	AY264636		AY264689					
	Acanthurus olivaceus	KC623669	KC623707	KC623745	AY264690	KC623778	KC623814	KC623844	KC623880	KC623918
	Acanthurus pyroferus	KC623670	KC623708	KC623746	AY264691	KC623779	KC623815	KC623845	KC623881	KC623919
	Acanthurus tennentii	KC623671	KC623709	KC623747		KC623780	KC623816	KC623846	KC623882	KC623920
	Acanthurus thompsoni	KC623672	KC623710	KC623748		KC623781	KC623817	KC623847	KC623883	KC623921
	Acanthurus tractus	KC623656	KC623694	KC623732		KC623765	KC623800	KC623830	KC623865	KC623904
	Acanthurus triostegus	KC623673	KC623711	EF539242	AY264692	EF536295	EF536257	EF530095	KC623884	EF533918
	Acanthurus xanthopterus	KC623674	KC623712	KC623749	AY264693	KC623782	KC623818	KC623848	KC623885	KC623922
	Ctenochaetus binotatus		KC623713	KC623750	AY264694	KC623783		KC623849	KC623886	KC623923
	Ctenochaetus flavicauda	HM034209								
	Ctenochaetus striatus	KC623675	KC623714	EF539243	AY264695	EF536296	EF536258	EF530096		EF533919
	Ctenochaetus strigosus	KC623676	FJ376811	KC623751		KC623784	KC623819	KC623850	KC623887	KC623924
	Ctenochaetus tominiensis	KC623677	KC623715	KC623752		KC623785	KC623820	KC623851		KC623925
	Ctenochaetus truncatus	KC623678	KC623716	KC623753		KC623786	KC623821	KC623852	KC623888	KC623926
	Naso annulatus	HM034159	AY264643		AY264696					
	Naso brachycentron		AY264644		AY264697					
	Naso brevirostris	KC623679	KC623717	EF539240	AY264698	EF536293	EF536255	EF530093	KC623889	EF533916
	Naso caeruleacauda		AY264646		AY264699					
	Naso caesius		AY264647		AY264700					
	Naso elegans	KC623680	KC623718	KC623754	AY264701			KC623853	KC623890	
	Naso fageni		AY264649		AY264702					
	Naso hexacanthus		AY264650		AY264703					
	Naso lituratus	HM034247	AB276964	EF539239	AY264704	EF536292	EF536254	EF530092	EU637984	EF533915
	Naso lopezi	AP009163	AP009163		AY264705					
	Naso maculatus		AY264653		AY264706					
	Naso mcdadei		AY264654		AY264707					
	Naso minor		AY264655		AY264708					
	Naso reticulatus		AY264656		AY264709					
	Naso thynnoides		AY264657		AY264710					
	Naso tonganus		AY264658		AY264711					
	Naso tuberosus		AY264659		AY264712					

(*continued on next page*)

Table 1 (*continued*)

Taxon name	*cox1*	*Cytb*	*ENC1*	*ETS2*	*myh6*	*plagl2*	*Rag1*	*Rh*	*zic1*
Naso unicornis	KC623681	KC623719	KC623755	AY264713	KC623787	KC623822	KC623854	KC623891	KC623927
Naso vlamingii	KC623682	KC623720	KC623756	AY264714	KC623788	KC623823	KC623855	KC623892	KC623928
Paracanthurus hepatus	KC623683	KC623721	EF539244	AY264715	EF536297	EF536259	EF530097	KC623893	EF533920
Prionurus biafraensis	KC623684	KC623722	KC623757		KC623789	KC623824	KC623856	KC623894	KC623929
Prionurus laticlavius	KC623685	KC623723	KC623758		KC623790	KC623825	KC623857	KC623895	KC623930
Prionurus maculatus	KC623687	KC623725			KC623792			KC623897	KC623932
Prionurus microlepidotus		AY264628		AY264681	EF536298	EF536260	EF530098		EF533921
Prionurus punctatus	KC623686	KC623724	KC623759		KC623791		KC623858	KC623896	KC623931
Prionurus scalprum		AB276963		AY264682					
Zebrasoma desjardinii	KC623688	KC623727	KC623760		KC623794		KC623860	KC623898	KC623934
Zebrasoma flavescens	KC623689	AP006032	KC623761		KC623795	KC623827	KC623861	KC623899	KC623935
Zebrasoma rostratum	HM034282								
Zebrasoma scopas	KC623690	KC623728	EF539238	AY264683	KC623796	EF536253	AY308776	KC623900	KC623936
Zebrasoma velifer	KC623691	KC623729	KC623762	AY264684	KC623797		KC623862	KC623901	KC623937

dle part of the Danatinsk Suite, Uylya-Kushlyuk, southwest Turkmenistan, (Lower Eocene, Ypresian, 55.8 My; see Gavrilov et al., 2003), was identified by Bannikov and Tyler (1995) as a stem luvarid. This result was based on nine synapomorphies, including the dorsal- and anal-fin pterygiophores being uniquely modified and broadly sutured around the dorsal and ventral margins of the body just below the skin; two or fewer large dorsal-fin spines; no anal-fin spines; unsegmented soft-dorsal and anal-fin rays; distal end of the first anal-fin basal pterygiophore is greatly prolonged anteriorly; hypurals 1–4 fused into a single hypural plate, with only the fifth hypural and the parhypural remaining autogenous; caudal-fin rays overlap deeply the hypural plate; and the pelvic fin becomes rudimentary with increasing specimen size (or is absent). The otoliths assigned to the "genus *Epigonidarum*" *weinbergi* from the Coniacian of Tiefe Gosau, Austria (Late Cretaceous, 89–84 Ma), considered to be the oldest record of the percomorphs, were used to establish a soft upper boundary (Sieber and Weinfurter, 1967).

We ran the analyses for 50 million generations, sampling every 5000 generations. Proper chain mixing and convergence was ensured by inspecting trace files in Tracer 1.5 (Drummond and Rambaut, 2007). We removed the first 10% of trees as burnin, and generated the timetree using TreeAnnotator (Drummond and Rambaut, 2007).

To test the hypothesis that thick-walled, gizzard-like stomachs evolved multiple times within the genus *Acanthurus*, we conducted a maximum likelihood ancestral state reconstruction of this morphology using the Geiger package (Harmon et al., 2008) in R 2.15.2 (R Development Team, 2012). Each *Acanthurus* and *Ctenochaetus* species in our timetree was coded as either having the thick-walled, gizzard-like stomach following descriptions from the literature (Jones, 1968; Randall, 1956; Randall and Clements, 2001; Hiatt and Strasburg, 1960), not having this particular morphology, or as unknown (Table S1). *Acanthurus tractus* was coded as having this morphology because of its close relationship to *A. bahianus*, which has the gizzard-like stomach.

3. Results

3.1. Phylogenetic analyses

The reduced and full datasets did not produce significantly different topologies for either the ML or Bayesian phylogenetic analyses (Figs. 2, S1), so we will present the results for the full dataset analyses and comment later on the differences between the full and reduced datasets.

The ML and Bayesian trees produced an identical tree topology for the intergeneric relationships, with the only differences observed in the arrangement among some *Naso* species and the placement of *Ctenochaetus striatus* and *C. tominiensis*. In both ML and Bayesian analyses we recover a highly supported (all with 100 bootstrap support, bsp; 1.0 posterior probability, pp) monophyletic Acanthuridae, Nasinae and Acanthurinae. Within Nasinae we recover *Naso lopezi* as the sister taxon to a clade containing the remaining *Naso* species (100 bsp, 1.0 pp). This clade contains several well-supported groups: *Naso maculatus* + *N. reticulatus* (88 bsp, 0.99 pp); *N. tonganus* + *N. tuberosus* (92 bsp, 0.98 pp); *N. caesius* + *N. hexacanthus* (100 bsp, 1.0 pp); *N. unicornis* + (*N. lituratus* + *N. elegans*) (98 bsp, 1.0 pp); however, the relationships among these groups are not well resolved (Fig. 2).

Within Acanthurinae we recover a strongly supported *Prionurus* clade, which is sister group to the remaining acanthurins (100 bsp, 1.0 pp). We recover high support for all the relationships among the *Prionurus* species (all nodes with $\geqslant$92 bsp and 1.0 pp), except for the sister relationship between *P. maculatus* and *P. scalprum* (62 bsp, 0.86 pp). The last four genera make up two major clades. We

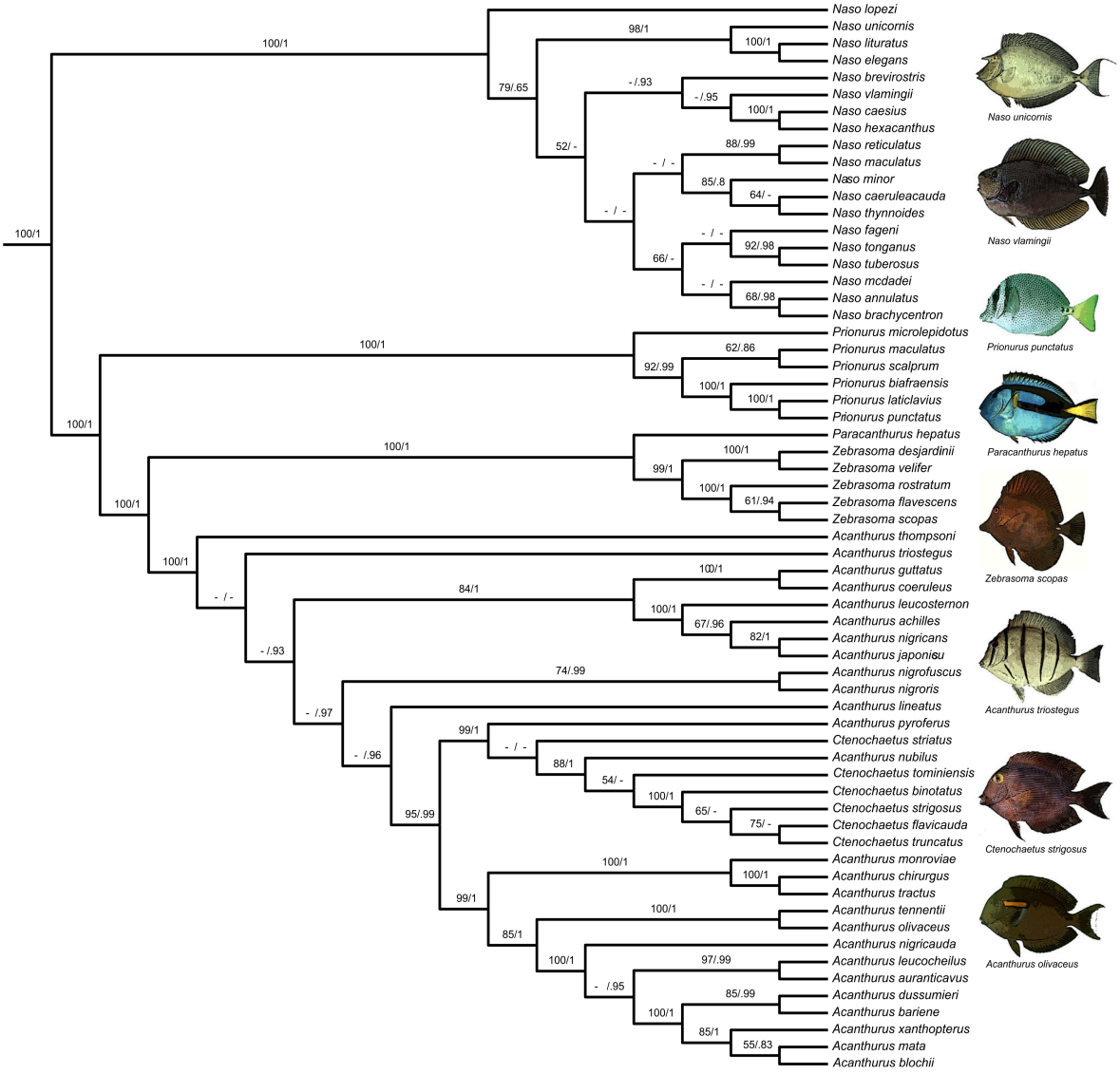

Fig. 2. Molecular phylogenetic tree based on the maximum likelihood analysis of the concatenated full dataset for all species included in this study. The bootstrap proportion (bsp), then the posterior probability (pp) values based on the Bayesian analysis are provided preceding the nodes. Only bsp ⩾ 50 and pp ⩾ 0.80 are shown. Fish drawings adapted from Fishbase.

find that *Paracanthurus* is sister to a *Zebrasoma* clade (100 bsp, 1.0 pp), and all relationships among *Zebrasoma* are highly supported, except for the sister relationship of *Z. flavescens* and *Z. scopas* in the ML tree (61 bsp, but 0.94 pp).

A final major clade contains the genera *Acanthurus* + *Ctenochaetus* (100 bsp, 1.0 pp), both of which are paraphyletic (Fig. 2). We recover strong support (99 bsp, 1.0 pp) for a clade made up of *Acanthurus pyroferus*, *A. nubilus*, and all *Ctenochaetus*. In the ML tree, *Acanthurus pyroferus*, then *Ctenochaetus striatus* (31 bsp), then *A. nubilus* (88 bsp), then *C. tominiensis* (54 bsp) serially branch off from a clade containing the remaining *Ctenochaetus* (100 bsp). In the Bayesian tree, *Acanthurus pyroferus* + *Ctenochaetus striatus* (0.94 pp) is sister to a polytomy (1.0 pp) of *A. nubilus*, *C. tominiensis*, and a clade containing the remaining *Ctenochaetus* (1.0 pp).

We recover identical relationships among the remaining *Acanthurus* species, with several well-supported subclades. In both analyses we recover a pectinate branching pattern where *Acanthurus thompsoni* (100 bsp, 1.0 pp), then *A. triostegus* branch off from the clade containing all other *Acanthurus* and *Ctenochaetus*, although the position of *A. triostegus* is weakly supported (<50 bsp, 0.53 pp). A subclade containing *Acanthurus guttatus* + *A. coeruleus* sister to *A. leucosternon* + *A. achilles* + (*A. nigricans* + *A. japonicus*) is recovered (84 bsp, 1.0 pp), as well as a derived clade containing the well-supported *Acanthurus* + *Ctenochaetus* subclade described above sister to a clade containing *A. monroviae*, *A. chirurgus*, *A. tractus*, *A. tennentii*, *A. olivaceus*, *A. nigricauda*, *A. leucocheilus*, *A. auranticavus*, *A. dussumieri*, *A. bariene*, *A. xanthopterus*, *A. mata*, and *A. blochii* (99 bsp, 1.0 pp). Most relationships among these major subclades are highly supported in the Bayesian analysis (⩾0.93 pp), but only the sister relationship between the *Acanthurus* + *Ctenochaetus* clade and the derived *Acanthurus* clade is highly supported in the ML tree (95 bsp).

Differences between the reduced and full datasets occurred in parts of the tree with low support (Fig. S1). For example, using

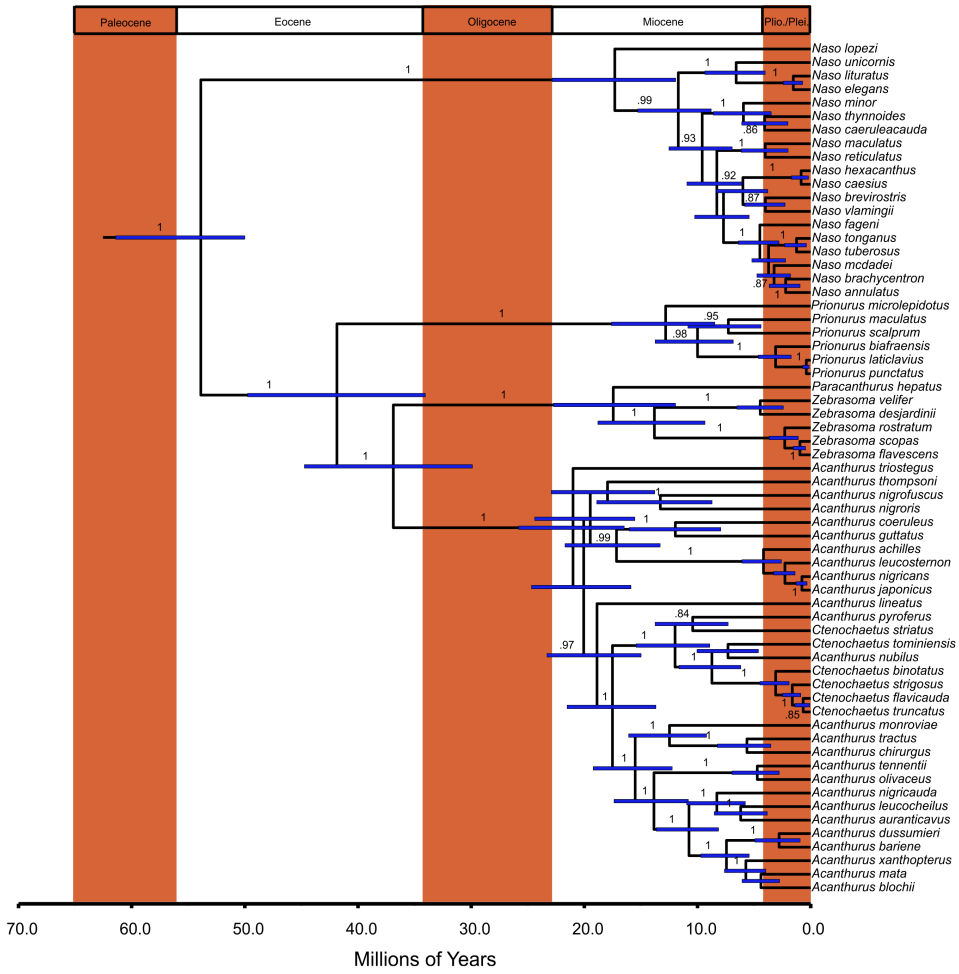

Fig. 3. BEAST timetree based on the concatenated full dataset. Posterior probabilities, pp, ⩾0.80 are shown.

the ML and Bayesian reduced datasets, *Naso brevirostris* and *N. vlamingii* are sister taxa, but are sequential sister taxa to *N. annulatus* + *N. brachycentron* in both full analyses. The placement of *Acanthurus thompsoni*, *A. nigroris* + *A. nigrofuscus*, and *A. triostegus* also differs at the base of the *Acanthurus* + *Ctenochaetus* clade in the ML analyses; *A. thompsoni* is the sister taxon to the *Acanthurus* + *Ctenochaetus* clade in the full dataset, but *A. thompsoni* + (*A. nigroris* + *A. nigrofuscus*) is the sister clade to the *Acanthurus* + *Ctenochaetus* clade in the reduced analysis. Additionally, *Acanthurus triostegus* is the sister taxon to the clade containing *A. guttatus*, *A. coeruleus*, *A. leucosternon*, *A. achilles*, *A. nigricans*, and *A. japonicus* in the reduced tree, but *A. triostegus* is the sister taxon to the *Acanthurus* + *Ctenochaetus* clade minus *A. thompsoni* in the full dataset tree. In the reduced Bayesian tree, *Acanthurus triostegus* forms a polytomy with *A. thompsoni* and the clade containing the remaining *Acanthurus* + *Ctenochaetus*, but *A. thompsoni* and *A. triostegus* are sequential sister taxa in the full tree. Finally, the relationship between *Acanthurus pyroferus* and *Ctenochaetus striatus* differs in the ML analyses; they are sequential lineages that branch off the *A. nubilus* + *Ctenochaetus* clade in the full dataset, but are sister taxa in the reduced analysis.

Table 2
Inferred divergence time estimates and 95% highest posterior density (95% HPD) for major nodes in the time-calibrated phylogeny.

Node	Crown age (Ma)	95% HPD
Acanthuridae	54	51–62
Nasinae (*Naso*)	17	12–23
Acanthurinae	42	34–51
Prionurus	13	8–18
Paracanthurus + *Zebrasoma*	17	12–23
Acanthurus + *Ctenochaetus*	21	16–26

Our gene tree species tree analysis (Fig. S2) is largely congruent with the ML and Bayesian trees except that the *Paracanthurus* + *Zebrasoma* clade is sister to the *Prionurus* clade, and there is some rearrangement within the *Acanthurus* + *Ctenochaetus* clade. We recover *Acanthurus triostegus* as the sister taxon to the remaining *Acanthurus* + *Ctenochaetus*. Similar to all other analyses, we find strong support for a paraphyletic *Acanthurus* and *Ctenochaetus*. *A. pyroferus* and *A. nubilus* form a clade with the remaining *Ctenochaetus* species (1.0 pp); *Acanthurus pyroferus* is sister to a clade containing *A. nubilus* + *Ctenochaetus striatus* (0.8 pp), which is sister to the other *Ctenochaetus*. Other major groups were also recovered with high support, including *Acanthurus guttatus* + *A. coeruleus*, and a clade including *A. monroviae*, *A. tractus*, *A. chirurgus*, *A. tennentii*, *A. olivaceus*, *A. nigricauda*, *A. auranticavus*, *A. leucocheilus*, *A. bariene*, *A. mata*, *A. blochii*, and *A. xanthopterus*, with high support for many relationships within this group.

The constrained ML topology we recovered placed *Acanthurus nubilus* as sister taxon to the *Ctenochaetus* clade with an extremely

short internode between them (Fig. S3). The AU test ranked the unconstrained tree ($p = 0.72$) higher than the constrained *Ctenochaetus* tree, but we could not reject the hypothesis of a monophyletic *Ctenochaetus* ($p = 0.28$). We did, however, reject a monophyletic *Ctenochaetus* (pp < 0.001) using the Bayesian posterior probability estimated from the log likelihood values.

3.2. Divergence time estimation

Our timetree analysis (Fig. 3) recovered a similar topology to those from the ML and Bayesian analyses (Fig. 2), differing only in species-level relationships with low support within the *Naso* and the *Acanthurus* + *Ctenochaetus* clades. *Naso lopezi* was identified as the sister taxon to the clade containing the remaining *Naso* diversity, and several other major groups were inferred that were recovered in the other phylogenetic analyses, including: *N. unicornis* + (*N. elegans* + *N. lituratus*); *N. caeruleacauda*, *N. minor*, and *N. thynnoides*; *N. maculatus* + *N. reticulatus*; *N. vlamingii*, *N. brevirostris*, *N. caesius* + *N. hexacanthus*; and *N. tonganus* + *N. tuberosus*; and *N. brachycentron* + *N. annulatus*.

The BEAST tree recovers *Acanthurus triostegus* as the sister taxon to the remaining *Acanthurus* + *Ctenochaetus* (instead of *A. thompsoni* in the ML and Bayesian trees); *A. thompsoni* is instead nested in one of the major *Acanthurus* subclades (Fig. 3). Many similar sister taxa relationships, compared to the ML and Bayesian analyses, are recovered by the BEAST analysis, such as *Acanthurus nigroris* + *A. nigrofuscus*, *A. coeruleus* + *A. guttatus*, *A. japonicus* + *A. nigricans*, and *A. chirurgus* + *A. tractus*. The BEAST tree also supports the paraphyly of *Acanthurus* and *Ctenochaetus*, as well as the placement of *A. lineatus* as the sister taxon to the clade containing *Ctenochaetus* and the major subclade of *Acanthurus* species. Identical relationships are recovered in the *Prionurus* and the *Paracanthurus* + *Zebrasoma* clades for all analyses.

The timetree analysis estimates a Late Paleocene–Early Eocene crown age for the Acanthuridae (54 Ma, 95% highest posterior density, HPD, 51–62 Ma), with all of the extant generic diversity arising between 17 and 21 Ma (Fig. 3, Table 2). *Naso* represents a relatively recent radiation; *Naso lopezi* split from the remaining *Naso* approximately 17 Ma (12–23 Ma HPD), and the major diversification occurred between ~12 and 2 Ma (Fig. 3, Table 2). The crown age of the Acanthurinae is much older (42 Ma, 34–51 Ma HPD). We find that the crown *Prionurus* originated in the Middle Miocene (13 Ma, 8–18 Ma HPD), and the crown *Paracanthurus* + *Zebrasoma* appeared around the same time as *Naso*, 17 Ma (12–23 Ma HPD) (Fig. 3, Table 2).

The *Acanthurus* + *Ctenochaetus* clade originated sometime in the Early Miocene (21 Ma, 16–26 Ma HPD) (Fig. 3, Table 2). Two major subclades began diversifying contemporaneously around 19 Ma, one leading to a clade of *Acanthurus* (*A. thompsoni*, *A. nigrofuscus*, *A. nigroris*, *A. coeruleus*, *A. guttatus*, *A. achilles*, *A. leucosternon*, *A. japonicus* and *A. nigricans*), the other leading to a clade of the remaining *Acanthurus* + *Ctenochaetus*. We estimate the age of the clade containing all *Ctenochaetus* and *A. pyroferus* and *A. nubilus* to be ~12 Ma (9–15 Ma HPD). *Ctenochaetus striatus* and *Acanthurus pyroferus* split from one another ~10 Ma (7–14 Ma HPD), and *C. tominiensis* and *A. nubilus* split ~7 Ma (5–10 Ma HPD). The remaining *Ctenochaetus* began radiating about 3 Ma (2–4 Ma HPD).

3.3. Ancestral state reconstruction of stomach morphology

Our ancestral reconstruction of the gizzard-like stomach morphology shows that it has evolved once in the *Acanthurus* + *Ctenochaetus* clade (Fig. S4). It appears that the trait evolved approximately 19 Ma in the stem lineage leading to a derived clade that includes all *Ctenochaetus* + *A. nubilus* + *A. pyroferus* and a clade containing *A. monroviae*, *A. tractus*, *A. chirurgus*, *A. tennentii*, *A. olivaceus*, *A. nigricauda*, *A. auranticavus*, *A. leucocheilus*, *A. bariene*, *A. dussumieri*, *A. mata*, *A. blochii*, and *A. xanthopterus*. At least one reversal from the gizzard-like stomach to the thin-walled stomach occurred within this clade in *Acanthurus nubilus*.

4. Discussion

4.1. Acanthurid relationships

Our analysis represents the most comprehensive species-level molecular phylogeny for the family Acanthuridae to date in both taxonomic sampling and number of loci. Our results using maximum likelihood and Bayesian methods are highly congruent with previously published studies based on morphological (Winterbottom, 1993; Guiasu and Winterbottom, 1993; Tyler et al., 1989) and molecular characters (Holcroft and Wiley, 2008; Klanten et al., 2004; Tang et al., 1999). Our tree topologies support the division of extant acanthurids into two subfamilies, Nasinae and Acanthurinae, as well as the relationships among the major acanthurid subclades (Winterbottom, 1993; Guiasu and Winterbottom, 1993; Holcroft and Wiley, 2008; Clements et al., 2003; Klanten et al., 2004; Tang et al., 1999; Tyler et al., 1989). We recovered a sister group relationship between Nasinae and all remaining acanthurids; *Prionurus* sister to all other acanthurins; and *Zebrasoma* + *Paracanthurus* sister to a strongly supported *Acanthurus* + *Ctenochaetus* clade (100 bsp, 1.0 pp). Our species tree is an exception, having recovered *Paracanthurus* + *Zebrasoma* sister to *Prionurus*. Because all other tree topologies based on both molecular and morphological evidence do not support this relationship, we consider the phylogenetic hypothesis of *Prionurus* sister to all remaining acanthurins to be the correct one.

We recovered paraphyly of *Acanthurus*, a result that had been predicted in generic-level studies that had failed to detect morphological synapomorphies for this genus (e.g., Winterbottom, 1993; Guiasu and Winterbottom, 1993). With increased sampling of both *Acanthurus* and *Ctenochaetus* compared to previous molecular studies, our analysis strongly supports *Ctenochaetus* paraphyly with respect to *Acanthurus*, a result already inferred by Clements et al. (2003) and Klanten et al. (2004). The ML tree of Clements et al. (2003) suggests that *Acanthurus pyroferus*, *A. mata*, *A. xanthopterus*, *A. triostegus*, *A. nigricans*, and *A. nigroris* all fall within *Ctenochaetus*. In contrast, we recover highly supported *Ctenochaetus* paraphyly (⩾99 bsp, 1.0 pp) with respect to only *Acanthurus pyroferus* and *A. nubilus*. We recover a close relationship between *Acanthurus pyroferus* and *Ctenochaetus*, as suggested by the ML analysis of Clements et al. (2003); however, *A. pyroferus* and *C. striatus* are sister taxa in all but our full ML analysis and the species tree. Support for *Ctenochaetus striatus* sister to the remaining *Ctenochaetus* (+ *Acanthurus nubilus* in the full dataset) was very low in the full ML tree (31 bsp), and *A. nubilus* + *C. striatus* was recovered with low support (0.8 pp) in the species tree.

The inclusion of *Acanthurus nubilus* in a clade with all *Ctenochaetus* (minus *C. striatus*) is highly supported (88 bsp, 1.0 pp), although the relationship of *Acanthurus nubilus* varies within the clade. The AU test results did not allow us to reject the hypothesis of a monophyletic *Ctenochaetus*. Considering the short internode separating *Acanthurus nubilus* and *Ctenochaetus* in the constrained tree topology, however, it is not surprising that the difference between the constrained and unconstrained tree likelihoods was not large enough to reject the constrained topology. All other evidence points to paraphyly of *Ctenochaetus*. In addition to rejecting a monophyletic *Ctenochaetus* based on the Bayesian posterior probability values calculated by the program Consel, we recovered *Acanthurus nubilus* within *Ctenochaetus* in all tree topologies including the individual gene analyses and the species tree analy-

sis, which suggests that this placement is not an artifact of individual gene histories. The placement of *Acanthurus nubilus* is not likely an artifact due to misidentification or contamination in published sequences either. *Acanthurus nubilus* is represented in our data matrix by three loci (*cox1*, *Cytb*, *ETS2*), but these data have been produced by two independent studies (Klanten et al., 2004; Hubert et al., 2010). Consistent placement of *Acanthurus nubilus* within *Ctenochaetus* in all individual gene tree analyses suggests that this reflects the true topology.

Guiasu and Winterbottom (1993) identified 14 osteological synapomorphies for the clade formed by the *Ctenochaetus* species in their study (*C. binotatus*, *C. striatus*, *C. strigosus*), with all but one of these characters found in the suspensorium and jaws, in the hyoid arch or in the branchial arches. Unfortunately neither *Acanthurus nubilus* nor *A. pyroferus* were included in their analysis, so at the moment it is unknown how many of the 14 traits are found in these two *Acanthurus* species. We think it is worth pointing out that *Acanthurus nubilus* (VI or VII dorsal spines), *A. pyroferus* (VIII), *A. chronixis* (VIII), and *A. tristis* (VIII) (e.g. Randall, 2001) are exceptions among most *Acanthurus* species, which possess nine dorsal spines. *Ctenochaetus* species consistently have eight dorsal spines (Randall and Clements, 2001), so the species in the *Acanthurus nubilus* + *A. pyroferus* + *Ctenochaetus* clade we recover are all distinguished from other *Acanthurus* by having eight or fewer dorsal spines. *Acanthurus chronixis* and *A. tristis* were not included in our study so their phylogenetic position could not be determined; however, morphological evidence has suggested a close relationship between *A. pyroferus* and *A. chronixis* (Randall, 1960) and *A. pyroferus* and *A. tristis* (Randall, 1993). *Acanthurus chronixis* has been described by a single specimen, so additional evidence of this relationship is limited, but it is important to note that *A. chronixis* also has the thick-walled, gizzard-like stomach. Additional lines of evidence beyond morphology link *Acanthurus pyroferus* and *A. tristis*: mimicry of angelfishes by *Acanthurus pyroferus* has been well-documented (e.g. see Randall, 2005) and juvenile *A. tristis* mimic the angelfish *Centropyge eibli* in the Indian Ocean; and hybridization between *A. pyroferus* and *A. tristis* has been described (Randall, 2001). A close relationship between the three *Acanthurus* species suggests that *A. chronixis* and *A. tristis* may also fall within the *Acanthurus nubilus* + *A. pyroferus* + *Ctenochaetus* clade we recovered, but further study is needed to confirm this hypothesis.

4.2. Timing of acanthurid evolution

Our relaxed molecular clock analysis reveals Late Paleocene/Early Eocene origin for the acanthurids, which possess a rich fossil record dating back to the Middle Eocene (~50 Ma). The split between Nasinae and Acanthurinae dates to ~56 Ma, right at the Paleocene/Eocene boundary. The two lineages experienced significantly different evolutionary paths: the Nasinae underwent a long time lag of ~40 My before their crown radiation ~17 Ma, while the Acanthurinae began diversifying during the Middle Eocene (~42 Ma).

Our estimated age for the origin of the root Nasinae is in close agreement with Klanten et al.'s (2004) estimate of 52–43 Ma; however, our timing of diversification within *Naso* is strongly incongruent. Klanten et al. (2004) estimated a *Naso* crown age between 46 and 39 Ma, which is much older than our estimate of 17 Ma. Divergence times of Klanten et al. (2004) were inferred using a non-parametric rate smoothing penalized likelihood approach, and an extrapolation of molecular evolution rates for selected gene regions. Previous studies have found that penalized likelihood methods, especially when using datasets with few molecular loci, can recover considerably different divergence time estimates compared to analyses using a large number of loci (e.g. Mulcahy et al., 2012). Our study includes more molecular loci (including seven nuclear genes) compared to Klanten et al. (2004), and our divergence time estimates are based on fossil calibration points that are more reliable than inferring divergence times based on molecular evolution rates extrapolated from other groups. We also utilize a Bayesian approach that explicitly incorporates uncertainty in calibration age and topology, all of which are advantages in inferring divergence times over penalized likelihood methods (e.g. Graur and Martin, 2004). Therefore, we feel our results reflect more closely the correct timing of diversification for extant *Naso*.

The stem ages of the various acanthurine subclades all date to the Eocene, and all extant surgeonfish diversity began radiating since the Early Miocene (~21 Ma for the *Acanthurus* + *Ctenochaetus* clade; ~17 Ma for *Zebrasoma* + *Paracanthurus*; ~17 Ma for *Naso*), or the Middle Miocene (~13 Ma for *Prionurus*). These results are congruent with patterns of diversification observed in other clades of marine organisms (e.g., pufferfishes and allies, Alfaro et al., 2007; Dornburg et al., 2011; Santini et al., 2013a, 2013b; wrasses, Alfaro et al., 2009; Cowman and Bellwood, 2011; Kazancioglu et al., 2009; butterflyfishes and cardinalfishes, Cowman and Bellwood, 2011; damselfishes, Cowman and Bellwood, 2011; Frédérich et al., 2013; several clades of gastropods, Williams and Duda, 2008), and may be linked to two main phenomena. First, geological events, such as the final closure of the Tethys Sea and the establishment of the circum-Antarctic currents, led to progressive regionalization of the marine biota (Hallam, 1994) that likely contributed to the fragmentation of previously more widespread taxa and an increase in cladogenesis. Second, the Miocene radiation of several major scleractinian coral lineages, such as the *Acropora* staghorn corals (Wood, 1999), contributed to an expansion of reefs that likely spurred diversification in at least some of the associated fish fauna.

Surgeonfishes possess one of the best studied fossil records among percomorph fishes, with at least 14 extinct genera and 16 species known from the Monte Bolca fossil site (Blot and Tyler, 1990; Sorbini and Tyler, 1998a, 1998b; Tyler, 1999, 2005a, 2005b; Tyler and Bannikov, 2000) and additional fossil taxa known from Oligocene and Miocene deposits (Tyler 1997, 2000; Tyler and Sorbini, 1998; Tyler and Micklich, 2011). Unfortunately, most acanthurid fossils have not yet been analyzed in a phylogenetic context (Tyler, 2000, study of Nasinae being the lone exception), thus preventing us from knowing if most of these taxa could be assigned to the crown or stem of this family. The rich fossil record, however, points to the acanthurids already having reached a significant diversity by the Middle Eocene, and the fact that several of the fossils could be assigned to the Nasinae supports a scenario of high turnover along this lineage, which could be inferred by its long stem.

4.3. Stomach morphology evolution

We reject the Clements et al. (2003) hypothesis that thick-walled, gizzard-like stomachs evolved independently in *Acanthurus pyroferus* and *A. xanthopterus* based on our phylogenetic analyses and ancestral state reconstruction. Our tree topologies recover a strongly supported *Acanthurus* subclade within the *Acanthurus* + *Ctenochaetus* clade which includes all 13 of the 19 *Acanthurus* species with this derived stomach morphology that are included in our study, as well as all *Ctenochaetus*. It is clear from our ancestral state reconstruction that the gizzard-like stomach evolved once in an early ancestor of this *Acanthurus* + *Ctenochaetus* subclade, alluding that the gizzard-like stomach has a common origin for both *Acanthurus* and *Ctenochaetus*.

The ancestral state reconstruction also suggests that a reversal from the gizzard-like stomach to thin-walled stomachs occurred at least once in *Acanthurus nubilus*. *Acanthurus nubilus* is a planktivorous species and this shift in diet may explain the loss of the

gizzard-like stomach that is used for mechanical trituration of detrital material in the other species of this subclade (e.g. Choat et al., 2004). The subclade we recover also includes *Acanthurus leucocheilus*, which was not considered in the morphological studies so we are unable to assess whether this species also reverted to the thin-walled stomach morphology or if it has the thick-walled, gizzard-like morphology. We recommend further research to assess whether *Acanthurus leucocheilus* and all other unexamined *Acanthurus* have gizzard-like stomachs.

4.4. Reclassification of Ctenochaetus

In all previously published morphological studies (Winterbottom, 1993; Guiasu and Winterbottom, 1993), the monophyly of the acanthurid genera (with the exception of *Acanthurus* and *Prionurus*) was supported, in some cases with multiple synapomorphies. The monophyly of *Ctenochaetus*, for example, is supported by 14 synapomorphies (Guiasu and Winterbottom, 1993). While our molecular topologies infer strong support for the monophyly of *Prionurus*, our results show a reciprocal paraphyly of *Acanthurus* and *Ctenochaetus*. Our result of a non-monophyletic *Acanthurus* had already been predicted by both morphological (Guiasu and Winterbottom, 1993) and molecular studies (Clements et al., 2003; Klanten et al., 2004); while the non-monophyly of *Ctenochaetus* had so far been supported only by DNA sequence data. Guiasu and Winterbottom, (1993) identified 14 osteological synapomorphiees for *Ctenochaetus*; several species from this genus, however, were not included in that morphological study, nor were *Acanthurus nubilus* or *A. pyroferus*, the two *Acanthurus* species that strongly grouped with *Ctenochaetus* in our study. It is possible that upon further examination some *Acanthurus* species (e.g. *A. nubilus* and *A. pyroferus*) will also share some/all of these synapomorphic traits.

In order to consider the information contained in our new phylogenetic hypothesis, and to allow the taxonomic nomenclature to reflect the evolutionary (i.e., phylogenetic) relationships, we recommend synonymizing the genus *Ctenochaetus* with *Acanthurus*, and suggest moving *Ctenochaetus binotatus*, *C. cyanocheilus*, *C. flavicauda*, *C. hawaiiensis*, *C. marginatus*, *C. striatus, C. strigosus*, *C. tominiensis*, and *C. truncatus* to the genus *Acanthurus*. An alternative would be to maintain the generic name of *Ctenochaetus* and change the generic status of *Acanthurus nubilus* and *A. pyroferus*; this would involve breaking the genus *Acanthurus* into several new genera. However, the relationships among some *Acanthurus* species in our study appear to be poorly supported, thus preventing us from knowing how many clades form the *Acanthurus* + *Ctenochaetus* group. Furthermore, 13 species of *Acanthurus* are missing from our sampling, and we would not know to which new genus they should be assigned. For these reasons we consider synonymizing *Ctenochaetus* with *Acanthurus* to be the most logical course of action.

4.5. Conclusions

Our findings reveal that the extant surgeonfish body plan appeared in the Late Paleocene/Early Eocene, and underwent a dramatic radiation by the Middle Eocene (50 Ma). Our timetree shows that most extant acanthurid diversification occurred throughout the Miocene contemporaneously with the radiation of scleractinian coral reef lineages. Our new phylogeny rejects the previous hypothesis that the evolution of a thick-walled, gizzard-like stomach evolved multiple times in *Acanthurus*; rather we recover a strongly supported subclade including all species in our study with this stomach morphology, and our ancestral state reconstruction supports common ancestry of the gizzard-like stomach for the *Acanthurus* and *Ctenochaetus* species. Finally, we find strong evidence of the paraphyly of *Acanthurus* and *Ctenochaetus*, and suggest revision to the acanthurid taxonomy by eliminating the genus *Ctenochaetus*, which we show to be a derived lineage within *Acanthurus*.

Acknowledgments

Funding for this project was provided by NSF Grant DEB 0842397 "Systematics and Influence of Coral Reefs on Diversification in Tetraodontiform Fishes". FS was supported by an ISI Lagrange fellowship. This research project was made possible by the generous loan or gift of tissues from a number of colleagues and institutions: Andrew Bentley and Ed Wiley (University of Kansas), H.J. Walker and Phil Hastings (Scripps Institute of Oceanography); Rick Feeney and Jeff Siegel (Los Angeles County Natural History Museum); and Luiz Rocha (California Academy of Sciences). We thank Peter Wainwright, Kendall Clements, and Giacomo Bernardi for helpful comments on an earlier version of this manuscript.

Appendix A. Supplementary data

Supplementary data associated with this article can be found, in the online version, at http://dx.doi.org/10.1016/j.ympev.2013.03.014.

References

Akaike, H., 1973. Information theory as an extension of the maximum likelihood principle. In: Petrov, B.N., Caski, F. (Eds.), Second International Symposium on Information Theory. Akademiai Kiado, Budapest, pp. 267–281.

Alfaro, M.E., Santini, F., Brock, C.D., 2007. Do reefs drive diversification in marine teleosts? Evidence from the pufferfishes and their allies (order Tetraodontiformes). Evolution 61, 2104–2126.

Alfaro, M.E., Santini, F., Brock, C.D., Alamillo, H., Dornburg, A., Rabosky, D.L., et al., 2009. Nine exceptional radiations plus high turnover explain species diversity in jawed vertebrates. Proc. Natl. Acad. Sci. USA 106, 13410–13414.

Bannikov, A.F., Tyler, J.C., 1995. Phylogenetic revision of the fish families Luvaridae and †Kushlukiidae (Acanthuroidei), with a new genus and two new species of Eocene luvarids. Smithson. Contr. Paleob. 81, 1–45.

Bernal, M.A., Rocha, L.A., 2011. *Acanthurus tractus* Poey, 1860, a valid western Atlantic species of surgeonfish (Teleostei, Acanthuridae), distinct from *Acanthurus bahianus* Castelnau, 1855. Zootaxa 2905, 63–68.

Blot, J., Tyler, J.C., 1990. New genera and species of fossil surgeonfishes and their relatives (Acanthuroidei, Teleostei) from the Eocene of Monte Bolca, Italy, with application of the Blot formula to both fossil and recent forms. St. Ric. Giac. Terz. Bolca 6, 13–92.

Borden, W.C., 1998. Phylogeny of the Unicornfishes (Naso, Acanthuridae) Based on soft anatomy. Copeia 1, 104–113.

Chen, W.-J., Bonillo, C., Lecointre, G., 2003. Repeatability of clades as a criterion of reliability: a case study for molecular phylogeny of Acanthomorpha (Teleostei) with larger number of taxa. Mol. Phylogenet. Evol. 26, 262–288.

Choat, J.H., Clements, K.D., Robbins, W.D., 2002. The trophic status of herbivorous fishes on coral reefs I: Dietary analyses. Mar. Biol. 140, 613–624.

Choat, J.H., Robbins, W.D., Clements, K.D., 2004. The trophic status of herbivorous fishes on coral reefs II: Food processing modes and trophodynamics. Mar. Biol. 145, 445–454.

Clements, K.D., Gray, R.D., Choat, J.H., 2003. Rapid evolutionary divergence in reef fishes of the family Acanthuridae (Perciformes; Teleostei). Mol. Phylogenet. Evol. 26, 190–201.

Cowman, P.F., Bellwood, D.R., 2011. Coral reefs as drivers of cladogenesis: expanding coral reefs, cryptic extinction events, and the development of biodiversity hotspots. J. Evol. Biol. 24, 2543–2562.

Dornburg, A., Sidlauskas, B., Santini, F., Sorenson, L., Near, T.J., Alfaro, M.E., 2011. The influence of an innovative locomotor strategy on the phenotypic diversification of triggerfish (Family: Balistidae). Evolution 65, 1912–1926.

Drummond, A.J., Rambaut, A., 2007. BEAST: Bayesian evolutionary analysis by sampling trees. BMC Evol. Biol. 7, 214.

Drummond, A.J., Suchard, M.A., Xie, D., Rambaut, A., 2012. Bayesian phylogenetics with BEAUti and the BEAST 1.7. Mol. Biol. Evol. 29, 1969–1973.

Edgar, R.C., 2004. MUSCLE: multiple sequence alignment with high accuracy and high throughput. Nucleic Acids Res. 32, 1792–1797.

Frédérich, B., Sorenson, L., Santini, F., Slater, G.J., Alfaro, M.E., 2013. Iterative ecological radiation and convergence during the evolutionary history of damselfishes (Pomacentridae). Am. Nat. 181, 94–113.

Froese, R., Pauly, D., 2012. FishBase. <http://ww.fishbase.org>.

Gavrilov, Y.O., Shcherbinina, E.A., Oberhänsli, H., 2003. Paleocene-Eocene boundary events in the northeastern Peri-Tethys. In: Wing, S.L., Gingerich, P.D., Schmitz, B., Thomas, E. (Eds.), Causes and Consequences of Globally Warm Climates in the Early Paleogene, Geol. Soc. Am. Spec. Pap. vol. 369, pp. 147–168.

Gosline, W.A., 1968. The suborders of perciform fishes. Proc. US Natl. Mus. 124, 1–77.
Graur, D., Martin, W., 2004. Reading the entrails of chickens: molecular timescales of evolution and the illusion of precision. Trends Genet. 20, 80–86.
Greenwood, P.H., Rosen, D.E., Weitzman, S.H., Myers, G.S., 1966. Phyletic studies of teleostean fishes with a provisional classification of living forms. Bull. Am. Mus. Nat. Hist. 131, 339–456.
Guiasu, C.R., Winterbottom, R., 1993. Osteological evidence for the phylogeny of recent genera of surgeonfishes (Percomorpha, Acanthuridae). Copeia 2, 300–312.
Hallam, A., 1994. An Outline of Phanerozoic Biogeography. Oxford University Press, Oxford.
Harmon, L.J., Weir, J.T., Brock, C.D., Glor, R.E., Challenger, W., 2008. GEIGER: investigating evolutionary radiations. Bioinformatics 24, 129–131.
Heled, J., Drummond, A.J., 2010. Bayesian inference of species trees from multilocus data. Mol. Biol. Evol. 27, 570–580.
Hiatt, R.W., Strasburg, D.W., 1960. Ecological relationships of the fish fauna on coral reefs of the Marshall Islands. Ecol. Monogr. 30, 65–127.
Holcroft, N.I., Wiley, E.O., 2008. Acanthuroid relationships revisited: a new nuclear gene-based analysis that incorporates tetraodontiforms representatives. Ichthyol. Res. 55, 274–283.
Hubert, N., Delrieu-Trottin, E., Irisson, J.-O., Meyer, C., Planes, S., 2010. Identifying coral reef fish larvae through DNA barcoding: a test case with the families Acanthuridae and Holocentridae. Mol. Phylogenet. Evol. 55, 1195–1203.
Johnson, G.D., Washington, B.B., 1987. Larvae of the Moorish idol, *Zanclus cornutus*, including a comparison with other larval acanthuroids. Bull. Mar. Sci. 40, 494–511.
Jones, R.S., 1968. Ecological relationships in Hawaiian and Johnson Island Acanthuridae (surgeonfishes). Micronesica 4, 309–361.
Kazancioglu, E., Near, T.J., Hanel, R., Wainwright, P.C., 2009. Influence of sexual selection and feeding functional morphology on diversification rate of parrotfishes (Scaridae). Proc. Roy. Soc. Lond. Ser. B 276, 3439–3446.
Klanten, S.O., van Herwerden, L., Choat, J.H., Blair, D., 2004. Patterns of lineage diversification in the genus *Naso* (Acanthuridae). Mol. Phylogenet. Evol. 32, 221–235.
Maddison, W.P., Maddison, D.R., 2011. Mesquite: A Modular System for Evolutionary Analysis, Version 2.75. <http://www.mesquiteproject.org>.
Mok, H.-K., 1977. Gut patterns of the Acanthuridae and Zanclidae. Jpn. J. Ichthyol. 23, 214–219.
Mulcahy, D.G., Noonan, B.P., Moss, T., Townsend, T.M., Reeder, T.W., Sites Jr., J.W., Wiens, J.J., 2012. Estimating divergence dates and evaluating dating methods using phylogenomic and mitochondrial data in squamate reptiles. Mol. Phylogenet. Evol. 65, 974–991.
Nursall, J.R., 1974. Some territorial behavioral attributes of the surgeonfish Acanthurus lineatus at Heron Island, Queensland. Copeia 1974, 950–959.
Papazzoni, C.A., Trevisani, E., 2006. Facies analysis, paleoenvironmental reconstruction, and biostratigraphy of the 'Pesciara di Bolca' (Verona, northern Italy): an Early Eocene Fossil-Lagerstätte. Palaeogeogr. Palaeoclimat. Palaeoecol. 242, 1–35.
Posada, D., 2008. JModelTest: phylogenetic model averaging. Mol. Biol. Evol. 25, 1253–1256.
R Development Core Team, 2012. R: A Language and Environment for Statistical Computing. <http://www.r-project.org>.
Randall, J.E., 1955. An analysis of the genera of surgeon fishes (Family Acanthuridae). Pac. Sci. 9, 360–367.
Randall, J.E., 1956. A revision of the surgeon fish genus *Acanthurus*. Pac. Sci. 10, 159–235.
Randall, J.E., 1960. A new species of *Acanthurus* from the Caroline Islands, with notes on the systematics of other Indo-Pacific surgeonfishes. Pac. Sci. 14, 267–279.
Randall, J.E., 1993. Acanthurus tristis, a valid Indian Ocean surgeonfish (Periciformes: Acanthuridae). J.L.B. Smith Inst. Ichthyol. 2, 1–8 (Spec. Publ.).
Randall, J.E., 2001. Surgeonfishes of Hawai'i and the World. Mutual Publishing and Bishop Museum Press, Hawai'i.
Randall, J.E., 2005. A review of mimicry in marine fishes. Zool. Stud. 44, 299–328.
Randall, J.E., Clements, K.D., 2001. Second revision of the surgeonfish genus *Ctenochaetus* (Perciformes: Acanthuridae), with descriptions of two new species. Indo-Pac. Fish. 32, 1–33.
Randall, J.E., DiBattista, J.D., Wilcox, C., 2011. *Acanthurus nigros* Günther, a valid species of surgeonfish, distinct from the Hawaiian *A. nigroris* Valenciennes. Pac. Sci. 65, 265–275.
Ronquist, F., Teslenko, M., van der Mark, P., Ayres, D.L., Darling, A., Höhna, S., et al., 2012. MrBayes 3.2: efficient Bayesian phylogenetic inference and model choice across a large model space. Syst. Biol. 61, 539–542.
Santini, F., Sorenson, L., Marcroft, T., Dornburg, A., Alfaro, M.E., 2013a. A multilocus molecular phylogeny of boxfishes (Aracanidae, Ostraciidae; Tetraodontiformes). Mol. Phylogenet. Evol. 66, 153–160.
Santini, F., Nguyen, M., Sorenson, L., Waltzek, T.B., Lynch Alfaro, J.W., Eastman, J.M., Alfaro, M.E., 2013b. Do habitat shifts drive the diversity in teleost fishes? An example from the pufferfishes (Tetraodontidae). J. Evolution Biol..
Sevilla, R.G., Diez, A., Noren, M., Mouchel, O., Jerome, M., Verrez-Bagnis, V., et al., 2007. Primers and polymerase chain reaction conditions for DNA barcoding teleost fish based on the mitochondrial cytochrome b and nuclear rhodopsin genes. Mol. Ecol. Resources 7, 730–734.
Shimodaira, H., 2002. An approximately unbiased test of phylogenetic tree selection. Syst. Biol. 51, 492–508.
Shimodaira, H., Hasegawa, M., 2001. CONSEL: for assessing the confidence of phylogenetic tree selection. Bioinformatics 17, 1246–1247.
Sieber, R., Weinfurter, E., 1967. Otolithen aus Tiefen Gosauschichten, Osterreichs. Ann. Naturhist. Mus. Wien. 71, 353–361.
Sorbini, L., Tyler, J.C., 1998a. A new genus and species of Eocene surgeonfish (Acanthuridae) from Monte Bolca, Italy, with similarities to the Recent *Zebrasoma*. St. Ric. Giac. Terz. Bolca 7, 7–19.
Sorbini, L., Tyler, J.C., 1998b. A new species of the Eocene surgeon fish genus *Pesciarichthys* from Monte Bolca, Italy, with comments on caudal peduncle armature and supraneurals in acanthurids. St. Ric. Giac. Terz. Bolca 7, 21–34.
Stamatakis, A., 2006. RAxML-VI-HPC: maximum likelihood-based phylogenetic analyses with thousands of taxa and mixed models. Bioinformatics 22, 2688–2690.
Tang, K.L., Berendzen, P.B., Wiley, E.O., Morrissey, J.F., Winterbottom, R., Johnson, G.D., 1999. The phylogenetic relationships of the suborder Acanthuroidei (Teleostei:Perciformes) based on molecular and morphological evidence. Mol. Phylogenet. Evol. 11, 415–425.
Tyler, J.C., 1970a. Osteological aspects of interrelationships of surgeon fish genera (Acanthuridae). Proc. Acad. Nat. Sci. Phila. 122, 87–124.
Tyler, J.C., 1970b. The dorsal and anal fin spine-locking apparatus of surgeon fishes (Acanthuridae). Proc. Cal. Acad. Sci. Ser. 4 (38), 391–410.
Tyler, J.C., 1997. The Miocene fish *Marosichthys*, a putative tetraodontiform, actually a perciform surgeon fish (Acanthuridae) related to the recent *Naso*. Beaufortia 47, 1–10.
Tyler, J.C., 1999. A new genus and species of surgeon fish (Acanthuridae) with a unique dorsal-fin pterygiophore arrangement from the Eocene of Monte Bolca, Italy. St. Ric. Giac. Terz. Bolca 7, 245–256.
Tyler, J.C., 2000. *Arambourgthurus*, a new genus of hypurostegic surgeon fish (Acanthuridae) from the Oligocene of Iran, with a phylogeny of the Nasinae. Geodiversitas 22, 525–537.
Tyler, J.C., 2005a. Redescription and basal phylogenetic placement of the acanthurid surgeon fish *Gazolaichthys vestenanovae* from the Eocene of Monte Bolca, Italy (Perciformes; Acanthuroidea). St. Ric. Giac. Terz. Bolca 11, 97–117.
Tyler, J.C., 2005b. A new genus for the surgeon fish *Acanthurus gaudryi* De Zigno 1887 from the Eocene of Monte Bolca, Italy, amorphologically primitive basal taxon of Acanthuridae (Acanthuroidea, Perciformes). St. Ric. Giac. Terz. Bolca 11, 149–163.
Tyler, J.C., Bannikov, A.F., 2000. A new species of the surgeon fish genus *Tauichthys* from the Eocene of Monte Bolca, Italy (Perciformes, Acanthuridae). Boll. Mus. Civ. St. Nat. Verona 24, 29–36.
Tyler, J.C., Micklich, N.R., 2011. A new genus and species of surgeon fish (Perciformes, Acanthuridae) from the Oligocene of Kanton Glarus. Switzerland. Swiss J. Palaeontol. 130, 203–216.
Tyler, J.C., Sorbini, L., 1998. On the relationships of *Eonaso*, an Antillean fossil surgeon fish (Acanthuridae). St. Ric. Giac. Terz. Bolca 7, 35–42.
Tyler, J.C., Johnson, G.D., Nakamura, I., Collette, B.B., 1989. Morphology of *Luvarus imperialis* (Luvaridae), with a phylogenetic analysis of the Acanthuroidei (Pisces). Smithson. Contrib. Zool. 485, 1–78.
Ward, R.D., Zemlak, T.S., Innes, B.H., Last, P.R., Hebert, P.D., 2005. DNA barcoding Australia's fish species. Philos. Trans. Roy. Soc. B 360, 1847–1857.
Williams, S.T., Duda, T.F.J., 2008. Did tectonic activity stimulate Oligo–Miocene speciation in the Indo-West Pacific? Evolution 62, 1618–1634.
Winterbottom, R., 1993. Myological evidence for the phylogeny of recent genera of surgeonfishes (Percomorpha, Acanthuridae), with comments on the Acanthuroidei. Copeia 1, 21–39.
Winterbottom, R., McLennan, D.A., 1993. Cladogram versatility: evolution and biogeography of acanthuroid fishes. Evolution 47, 1557–1571.
Wood, R., 1999. Reef Evolution. Oxford University Press, New York.
Yang, Z., 2006. Computational Molecular Evolution. Oxford University Press, Oxford.

APPENDIX 1

Table A1-S1: Stomach morphology coding for maximum likelihood ancestral state reconstruction. *Ctenochaetus* species and nineteen *Acanthurus* species have the thick-walled, gizzard-like stomach morphology (Jones, 1968; Randall, 1956; Randall and Clements, 2001; Hiatt and Strasburg, 1960). Thirteen of the nineteen *Acanthurus* are included in this study.

Taxon name	Morphology
Acanthurus achilles	thin-walled
Acanthurus auranticavus	gizzard-like
Acanthurus tractus	gizzard-like
Acanthurus bariene	gizzard-like
Acanthurus blochii	gizzard-like
Acanthurus chirurgus	gizzard-like
Acanthurus coeruleus	thin-walled
Acanthurus dussumieri	gizzard-like
Acanthurus guttatus	thin-walled
Acanthurus japonicus	NA
Acanthurus leucocheilus	NA
Acanthurus leucosternon	thin-walled
Acanthurus lineatus	thin-walled
Acanthurus mata	gizzard-like
Acanthurus monroviae	gizzard-like
Acanthurus nigricans	NA
Acanthurus nigricauda	gizzard-like
Acanthurus nigrofuscus	thin-walled
Acanthurus nigroris	thin-walled
Acanthurus nubilus	thin-walled
Acanthurus olivaceus	gizzard-like
Acanthurus pyroferus	gizzard-like
Acanthurus tennentii	gizzard-like
Acanthurus thompsoni	thin-walled
Acanthurus triostegus	thin-walled
Acanthurus xanthopterus	gizzard-like
Ctenochaetus binotatus	gizzard-like
Ctenochaetus flavicauda	gizzard-like
Ctenochaetus striatus	gizzard-like
Ctenochaetus strigosus	gizzard-like
Ctenochaetus tominiensis	gizzard-like
Ctenochaetus truncatus	gizzard-like

Figure A1-S1: Bayesian tree based on the analysis of the concatenated reduced dataset. The posterior probability (pp) values are provided preceding the nodes. Only pp ≥ 0.80 are shown.

Figure A1-S2: Species tree inferred using a reduced concatenated dataset and *BEAST. Only pp ≥ 0.80 are shown.

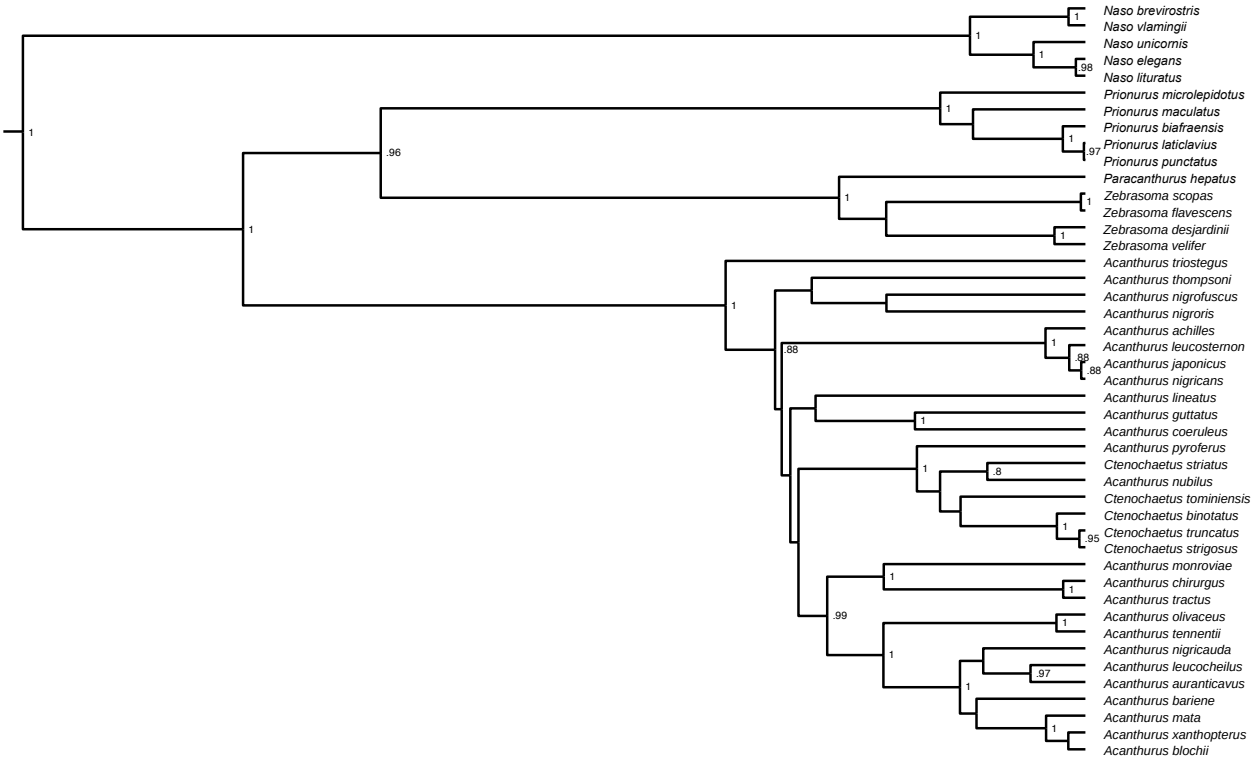

Figure A1-S3: Maximum likelihood tree topology with *Ctenochaetus* monophyly enforced. An extremely short internode separates *Acanthurus nubilus* from the *Ctenochaetus* clade.

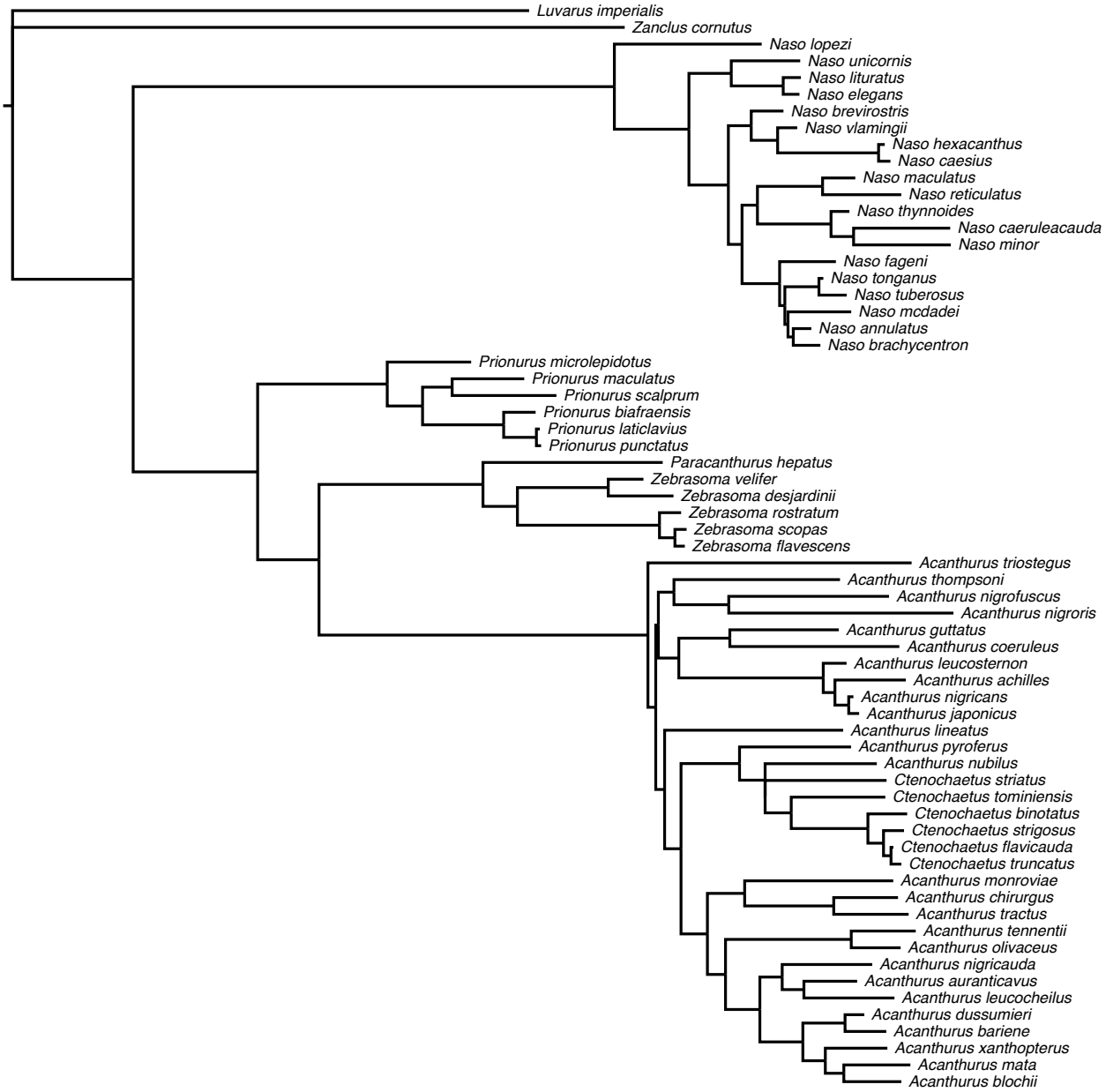

Figure A1-S4: Maximum likelihood ancestral state reconstruction of stomach morphology in *Acanthurus* and *Ctenochaetus*. At least two reversals from the gizzard-like stomach to the thin-walled stomach morphology occurred in *Acanthurus lineatus* and *A. nubilus*.

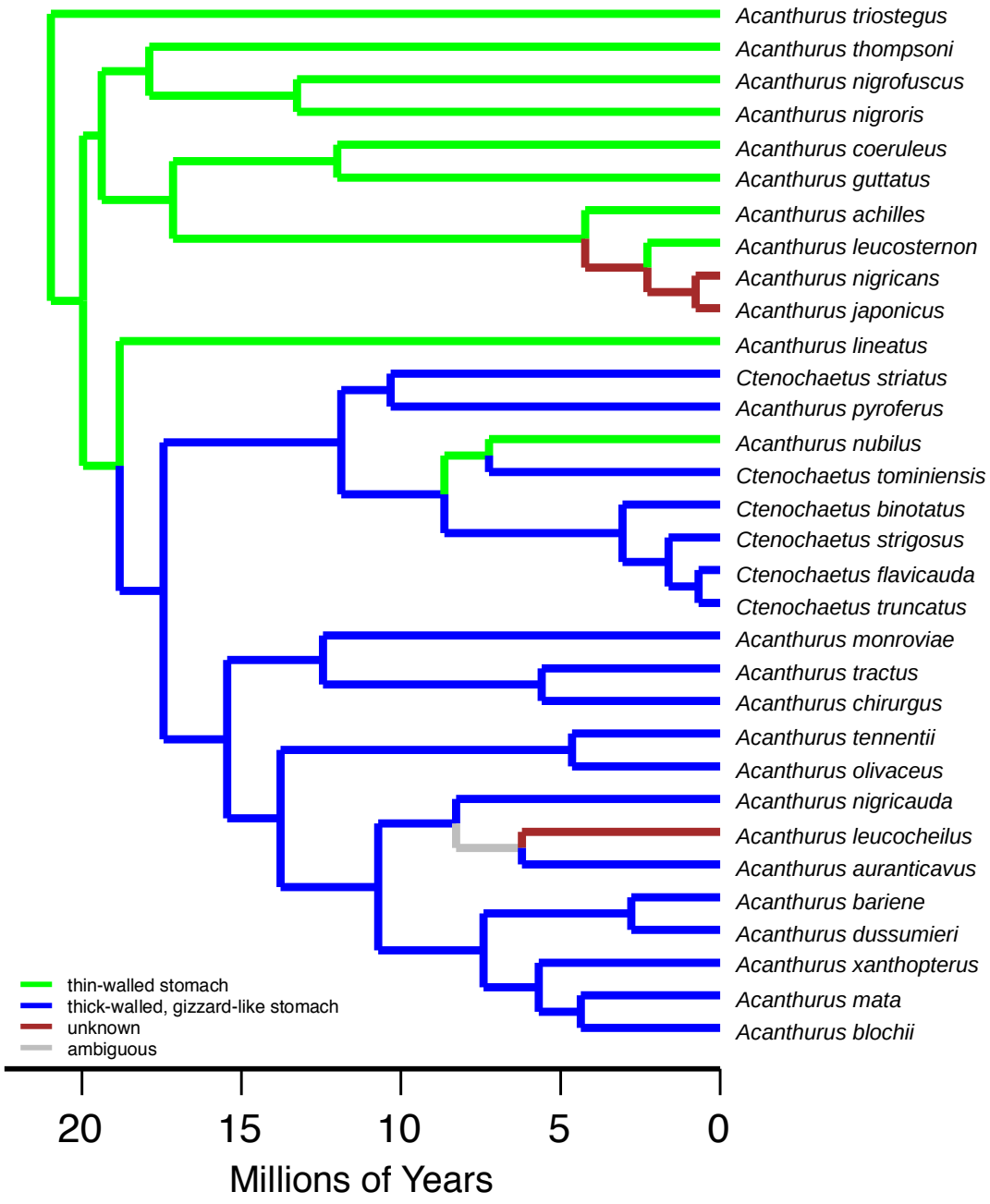

CHAPTER 2:

A phylogenomic perspective on the radiation of ray-finned fishes base upon targeted sequencing of ultraconserved elements (UCEs)

OPEN ACCESS Freely available online

PLOS ONE

A Phylogenomic Perspective on the Radiation of Ray-Finned Fishes Based upon Targeted Sequencing of Ultraconserved Elements (UCEs)

Brant C. Faircloth[•], **Laurie Sorenson, Francesco Santini, Michael E. Alfaro***[•]

Department of Ecology and Evolutionary Biology, University of California Los Angeles, Los Angeles, California, United States of America

Abstract

Ray-finned fishes constitute the dominant radiation of vertebrates with over 32,000 species. Although molecular phylogenetics has begun to disentangle major evolutionary relationships within this vast section of the Tree of Life, there is no widely available approach for efficiently collecting phylogenomic data within fishes, leaving much of the enormous potential of massively parallel sequencing technologies for resolving major radiations in ray-finned fishes unrealized. Here, we provide a genomic perspective on longstanding questions regarding the diversification of major groups of ray-finned fishes through targeted enrichment of ultraconserved nuclear DNA elements (UCEs) and their flanking sequence. Our workflow efficiently and economically generates data sets that are orders of magnitude larger than those produced by traditional approaches and is well-suited to working with museum specimens. Analysis of the UCE data set recovers a well-supported phylogeny at both shallow and deep time-scales that supports a monophyletic relationship between *Amia* and *Lepisosteus* (Holostei) and reveals elopomorphs and then osteoglossomorphs to be the earliest diverging teleost lineages. Our approach additionally reveals that sequence capture of UCE regions and their flanking sequence offers enormous potential for resolving phylogenetic relationships within ray-finned fishes.

Citation: Faircloth BC, Sorenson L, Santini F, Alfaro ME (2013) A Phylogenomic Perspective on the Radiation of Ray-Finned Fishes Based upon Targeted Sequencing of Ultraconserved Elements (UCEs). PLoS ONE 8(6): e65923. doi:10.1371/journal.pone.0065923

Editor: Corrie S. Moreau, Field Museum of Natural History, United States of America

Received February 1, 2013; **Accepted** May 1, 2013; **Published** June 18, 2013

Funding: National Science Foundation grants DEB-6861953 and DEB-6701648 (to MEA) and DEB-1242260 (to BCF) provided partial support for this work. Funds from an Amazon Web Services education grant (to BCF) supported computational portions of this work. The funders had no role in study design, data collection and analysis, decision to publish, or preparation of the manuscript.

Competing Interests: The authors have received commercial funding from Amazon Web Services for this project to support computational analyses using the Amazon Web Services platform. This does not alter the authors' adherence to all the PLOS ONE policies on sharing data and materials.

* E-mail: michaelalfaro@ucla.edu

[•] These authors contributed equally to this work.

Introduction

The ray-finned fishes (Actinopterygii) constitute the dominant radiation of vertebrates on the planet including more than 32,000 species and equaling or exceeding richness estimates for the combined total of birds, mammals, and reptiles. Despite a long history of systematic study, resolution of phylogenetic relationships within this vast radiation remains an area of active research. Studies based upon traditional morphological and single-gene, PCR-based molecular approaches have succeeded in delineating several major lineages of ray-finned fishes, but conflict over how these lineages are related to one another remains. For example, the earliest morphological studies of ray-finned fishes unite gar (*Lepisosteus*) with the bowfin (*Amia*) in the clade Holostei [1] though this clade is not recovered in some later analyses [2,3]. The early branching of teleost lineages has also been historically contentious. Systematists agree on the four earliest-diverging lineages: the osteoglossomorphs (bony-tongues; arawanas, elephant fishes, and allies), the elopomorphs (tarpons, bonefishes, and eels), the ostarioclupeomorphs (anchovies and herrings, minnows, characins, catfishes, and electric eels), and the euteleosts (salmons, pikes, lizardfishes, and perch-like fishes). However, there is disagreement over both the relationships among these groups and the basal divergences within euteleosts. Recent morphological and molecular studies have produced conflicting hypotheses of relationships among these lineages [4,5,7,14]. Morphological analyses alternatively place the osteoglossomorphs [6] or the elopomorphs [7–10] as the sister group to all other teleosts and the remaining lineages sister to the ostarioclupeomorph/euteleost clade. Some molecular analyses place elopomorphs and osteoglossomorphs as the sister group to remaining teleosts [11,12] while others recover a basal divergence between osteoglossomorphs and other teleosts [5,13].

Recently, Near *et al.* [14] used wide-spread taxonomic sampling, in conjunction with sequence collected from nine commonly used nuclear genes, to provide a more comprehensive phylogenetic hypothesis of relationships among fishes. Their results supported the monophyly of the Holostei, suggesting that the elopomorphs formed the earliest diverging teleost lineage [14], and provided a new timescale for the divergence of ray-finned fishes. Although promising, these new insights into the radiation of actinopterygians relied upon a relatively modest number of genomic markers, and the stability and timing of these relationships encoded throughout the genomes of the target groups remain largely untested. One exception to this statement includes a recent study by Zou *et al.* [15] that used transcriptome sequences to examine basal divergences within euteleosts. However, the Zou *et al.* [15] study did not include several anciently diverging lineages

(e.g. *Amia*, osteoglossomorphs) informing questions about the early evolution of major groups of ray-finned fishes.

Phylogenomics and next-generation sequencing technologies offer enormous promise for resolving relationships within actinopterygians and other major sections of the Tree of Life. However, revolutions within genomics and informatics have had a surprisingly modest effect on data collection practices within the phylogenetics community: most studies of non-model organisms continue to rely upon direct sequencing of a moderate number of loci, and workflows that do take advantage of massively parallel sequencing platforms remain bottlenecked by cross-species amplification of phylogenetically informative loci. Several alternatives to traditional phylogenetic workflows exist that help to overcome the inefficiencies of gene-based sequencing. One class of these methods is exemplified by the recent work of Zou *et al.* [15], who used a combination of *de novo* transcriptome sequencing, existing transcript data, and computational methods to identify 274 orthologous groups from which they inferred the phylogeny of the Actinopterygii. The benefits of their approach include the use of existing, transcript-related data sets (ESTs in GenBank); reasonably well-established data generation methods; and the collection of data from hundreds of loci across the genomes of the focal taxa. Limitations of this approach include reliance on sampling fresh or properly preserved tissues (generally precluding the use of thousands of existing museum samples), dependence of the approach on expression patterns of the tissue sampled, and collection of data from fewer genomic locations than alternative methodologies.

A second class of phylogenomic methods involves sequence capture of nuclear regions flanking and including ultraconserved elements (UCEs) [16]. Rather than sequencing expressed portions of the genome, the UCE-based approach involves enriching organismal DNA libraries for hundreds to thousands of UCEs and their flanking regions; sequencing these libraries using massively parallel sequencing; and assembling, aligning, and analyzing the resulting data using informatic tools. This approach has been successfully used in mammals [17], birds [16,18], and reptiles [19] to generate phylogenomic data sets that contain at least one order of magnitude more characters than those generated using PCR and to resolve historically contentious sections of the Tree of Life [17,19]. The UCE approach differs from transcript-based phylogenomic studies [15] because data collection is independent of expression pattern, researchers can prepare and enrich libraries from existing tissue collections, and UCE loci may be better conserved and more numerous across distantly related taxa [17].

Here, we apply the UCE approach to ray-finned fishes by developing a novel set of sequence capture probes targeting almost 500 UCE regions in ray-finned fishes. We use the UCE data to provide the first phylogenomic perspective based upon widespread sampling of hundreds of markers across the genome on long-standing controversies regarding relationships at the base of the ray-finned fish Tree of Life. These include whether *Lepisosteus* and *Amia* form a monophyletic group (the Holostei [1,20]) and how the major lineages of teleosts, which constitute >99% of ray-finned fishes, are related to one another [4,5,7–10,21,22]. Our results reveal that sequence capture of UCE regions can efficiently and economically generate massive data sets with strong resolving power at both deep and shallow phylogenetic scales within fishes.

Results and Discussion

Probe design, UCE enrichment, and sequencing

We located 500 UCEs shared among all actinopterygian fishes. The total number of UCEs we found in actinopterygians is smaller than in birds [16] and in mammals [17] which likely reflects both the greater phylogenetic depth spanned by fishes and the paucity of genome-enabled taxa allowing comparisons across this clade. We designed a set of 2,000 capture probes targeting each of these loci (4× tiling). Following enrichment and sequencing, we obtained an average of 2,819,047 reads per species, which we assembled into an average of 665 contigs having an average length of 457 bp (Table 1). After removing contigs that matched no UCEs and UCE loci that matched multiple contigs, we enriched an average of 332 unique contigs matching UCE loci from each species. Average sequencing depth across unique UCE loci was 498X. An average of 55% of assembled contigs (95% CI ± 0.10; min = 0.15; max = 0.88) were on-target while an average of 32% of reads were on-target (95% CI ± 0.08; min = 0.07; max = 0.62). The variance in the proportion of reads and contigs on-target suggests that input DNA quality, insert length of DNA libraries, and taxonomic distance between the taxon used to design probes and taxa from which we enriched UCEs may play a role in enrichment efficiency. However, the lowest enrichment efficiencies we observed resulted from our removal of duplicated ultraconserved elements that may result from lineage-specific duplication events (e.g., *Salvelinus fontinalis* [23] prior to computing the proportion of reads and contigs on-target.

We integrated extant genomic data from several fish species to this group of unique UCE contigs, and we constructed 491 alignments ($\bar{x}_{length}$ = 305 bp, 95% CI ± 16.0) comprising 149,366 characters. After trimming alignment edges and removing taxa with excessively trimmed data, each alignment contained an average of 21 target taxa (95% CI ± 0.4; min = 3 taxa; max = 27 taxa). We removed two loci from further consideration because we were unable to estimate site-rate substitution models for these loci due to their short lengths. The resulting incomplete data matrix contained 489 loci (149,246 characters; $\bar{x}_{length}$ = 305 bp, 95% CI ± 16.0). We used this incomplete data matrix for subsequent analyses with RAxML and MrBayes. After removing loci having missing data for *Polypterus* and *Acipenser*, we input 136 alignments (41,731 characters; $\bar{x}_{length}$ = 307 bp, 95% CI ± 27.7) to CloudForest for model selection and subsequent species tree estimation using STAR.

A phylogenomic perspective on the basal radiation of ray-finned fishes

Maximum likelihood analysis produced a single, completely resolved topology wherein all but two nodes received high (≥0.99) bootstrap proportions and Bayesian posterior probabilities (Fig. 1). This topology provides new insight into several long-standing questions concerning the evolution of ray-finned fishes. Our analysis strongly supports the monophyly of the Holostei (*Amia+Lepisoteus*). This clade is historically controversial because morphological studies alternatively support [1,20] and refute [2,3] the monophyly of this group, while recent molecular studies generally recover the relationship [14,24,25]. Additionally, our analyses do not support prior findings of an "ancient fish clade" including the Holostei+Acipenseriformes as the sister group to the teleosts [25,26]. Rather, our results strongly suggest a traditional relationship in which these lineages form successive sister groups to the teleosts.

Our phylogenomic data provide strong evidence for the placement of elopomorphs as the sister group to all other teleosts and osteoglossomorphs and ostarioclupeomorphs as successive sister lineages to the euteleosts (Fig. 1). Our maximum likelihood topology is strongly incongruent with mitogenomic studies [5,13] but consistent with both a recent analysis of multiple nuclear genes [14] and some of the earliest morphological analyses of the group

Table 1. Sequence read and assembly statistics for fish species used in this study.

Scientific name	Common name	Number of trimmed reads	Contigs assembled	Reads in contigs	UCE contigs	Reads in UCE contigs	Avg. size	Avg. coverage	Contigs on target	Reads on target
Umbra limi	central mudminnow	2,727,071	1109	740,079	409	564,715	508.8	267.4	0.37	0.21
Diaphus theta	California headlightfish	2,626,413	584	688,635	401	604,295	502.4	299.1	0.69	0.23
Antennarius striatus	striated frogfish	3,724,320	474	2,462,193	418	2,310,186	649.7	850.2	0.88	0.62
Megalops sp.	tarpon	2,771,805	786	650,577	247	231,314	485.4	191.5	0.31	0.08
Astyanax fasciatus	banded astyanax	2,731,668	543	1,444,767	355	1,211,903	526.2	657.2	0.65	0.44
Acanthurus japonicus	Japan surgeonfish	2,017,174	613	1,242,932	454	1,125,871	600.8	405.9	0.74	0.56
Amia calva	bowfin	2,619,643	562	1,608,614	366	1,368,091	578.9	646	0.65	0.52
Lampris guttatus	opah	2,472,439	486	1,350,852	418	1,237,650	568.7	520.2	0.86	0.50
Acipenser fulvescens	lake sturgeon	3,083,152	577	1,129,829	167	467,414	426.9	665.4	0.29	0.15
Anchoa compressa	deep body anchovy	2,617,717	533	783,323	287	625,862	448.6	479.2	0.54	0.24
Danio rerio	zebrafish	2,777,132	518	1,367,065	382	1,166,020	463.4	657.1	0.74	0.42
Polypterus senegalus	gray bichir	3,206,418	576	873,104	294	726,100	557.6	440	0.51	0.23
Pantodon buchholzi	freshwater butterflyfish	3,329,691	466	2,058,929	272	1,399,286	550.4	930.5	0.58	0.42
Strophidon sathete	slender giant moray	3,159,269	1007	448,390	277	246,758	510.6	172.9	0.28	0.08
Osteoglossum bicirrhosum	silver arawana	2,735,138	643	1,565,346	276	813,175	467	623.9	0.43	0.30
Salvelinus fontinalis	brook trout	2,466,696	1118	688,684	166	161,214	408.7	234.8	0.15	0.07
Taenianotus triacanthus	leaf scorpionfish	3,245,453	712	1,423,244	447	1,252,564	652.5	431.4	0.63	0.39

doi:10.1371/journal.pone.0065923.t001

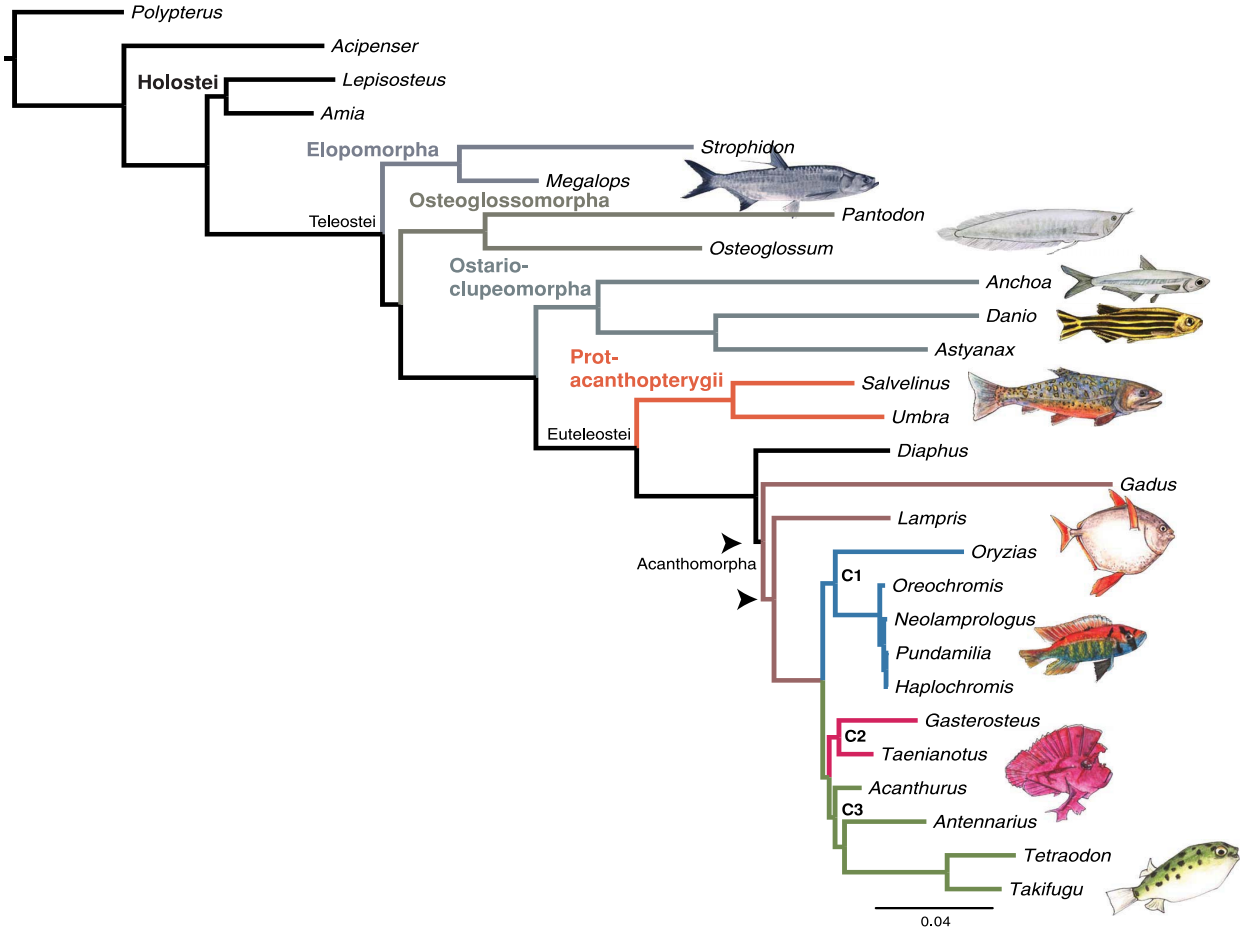

Figure 1. Maximum likelihood phylogram of ray-finned fish relationships based upon UCE sequences. All nodes except for two (indicated by arrows) supported by bootstrap proportions and Bayesian posterior probabilities >0.99. Our analysis supports a monophyletic Holostei and reveals the elopomorphs to be the earliest diverging lineage of teleosts. C1, C2, and C3 indicate clades within acanthomorphs consistent with other recent molecular studies (see Discussion).
doi:10.1371/journal.pone.0065923.g001

[7–10]. Within euteleosts, our results are congruent with recent molecular studies [4,14,15] in placing esociforms as the sister to salmoniforms rather than any neoteleost lineages.

Within acanthomorphs, the largest clade of euteleosts, UCEs recover several intriguing clades that agree with results from recent molecular phylogenetic studies. These include the African cichlids+medaka (Clade C1, Fig. 1), corresponding to an expanded clade of atherinomorphs suggested by recent studies [15,27,28]; a clade of gasterosteiforms (stickleback) and scorpaeniforms (*Taenionotus*) that is congruent with recent molecular and morphological studies [15,29,30]; and a clade including surgeonfish, frogfishes, and pufferfishes (acanthuroids, lophiiforms, and tetraodontiforms) corresponding to acanthomorph clade "N" of Dettai and Lecointre [14,31]. Based upon previous time-calibrated studies [14,32] and preliminary divergence time analyses of the UCE data set [33], our results suggest that UCEs provide sufficient phylogenetic signal to resolve splits within haplochromine cichlids that may be less than 5 Ma old [32] as well as the most basal actinopterygian divergences that exceed 400 Ma.

The STAR topology was less resolved than topologies based upon analyses of the concatenated data set (Fig. S1) but recovered largely congruent relationships including a monophyletic Holostei as the sister to other actinopterygians; monophyly of elopomorphs, osteoglossomorphs, ostarioclupeomorphs, and euteleosts; and a successive sister group relationship between ostarioclupeomorphs, *Salvelinus*+*Umbra*, and all remaining euteleosts. The species tree switched the position of the Gadiformes, represented by cod (*Gadus*) and Myctophiformes, represented by *Diaphus*. This position is not congruent with results from Near *et al.* [14] but has been suggested by previous molecular studies [4,24,34]. Relationships within cichlids are not fully resolved, but we recovered strong support for a clade consisting of *Neolamprologus*, *Haplochromis*, and *Oreochromis* that is not congruent with the concatenated topology (Fig. 1) or with accepted cichlid relationships [35].

Although UCE data would seem to provide a good fit to gene-tree species tree approaches because of the large number of loci that the approach generates, there are several challenges that genomic scale empirical data sets pose to accurate species tree reconstruction. These include pervasive incomplete taxonomic

sampling across UCE loci and insufficient resolution of individual gene trees due to the recovery of relatively short contigs. Further refinement of the protocols developed here, including modification of the in vitro transposition reaction to yield longer insert lengths; replacement of transposase-mediated library preparation with physical shearing by sonication and T/A ligation; size-selection of enriched, amplified libraries; deeper sequencing of longer libraries; paired-end reads; and longer sequence read lengths should improve gene-tree species tree reconstruction by increasing the amount of flanking sequence recovered across individual UCEs. Additional optimization of probe-designs, tiling densities, hybridization conditions, and hybridization reactions should increase the proportion of UCE loci recovered across individual taxa.

Conclusions

Sequence capture of regions anchored by UCEs offers a powerful and efficient means of generating massive genomic data sets capable of resolving phylogenetic relationships at both deep and shallow scales in non-model organisms. Our UCE-based approach offers several advantages over previous studies that should contribute to the reliability of our topology. These benefits include efficient sampling of sequence data across individual genomes and among divergent taxa, collection of data from an order of magnitude more loci than studies based upon traditionally used genetic markers and almost twice as many loci as transcriptome-based genomic studies [15], validity of the UCE probe set across bony fishes spanning 400 Ma of evolutionary history, and utility of the UCE enrichment approach with tissues collected from museum specimens. Additionally, these data illustrate that biologists can use UCE-based genetic markers to reconstruct the phylogeny of taxa other than amniotes, supporting the observation that UCE-based markers are a universal source of phylogenetically informative characters [16,17].

Availability

Contigs assembled from raw read data are available from NCBI Genbank (Accession #s: JQ717376–JQ723011). Probe data, assembled contigs, alignments, and data sets we used for analysis are available from Dryad (doi: 10.5061/dryad.j015n). Software used for the analysis of raw sequence data are available under an open-source, BSD license from https://github.com/faircloth-lab/phyluce, https://github.com/faircloth-lab/illumiprocessor, and https://github.com/ngcrawford/cloudforest. Protocols for library preparation and UCE enrichment are available under Creative Commons license from http://ultraconserved.org.

Materials and Methods

Ethics statement

All tissues used in this study were either received as loans from the Field Museum, Virginia Institute of Marine Science, or Scripps Institution of Oceanography or collected under Institutional Animal Care and Use Committee (IACUC) protocols #17611 (University of California, Los Angeles), #12790 (University of California, Davis), or #16956 (University of California, Davis).

Identification of UCE regions

To identify ultraconserved elements (UCEs) in fishes, we used genome-to-genome alignments of stickleback (*Gasterosteus aculeatus*) to medaka (*Oryzias latipes*) to locate nuclear DNA regions of 100% conservation greater than 80 bp in length. To enable efficient capture-probe design, we buffered these regions to 180 bp (where needed) by including equal amounts of medaka sequence 5′ and 3′ to each UCE. We aligned or re-aligned these buffered regions to the genome-enabled fishes (zebrafish, *Danio rerio*, stickleback, medaka, and two species of puffers, *Tetraodon nigroviridis* and *Takifugu rubripes*) using LASTZ [36], keeping only non-duplicate matches of $\geq$120 bp and $\geq$80% sequence identity across all species in the set. Based on the intersection of UCE loci across all fishes that were greater than 10 Kbp apart, we designed a pilot set of 120 bp sequence capture probes for each of the UCEs present among all members of the set by tiling probes at 4× density. We had these probes commercially synthesized into a custom SureSelect target enrichment kit (Agilent, Inc.). We used a higher than normal [37] tiling density to help ameliorate potential sequence differences among species introduced by buffering shorter UCEs to 180 bp.

Library preparation, UCE enrichment, sequencing, and assembly

Tissues used in this study were received as loans with permission from the Field Museum, Virginia Institute of Marine Science, or Scripps Institution of Oceanography or collected under IACUC protocols #17611, #12790, and #16956.

We extracted DNA from tissues using phenol-chloroform techniques or DNEasy kits (Qiagen Inc.), treated extracts with RNase, and followed RNase treatment with column-based cleanup (Qiagen Inc.). We prepared DNA libraries from 18 fish species, including representatives of five acanthomorph orders and two families of perciforms (Table 1), by slightly modifying the Nextera (Epicentre Biotechnologies) library preparation protocol for solution-based target enrichment [16] and increasing the number of PCR cycles following the tagmentation reaction to 20. The Nextera library preparation protocol uses in vitro transposition followed by PCR to shear DNA and attach indexed sequencing adapters [38] rather than relying on physical shearing followed by standard T/A ligation. Transposase-mediated library preparation using the Epicentre Nextera kit produces libraries with insert sizes averaging 100 bp (95% CI: 45 bp) [38]. Following library preparation, we substituted a blocking mix of 500 μM (each) oligos composed of the forward and reverse complements of the Nextera adapters for the Agilent-provided adapter blocking mix (Block #3). We incubated species-specific libraries (500 ng) with synthetic RNA probes from the SureSelect kit for 24 h at 65°C. We followed the standard SureSelect protocol to enrich DNA libraries following hybridization; we eluted clean, enriched DNA in 30 μL of nuclease free water; and we used 15 μL of enriched template in a 50 μL PCR reaction of 20 cycles combining forward, reverse, and indexing primers with Nextera polymerase to add a custom set of 24 indexed adapters [39]. We cleaned PCR reactions using Agencourt AMPure XP. We quantified enriched, indexed libraries using qPCR (Kapa Biosystems), and we prepared two library pools containing 10 libraries at equimolar ratios prior to sequencing.

We sequenced each pool of enriched DNA using two lanes of a single-end 100 bp Illumina Genome Analyser (GAIIx) run. After sequencing, we trimmed adapter contamination, low quality bases, and sequences containing ambiguous base calls using a pipeline we constructed (https://github.com/faircloth-lab/illumiprocessor). We assembled reads, on a species-by-species basis, into contigs using Velvet [40] and VelvetOptimiser (https://github.com/Victorian-Bioinformatics-Consortium/VelvetOptimiser). Following assembly, we used a software package (https://github.com/faircloth-lab/phyluce) containing a custom Python program (match_contigs_to_probes.py) integrating LASTZ [36] to align species-specific contigs to the set of probes/UCEs we used for enrichment while removing reciprocal and non-reciprocal duplicate hits from the data set. During matching, this program creates

a relational database of matches to UCE loci by taxon. This program also has the ability to include UCE loci drawn from existing genome sequences, for the primary purpose of including available data from genome-enabled taxa as outgroups or to extend taxonomic sampling. We used this feature to include UCE loci we identified in the genome sequences of *Gasterosteus aculeatus*, *Haplochromis burtoni*, *Neolamprologus brichardi*, *Oreochromis niloticus*, *Oryzias latipes*, *Pundamilia nyererei*, *Takifugu rubripes*, *Tetraodon nigroviridis*, *Gadus morhua*, and *Lepisosteus oculatus*. After generating the relational database of matches to enriched sequences and genome-enabled taxa, we used additional components of PHYLUCE (get_match_counts.py) to query the database and generate fasta files for the UCE loci we identified across all taxa. Then, we used a custom Python program (seqcap_align_2.py) to align contigs with MAFFT [41] and trim contigs representing UCEs, in parallel, across the selected taxa prior to phylogenetic analysis [16].

Phylogenetic Analyses

The large number of UCE loci we collected create a vast potential space for partitioning data that makes a traditional evaluation of alternative partitioning strategies computationally challenging. As a result, we modeled nucleotide substitutions across the concatenated data set using two approaches. For Bayesian analysis, we used a custom script (run_mraic.py) wrapping a modified MrAIC 1.4.4 [42] to find the best-fitting, finite-sites substitution model for each UCE locus, we grouped loci having similar substitution models (selected by AICc) into the same partition, and we assigned the partition specific substitution model to all loci concatenated within each partition. For maximum likelihood analyses, we maintained the partitions identified in the Bayesian analysis and we modeled each partition using the GTR+CAT approximation. We performed Bayesian analysis of the concatenated data set using MrBayes 3.1 [43] and two independent runs (4 chains each) of 5,000,000 iterations each, sampling trees every 500 iterations, to yield a total of 10,000 trees. We sampled the last 5,000 trees after checking results for convergence by visualizing the log of posterior probability within and between the independent runs for each analysis, ensuring the average standard deviation of split frequencies was <0.001, and ensuring the potential scale reduction factor for estimated parameters was approximately 1.0. We performed maximum likelihood analysis of the concatenated data in RAxML [44] using the rapid bootstrapping algorithm and 500 bootstrap replicates.

Gene tree-species tree methods enjoy some advantages over the analysis of concatenated data sets under certain conditions [45–47] but may also be sensitive to missing data [48] and to the resolution of individual gene trees [49]. To minimize the number of unresolved gene tree topologies and maximize the number of topologies that overlapped in sampling the base of the actinopterygian tree, we selected a subset of the UCE contigs containing complete data for *Polypterus* and *Acipenser* and loci ≥ 50 bp, and we used this subset to estimate a species tree with CloudForest (https://github.com/ngcrawford/CloudForest), a parallel implementation of a workflow combining substitution model selection (similar to MrAIC 1.4.4 [42]) and gene tree estimation using PhyML [50]. We estimated the species tree by summarizing gene trees using STAR [51–53]. To assess confidence in the resulting species tree, we used CloudForest to generate 1000, multi-locus, non-parametric bootstrap replicates by resampling nucleotides within loci as well as resampling loci within the data set [54], we summarized bootstrap replicates using STAR, and we reconciled bootstrap replicates with the species tree using RAxML.

Supporting Information

Figure S1 Species tree based upon STAR analysis. Topology based upon analysis of all loci ≥ 50 base pairs that contained both *Polypterus* and *Acipenser* ($N = 136$). Node values indicate bootstrap proportion based upon 1000 replicates. We collapsed nodes having $\leq 50\%$ bootstrap support.
(EPS)

Acknowledgments

We thank Bryan Carstens, Scott Herke, and the LSU Genomics Facility for help with Illumina sequencing. We thank Travis Glenn for helpful discussion of several laboratory methods, and we thank John Huelsenbeck and Brian Moore for helpful discussions relative to phylogenetic analyses. Guillermo Orti and an anonymous referee provided helpful comments on the manuscript text. Amisha Gadani provided illustrations. We thank Mark Westneat, Patrick McGrath, Eric Hilton, H.J. Walker, Phil Hastings, Peter Wainwright, Rita Metha, and Anindo Choudhury for help with tissues and specimens.

Author Contributions

Conceived and designed the experiments: MEA BCF FS. Performed the experiments: BCF LS. Analyzed the data: BCF MEA. Contributed reagents/materials/analysis tools: BCF LS FS MEA. Wrote the paper: BCF MEA.

References

1. Nelson G (1969) Gill arches and the phylogeny of fishes, with notes on the classification of verte-brates. Bull Am Mus Nat Hist 141: 465–552.
2. Olsen P (1984) The skull and pectoral girdle of the parasemionotid fish *Watsonulus eugnathoides* from the Early Triassic Sakamena Group of Madagascar, with comments on the relationships of the holostean fishes. J Vert Paleontol 4: 481–499.
3. Patterson C (1973) Interrelationships of holosteans. In: Greenwood P, Miles R, Patterson C, editors, Interrelationships of fishes, London: Academic Press. pp. 207–226.
4. Li C, Lu G, Orti G (2008) Optimal data partitioning and a test case for ray-finned fishes (Actinopterygii) based on ten nuclear loci. Syst Biol 57: 519.
5. Inoue JG, Miya M, Tsukamoto K, Nishida M (2003) Basal actinopterygian relationships: A mi-togenomic perspective on the phylogeny of the ''ancient fish''. Mol Phylogenet Evol 26: 110–120.
6. Patterson C, Rosen D (1977) Review of ichthyodectiform and other Mesozoic teleost fishes and the theory and practice of classifying fossils. Bull Am Mus Nat Hist 158: 83–172.
7. Arratia G (2001) The sister-group of Teleostei: Consensus and disagreements. J Vert Paleontol 21: 767–773.
8. Arratia G (2010) The clupeocephala re-visited: Analysis of characters and homologies. Rev Biol Mar Oceanog 45: 635–657.
9. Arratia G (2004) Mesozoic halecostomes and the early radiation of teleosts. In: Arratia G, Tintori A, editors, Mesozoic fishes 3, Munich, Germany: Verlag Dr. Friedrich Pfeil. pp. 279–315.
10. Cloutier R, Arratia G (2004) Early diversification of actinopterygians. In: Arratia G, Wilson MVH, Cloutier R, editors, Recent advances in the Origin and Early Radiation of Vertebrates, Munich, Germany: Verlag Dr. Friedrich Pfeil. pp. 217–270.
11. Le H, Lecointre G, Perasso R (1993) A 28S rRNA-based phylogeny of the gnathostomes: First steps in the analysis of conict and congruence with morphologically based cladograms. Mol Phylogenet Evol 2: 31–51.
12. Broughton RI (2010) Phylogeny of teleosts based on motochondrial genome sequences. In: Nelson J, Schultz H, Wilson M, editors, Origin and Phylogenetic Interrelationships of Teleosts, Munchen: Verlag. pp. 61–76.
13. Inoue JG, Miya M, Venkatesh B, Nishida M (2005) The mitochondrial genome of Indonesian coela-canth *Latimeria menadoensis (Sarcopterygii: Coelacanthiformes)* and divergence time estimation between the two coelacanths. Gene 349: 227–235.
14. Near TJ, Eytan RI, Dornburg A, Kuhn KL, Moore JA, et al. (2012) Resolution of ray-finned fish phylogeny and timing of diversification. Proc Natl Acad Sci USA 109: 13698–13703.
15. Zou M, Guo B, Tao W, Arratia G, He S (2012) Integrating multi-origin expression data improves the resolution of deep phylogeny of ray-finned fish (Actinopterygii). Sci Rep 2.

16. Faircloth B, McCormack J, Crawford N, Harvey M, Brumfield R, et al. (2012) Ultraconserved elements anchor thousands of genetic markers for target enrichment spanning multiple evolutionary timescales. Syst Biol 61: 717–726.
17. McCormack J, Faircloth B, Crawford N, Gowaty P, Brumfield R, et al. (2012) DNA anking ultra-conserved elements provides novel phylogenetic markers and resolves placental mammal phylogeny when combined with species tree analysis. Genome Res 22: 746–754.
18. McCormack J, Harvey M, Faircloth B, Crawford N, Glenn T, et al. (2013) A phylogeny of birds based on over 1,500 loci collected by target enrichment and high-throughput sequencing. PLoS ONE 8: e54848.
19. Crawford NG, Faircloth BC, McCormack JE, Brumfield RT, Winker K, et al. (2012) More than 1000 ultraconserved elements provide evidence that turtles are the sister group of archosaurs. Biol Lett 8: 783–786.
20. Grande L (2010) An empirical synthetic pattern study of gars (Lepisosteiformes) and closely related species, based mostly on skeletal anatomy: the resurrection of Holostei. Supplementary issue of Copeia 10: 1–863.
21. De Pinna M (1996) Teleostean monophyly. In: Stiassny ML, Parenti LR, Johnson GD, editors, Interrelationships of Fishes, San Diego: Academic Press. pp. 147–162.
22. Zaragueta-Bagils R, Lavoue S, Tillier A, Bonillo C, Lecointre G (2002) Assessment of otocephalan and protacanthopterygian concepts in the light of multiple molecular phylogenies. C R Biol 325: 1191–1207.
23. Davidson WS, Koop BF, Jones SJM, Iturra P, Vidal R, et al. (2010) Sequencing the genome of the Atlantic salmon (Salmo salar). Genome Biology 11: 403.
24. Li C, Lu G, Orti G (2008) Optimal data partitioning and a test case for ray-finned fishes (Actinopterygii) based on ten nuclear loci. Syst Biol 57: 519–539.
25. Inoue JG, Miya M, Tsukamoto K, Nishida M (2003) Basal actinopterygian relationships: A mi-togenomic perspective on the phylogeny of the ''ancient fish''. Mol Phylogenet Evol 26: 110–120.
26. Venkatesh B, Erdmann M, Brenner S (2001) Molecular synapomorphies resolve evolutionary rela-tionships of extant jawed vertebrates. Proc Natl Acad Sci USA 98: 11382–11387.
27. Mabuchi K, Miya M, Azuma Y, Nishida M (2007) Independent evolution of the specialized pha-ryngeal jaw apparatus in cichlid and labrid fishes. BMC Evol Biol 7: 10.
28. Wainwright P, Smith W, Price S (2012) The evolution of pharyngognathy: A phylogenetic and functional appraisal of the pharyngeal jaw key innovation in labroid fishes and beyond. Syst Biol 61: 1001–1027.
29. Smith W, Wheeler W (2006) Venom evolution widespread in fishes: A phylogenetic road map for the bioprospecting of piscine venoms. J Hered 97: 206–217.
30. Smith W, Craig M (2007) Casting the percomorph net widely: The importance of broad taxonomic sampling in the search for the placement of serranid and percid fishes. Copeia 1: 35–55.
31. Dettai A, Lecointre G (2005) Further support for the clades obtained by multiple molecular phy-logenies in the acanthomorph bush. C R Biol 328: 674–689.
32. Santini F, Harmon L, Carnevale G, Alfaro M (2009) Did genome duplication drive the origin of teleosts? A comparative study of diversification in ray-finned fishes. BMC Evol Biol 9: 194.
33. Alfaro M, Faircloth B, Sorenson L, Santini F (2012) A phylogenomic perspective on the radiation of ray-finned fishes based upon targeted sequencing of ultraconserved elements (UCEs). arXiv preprint: 1210.0120.
34. Meynard CN, Mouillot D, Mouquet N, Douzery EJP (2012) A phylogenetic perspective on the evolution of mediterranean teleost fishes. PLoS ONE 7: e36443.
35. Genner MJ, Seehausen O, Lunt DH, Joyce DA, Shaw PW, et al. (2007) Age of cichlids: new dates for ancient lake fish radiations. Molecular Biology and Evolution 24: 1269–1282.
36. Harris R (2007) Improved pairwise alignment of genomic DNA. Ph.D. thesis, The Pennsylvania State University.
37. Tewhey R, Nakano M, Wang X, Pabon-Pena C, Novak B, et al. (2009) Enrichment of sequencing targets from the human genome by solution hybridization. Genome Biol 10: R116.
38. Adey A, Morrison HG, Asan, Xun X, Kitzman JO, et al. (2010) Rapid, low-input, low-bias con-struction of shotgun fragment libraries by high-density in vitro transposition. Genome Biology 11: R119.
39. Faircloth BC, Glenn TC (2012) Not all sequence tags are created equal: Designing and validating sequence identification tags robust to indels. PLoS ONE 7: e42543.
40. Zerbino D, Birney E (2008) Velvet: Algorithms for de novo short read assembly using de Bruijn graphs. Genome Res 18: 821–829.
41. Katoh K, Kuma K, Toh H, Miyata T (2005) MAFFT version 5: Improvement in accuracy of multiple sequence alignment. Nucleic Acids Res 33: 511–518.
42. Nylander J (2004) MrAIC.pl. Evolutionary Biology Centre, Uppsala University: Program dis-tributed by the author.
43. Ronquist F, Huelsenbeck JP (2003) MrBayes 3: Bayesian phylogenetic inference under mixed models. Bioinformatics 19: 1572–1574.
44. Stamatakis A, Ott M (2008) Effcient computation of the phylogenetic likelihood function on multi-gene alignments and multi-core architectures. Philos Trans R Soc Lond, B, Biol Sci 363: 3977–3984.
45. Kubatko L, Degnan J (2007) Inconsistency of phylogenetic estimates from concatenated data under coalescence. Syst Biol 56: 17–24.
46. Edwards S, Liu L, Pearl D (2007) High-resolution species trees without concatenation. Proc Natl Acad Sci USA 104: 5936–5941.
47. Edwards S (2009) Is a new and general theory of molecular systematics emerging? Evolution 63: 1–19.
48. Bayzid MS, Warnow T (2012) Estimating optimal species trees from incomplete gene trees under deep coalescence. J Comput Biol 19: 591–605.
49. Castillo-Ramrez S, Liu L, Pearl D, Edwards S, Knowles L, et al. (2010) Bayesian estimation of species trees: A practical guide to optimal sampling and analysis. In: Estimating species trees: Practical and theoretical aspects, Hoboken: Wiley-Blackwell. pp. 15–33.
50. Guindon S, Dufayard JF, Lefort V, Anisimova M, Hordijk W, et al. (2010) New algorithms and methods to estimate maximum-likelihood phylogenies: Assessing the performance of PhyML 3.0. Syst Biol 59: 307–321.
51. Liu L, Yu L, Kubatko L, Pearl DK, Edwards SV (2009) Coalescent methods for estimating phylo-genetic trees. Mol Phylogenet Evol 53: 320–328.
52. Liu L, Yu L, Pearl DK, Edwards SV (2009) Estimating species phylogenies using coalescence times among sequences. Syst Biol 58: 468–477.
53. Liu L, Yu L (2010) Phybase: an R package for species tree analysis. Bioinformatics 26: 962–963.
54. Seo TK (2008) Calculating bootstrap probabilities of phylogeny using multilocus sequence data. Mol Biol and Evol 25: 960–971.

APPENDIX 2

Figure A2-S1: Species tree based upon STAR analysis. Topology based upon analysis of all loci ≥ 50 base pairs that contained both *Polypterus* and *Acipenser* (N = 136). Node values indicated bootstrap proportion based upon 1000 replicates. We collapsed nodes having ≤ 50% bootstrap support.

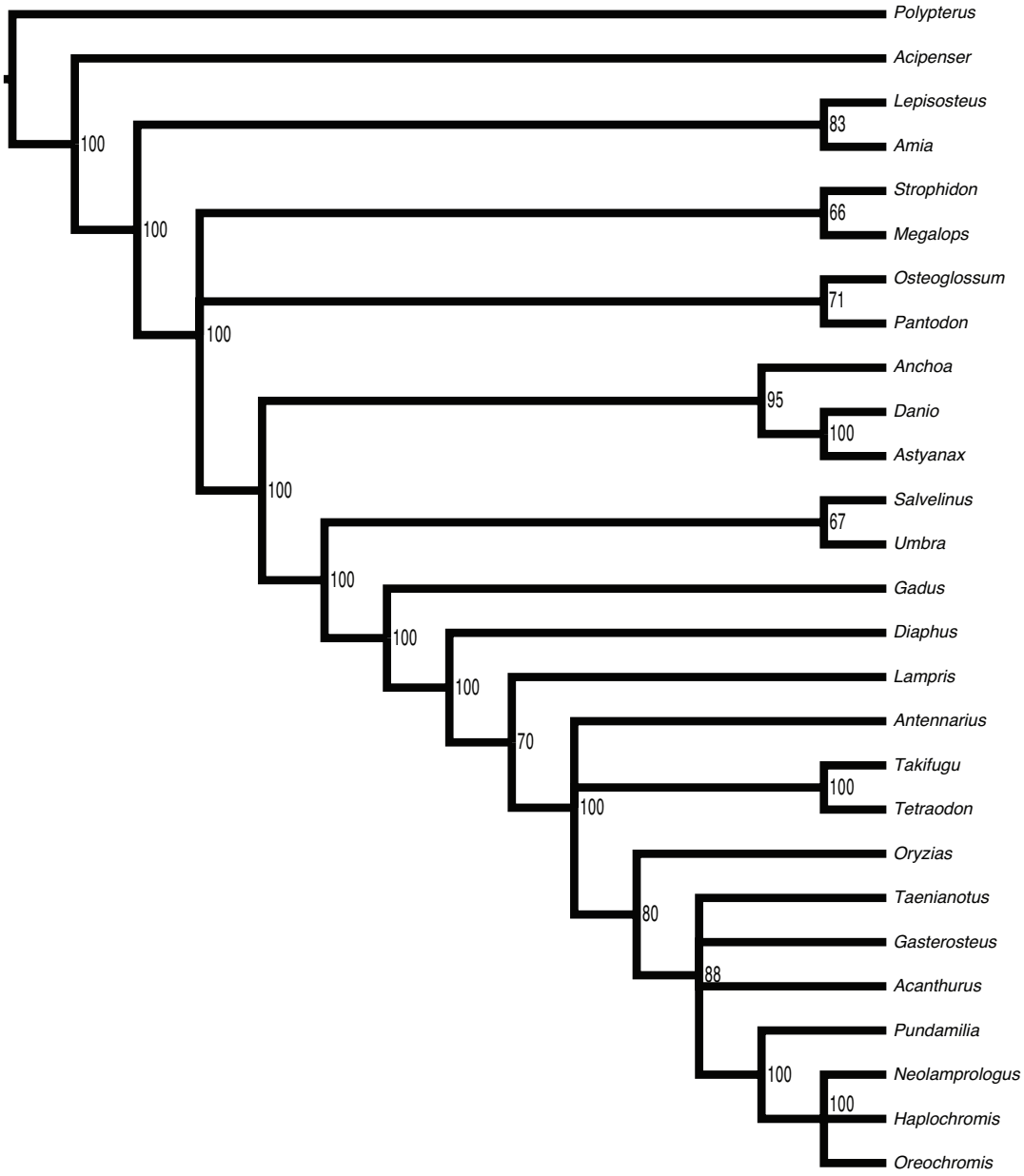

CHAPTER 3:

The influence of shallow and deepwater habitats on the radiation of modern sharks

INTRODUCTION

In the marine realm, biodiversity dynamics at the macroevolutionary scale are strongly influenced by the environment. Differential patterns of evolutionary rates relating to habitat have been documented by paleobiologists based on evidence from the fossil record, particularly for invertebrates (e.g. Jablonski 2005; Kiessling & Aberhan 2007; Kiessling *et al.* 2010). Higher taxonomic groups occupying shallow, carbonate substrate, or onshore environments have been shown to enjoy elevated origination rates compared to groups occupying deepwater, siliciclastic, or offshore habitats (e.g. Kiessling & Aberhan 2007; Kiessling *et al.* 2010). Among shelf environments, lineages preferring coral reefs tend to have higher speciation rates than non-reef-associated groups (Kiessling & Aberhan 2007; Kiessling *et al.* 2010). Mechanisms proposed to explain differences in evolutionary rates among habitats include: higher temperature and solar radiation that may increase mutation rates (e.g. Davies *et al.* 2004; Allen *et al.* 2006), environmental heterogeneity among inshore habitats that can increase speciation by generating and sustaining genetic variation (e.g. Hoffmann & Hercus 2000; Nevo 2001; Tainaka *et al.* 2006), competition and predation pressure in high energy environments that can elevate rates of evolution (e.g. Leighton 1999; Aberhan *et al.* 2006), and habitat complexity in coral reefs that provides ecological opportunity for complex species interactions and niche partitioning (e.g. Gratwicke & Speight 2005; Lingo & Szedlmayer 2006). Similar patterns of habitat-mediated diversification have been described in comparative phylogenetic studies of extant marine fishes. Several studies have linked coral reef colonization with accelerated cladogenesis and phenotypic evolution (e.g. Alfaro *et al.* 2007; Bellwood *et al.* 2010; Cowman & Bellwood 2011; Price *et al.* 2011; Frédérich *et al.* 2013; Santini *et al.* 2013). However, studies of marine habitat-mediated

diversification have primarily focused on reef environments, and previous work has relied upon limited sampling of taxonomic and ecological diversity. Nearly all of the study species are relatively small-bodied omnivores, herbivores, molluscivores, and zooplanktivores (Bellwood & Wainwright 2002). In particular, we currently have a limited understanding of how cladogenesis rates differ among major habitat types (e.g. shelf versus deepwater), especially for lineages of specialized predators.

Extant sharks and rays represent a relatively recent radiation of an ancient vertebrate lineage, though most details of their macroevolutionary history are poorly understood. The first recorded neoselachian appeared in the Early Triassic (Cuny 1998) and the fossil record reveals three periods of exceptional diversification during the Mesozoic: the Upper Triassic (Cuny & Benton 1999), throughout the Jurassic, and during the Cretaceous (Underwood 2006; Kriwet *et al.* 2009; Guinot *et al.* 2012). Ecological expansion during post-extinction recoveries following the Permian-Triassic and Triassic-Jurassic extinction events may have played an important role in fueling neoselachian diversification (e.g. Kriwet *et al.* 2009). However, the extent to which modern shark fauna biodiversity reflects any of these Mesozoic events is currently not known.

Modern sharks are found in nearly all marine habitats, but are conspicuous members of communities where they play a vital role in maintaining ecosystem health as apex predators (e.g. Bascompte *et al.* 2005; Friedlander & DeMartini 2002). Sharks comprise over 500 described species in eight orders: Carcharhiniformes, Squaliformes, Squatiniformes, Pristiophoriformes, Orectolobiformes, Heterodontiformes, Lamniformes, and the Hexanchiformes. Diversity patterns across these shark lineages are highly uneven. Over 75% of extant shark diversity is found within two lineages, the Carcharhiniformes and the Squaliformes. The Squatiniformes, Lamniformes,

and Orectolobiformes are moderately species rich in comparison, with ~4%, ~3% and ~12% of the species diversity, respectively. The Heterodontiformes and the Pristiophoriformes are species poor, containing ~3% of the total shark species diversity combined.

The causal factors of this uneven species distribution are not known; however, diversity patterns may, in part, be correlated with habitats. Carcharhiniforms comprise many important shallow-water species including the Carcharhinidae, which includes the largest radiation of reef-associated shark species (Froese & Pauly 2012). In contrast, the Squaliformes represent a deepwater radiation and Lamniformes represent a successful radiation in pelagic ecosystems. Although habitat has been suggested to underlie radiations of extinct (e.g. Cuny & Benton 1999; Underwood 2006) and extant sharks (Straube *et al.* 2010), there have been few quantitative shark macroevolutionary studies and no rigorous tests to determine the relationship between habitat and cladogenesis rates. This is due in part to the lack of an adequate phylogenetic framework for comparative analysis of habitat and diversity.

Here we present the most comprehensive time-calibrated phylogeny to date that includes 268 shark species, representing all orders and 94% of shark families. Our analysis provides a general timescale for shark evolution and we examine the tempo and mode of evolution using our timetree. We test the hypothesis that shark lineages occupying shelf habitats have higher speciation rates compared to those occupying deepwater and pelagic habitats, following a common pattern of habitat-dependent speciation rates described in other groups. We also test the hypothesis that reef-associated carcharhinid lineages have elevated speciation rates compared to non-reef lineages. Finally, we use our timetree to determine whether the origins of major extant lineages coincide with the timing of recovery periods following mass extinction events as

suggested by the fossil record. We find that diversification in both shallow and deepwater habitats has been important to producing shark biodiversity, and that transitions onto coral reefs have been especially integral to generating carcharhinid biodiversity.

MATERIALS AND METHODS

Phylogeny and divergence time inference

We obtained sequence data for one nuclear (Rag1) and four mitochondrial genes (cox1, *Cytb, 16S,* and *NADH2)* from GenBank through the Phylota browser 1.4 (Sanderson *et al.* 2008) for 268 species, representing all eight orders and 32 shark families (Table A3-S1). Sequences for *Amblyraja radiata, Manta birostris, Chimaera monstrosa,* and *Hydrolagus colliei* were collected to serve as outgroups, following the example of Vélez-Zuazo & Agnarsson (2011). Sequences were aligned using MUSCLE (Edgar 2004), and alignments were adjusted by eye in MEGA v.5 (Tamura *et al.* 2011). The five loci were trimmed at the 5' and 3' ends to minimize missing data, and highly variable *16S* gene regions were removed. The final gene alignments contained 651 bp for *cox1,* 999 bp for *Cytb,* 1047 bp for *NADH2,* 1259 bp for *16S,* and 1476 bp for *Rag1,* for a total of 5432 bp.

The nucleotide substitution models for each gene were selected using the Akaike Information Criterion (AIC) in jModelTest (Posada 2008). The GTR + I + γ was the best fitting model for all genes except *Cytb,* where the best fitting model was TPM1uf + I + γ. However, there was no significant difference in AIC scores between this model and the GTR + I + γ, so the generalized time-reversible model was also selected for the *Cytb* locus. We did not include the proportion of invariant sites because this parameter is already accounted for by the gamma parameter (Yang 2006). Maximum likelihood (ML) phylogenetic analyses on the gene trees and

the concatenated dataset, partitioned by locus, were conducted using the GTRGAMMA setting in RAxML (Stamatakis 2006) using 500 fast bootstrap replicates. Topologies were compared to assess the degree of congruence. Taxa based on sequences from a single specimen that appeared in parts of the topology strongly contradictory to previous studies or to traditional taxonomy were assumed to be the potential result of misidentification or contamination in the original studies. These sequences were removed from the alignment and were not included in subsequent analyses.

Divergence time estimation was conducted using BEAST 1.6 (Drummond & Rambaut 2007). The concatenated alignment was partitioned by locus and analyzed using a birth-death prior for cladogenesis rates and uncorrelated exponential priors, except for the root, for which a uniform distribution was applied. Fourteen fossils were used to calibrate the timetree (Table A3-S2). To increase computational tractability, we constrained 33 nodes in the BEAST analysis that received > 90% bootstrap support in the ML analysis (Table A3-S3). The BEAST analysis was run for 100 million generations, sampling every 10,000 generations. Chain mixing and convergence were visually assessed in Tracer 1.5 (Drummond & Rambaut 2007). We removed 20% of trees as burnin, and generated the timetree in TreeAnnotator (Drummond & Rambaut 2007).

Habitat comparative analyses

We used Fishbase (Froese & Pauly 2012) to collect habitat preference data for all described shark species, and coded each species as shelf, deepwater (> 200 m depth), or pelagic (Table A3-S4). Using these habitat character states, we compared the fit of three discrete trait

models using the Geiger 1.99-3 (Harmon *et al.* 2008) package in R 2.15 (R Core Team 2012). We assessed fit for models where: (1) all transition rates were equal (ER); (2) forward and reverse transitions were equal (SYM); and (3) all transition rates were different (ARD) using corrected Akaike Information Criterion (AICc). We used a ΔAICc of four units as an indication of better model fit.

To test whether habitat affects shark speciation rates we ran MuSSE (Maddison *et al.* 2007) using maximum likelihood implemented in the DIVERSITREE 0.9-3 (FitzJohn 2012) package in R 2.15 (R Core Team 2012). DIVERSITREE applies a correction for random incomplete sampling (FitzJohn 2012), so we incorporated the proportion of missing diversity for each habitat category, and assumed it to be randomly distributed. We compared the fit of two models: the first was a habitat-independent speciation model where each habitat type was constrained to have the same rate ($\lambda_{shelf} = \lambda_{deep} = \lambda_{oceanic}$); the second was a habitat-dependent speciation model where each habitat type was free to evolve at independent speciation rates ($\lambda_{shelf} \neq \lambda_{deep} \neq \lambda_{oceanic}$). Since we were interested in testing the affect of habitat on speciation rates, and because extinction rate estimates from molecular phylogenies are often unreliable (e.g. Rabosky 2009), we constrained the extinction rates to be equal for each habitat state ($\mu_{shelf} = \mu_{deep} = \mu_{oceanic}$). We constrained transition rates among habitat types to be equal ($q_{shelf} = q_{deep}$, $q_{shelf} = q_{oceanic}$) after preliminary analyses using the fitDiscrete function in Geiger. Although the SYM model fit slightly better than the ER (ΔAICc = 2.8) and the ARD (ΔAICc = 1.1), neither the SYM or the ARD provided significant improvement in model fit, so we chose to use the simplest model, ER, for the analysis. To accommodate topological uncertainty, we ran the analysis over 100 randomly selected trees from the post-burnin sample. We averaged the results across all runs

and model fit was assessed using AIC. We used an AIC score improvement of four units as an indication of better model fit. If occupying shelf habitats elevates speciation rates, we expected to estimate higher speciation rates in shelf lineages and accept the habitat-dependent model.

We also tested whether coral reef-association affects carcharhinid speciation rates by using the same approach described above, including discrete model fitting in Geiger (Harmon *et al.* 2008). We divided the shelf habitat into four sub-categories and coded carcharhinid species as: brackish, shelf (inshore, non-reef), coastal-pelagic (cp), or reef-associated (Table A3-S5). Habitat preference was scored as shelf (inshore, non-reef) for species with unknown habitat preference. Two models were compared, a habitat-independent model where speciation rates were constrained ($\lambda_{brackish} = \lambda_{shelf} = \lambda_{cp} = \lambda_{reef}$), and a second where speciation rates were habitat-dependent ($\lambda_{brackish} \neq \lambda_{shelf} \neq \lambda_{cp} \neq \lambda_{reef}$). Extinction rates and transition rates were constrained based on our results from the discrete model fitting. We were able to reject the ARD model (ΔAICc = 16.2), and the ER model fit slightly better than the SYM model (but was not statistically preferred SYM ΔAICc = 3.6). MuSSE analyses were run over 100 randomly selected trees from the post-burnin sample; the results were averaged across runs and model fit was assessed using an AIC score threshold of four units. If reef-association results in elevated cladogenesis rates, we expected to estimate higher speciation rates in reef-associated lineages and accept the model where speciation rates are habitat dependent. This test is separate from the analysis conducted across the entire shark tree; therefore the rate estimates cannot be directly compared between the two tests.

To date no information is available on whether extant shark species tend to retain their ancestral lineage habitat type, or if habitat shifts are common among sharks. To examine whether

major shark groups evolved in different habitats and how frequent habitat shifts have occurred, we used SIMMAP in Phytools 0.3 (Revell 2012) to stochastically map ancestral habitat preferences on the timetree. We used the same habitat preference data (shelf, deepwater, or pelagic) collected for DIVERSITREE analyses (Table A3-S4), assumed an ER model, and ran the analysis for 1000 simulations. We also reconstructed habitat preference in Carcharhinidae (minus *Galeocerdo)* to determine how many times reef-association has evolved in this family, coding species as brackish, shelf, reef-associated, or coastal-pelagic (Table A3-S5). We stochastically mapped habitat on the carcharhinid timetree using SIMMAP and 1000 simulations. We were unable to conclusively reconstruct ancestral states at the internal nodes based on the SIMMAP analysis, so we used Geiger (Harmon *et al.* 2008) to reconstruct ancestral habitats using a maximum likelihood approach (Schluter *et al.* 1997).

RESULTS

Our maximum likelihood topology recovers a strongly supported monophyletic sharks (96% bootstrap proportion (BSP)), which appears as the sister group to the batoids (Fig. A3-S1). Within sharks two large clades are identified: the first one includes the traditional squalimorphs (96% BSP), while the second contains the groups traditionally assigned to the galeomorphs (albeit with only 36% BSP). Within squalimorphs we recover monophyletic hexanchiforms (100% BSP) as sister clade to the rest of this group. Pristiophoriforms + squatiniforms (sister taxa) appear sister to the largest order, the squaliforms. Within galeomorphs we recover monophyly for all orders: the heterodontiforms (100% BSP), the lamniforms and the orectolobiforms (both 99% BSP), and the carcharhiniforms (95% BSP).

The BEAST timetree (Fig. A3-S2) reveals that sharks diverged from batoids in the Lower Carboniferous (Table 1), ~364 Ma (319-402 Ma 95% highest posterior density (HPD)), and have a crown age dating to the upper Carboniferious/Lower Permian (300 Ma; 263-338 95% HPD). We recovered two major clades: the first, comprising Hexanchiformes + Pristiophoriformes + Squatiniformes + Squaliformes, dates to 238 Ma (201-276 Ma 95% HPD). The four ordinal lineages within this clade all originated in the early Mesozoic (the hexanchiforms originated 238 Ma, the pristiophoriforms and squatiniforms 200 Ma, and the squaliforms 216 Ma), although the crown ages for these four clades are much younger and date to the late Jurassic or Cretaceous (130 Ma, 73 Ma, 155 Ma and 162 Ma for hexanchiforms, pristiophoriforms, squatiniforms and squaliforms, respectively). All major squaliform clades, which together contain the bulk of the squalimorph diversity, have stem ages between 119 and 114 Ma, dating to the early Cretaceous, although most of the diversity originated more recently (25 - 75 Ma) during the late Cretaceous and the Paleogene.

Galeomorphs originated around 273 Ma (239-310 Ma 95% HPD) with the split between the heterodontiforms and the remaining galeomorphs (Table 1). In spite of their ancient origin, crown heterodontiforms are the product of a recent radiation, having originated in the Mid-Eocene around 47 Ma (20-80 Ma 95% HPD). Within galeomorphs, the orectolobiforms and carcharhiniforms all show a late Jurassic origin, with crown ages of 166 Ma (126-208 Ma 95% HPD) for the orectolobiforms, 162 Ma (137-189 Ma 95% HPD) for the lamniforms, and 179 Ma (165-199 Ma 95% HPD) for the carcharhiniforms. In spite of Paleozoic or Mesozoic origins for all the major groups, several important crown radiations occurred in the Cenozoic including: the

above mentioned heterodontiforms; the orectolobids (25 Ma, 13-40 Ma 95% HPD); and the bulk of the carcharhinid diversity (63 Ma, 50-79 Ma 95% HPD).

The habitat-dependent model fit our data best based on the DIVERSITREE results, but we could not exclude the habitat-independent model when habitat was coded as shelf, deepwater, or pelagic (ΔAIC = 0.511). The shelf habitat speciation rate was lower than for deepwater environments (λ_{shelf} = 0.048 lineages My^{-1}; λ_{deep} = 0.053 lineages My^{-1}). The shelf habitat speciation rate estimate was slightly higher than that estimated for pelagic environments ($\lambda_{pelagic}$ = 0.042 lineages My^{-1}).

For our carcharhinid analysis we found strong evidence for increased speciation rates corresponding to transitions to reef habitats (ΔAIC = 5.76). The speciation rate for reef-associated lineages was ~1.7x higher (λ_{reef} = 0.046 lineages My^{-1}) compared to their non-reef shelf counterparts (λ_{shelf} = 0.027 lineages My^{-1}). Species inhabiting brackish water had a similar net diversification rate compared to non-brackish, non-reef-associated shelf lineages ($\lambda_{brackish}$ = 0.028 lineages My^{-1}), whereas coastal-pelagic lineages diversified much slower (λ_{cp} = 0.017 lineages My^{-1}).

The ancestral habitat stochastic mapping results indicated that the squalimorph most common recent ancestor (MRCA) was a deepwater species, while the galeomorph MRCA was a coastal taxon. Both groups largely retained the habitat type of their last common ancestor, but a number of transitions between the shelf, deepwater and pelagic realms occurred in each clade (Fig. 1). Within squalimorphs, deepwater lineages have shifted to coastal habitats in hexanchiforms, pristiophoriforms, *Squatina* (with several reversals to deeper habitats), and two

recent lineages of *Squalus.* Within squaliforms there have also been two transitions to pelagic habitats. Within galeomorphs, the ancestral shelf habitat is retained by all heterodontids, by almost all orectolobids and by most carcharhiniforms. The last galeomorph order, the lamniforms, includes most of the pelagic sharks, although some lamniforms are found in shelf habitats and others have transitioned to deepwater. A number of pelagic species are also found within the carcharhinids, one of the largest shark families, with at least three lineages having transitioned from shelf habitats to open water environments. Carcharhinidae maximum likelihood habitat reconstruction revealed that the MRCA to all carcharhinids was either a shelf (non-reef) or reef-associated species (Fig. 2). It appears that transitions to reefs may have occurred in multiple carcharhinid lineages: at least once in *Rhizoprionodon;* once in *Negaprion;* and several times within *Carcharhinus.* It is clear that reef-association is highly concentrated within a large carcharhinid radiation. The MRCA of this radiation diverged and transitioned to reef habitats ~80 Ma, and this lineage subsequently radiated to a dense reef-associated clade ~45 Ma.

DISCUSSION

A timescale for the radiation of sharks

The maximum likelihood tree topology was largely congruent with other molecular studies (e.g. Naylor *et al.* 2005; Vélez-Zuazo & Agnarsson 2011; Li *et al.* 2012), particularly concerning the higher level relationships. Sharks split from batoids towards the end of the Devonian (~364 Ma), and crown sharks appeared at the end of the Carboniferous (~300 Ma). Both squalimorphs and galeomorphs began diversifying immediately following the end-Permian

mass extinction suggesting that diversity in these taxa reflects ecological expansion during the post-Permian extinction recovery phase along with other components of the marine fauna (e.g. Sepkoski 1982).

All ordinal lineages originated in the Early to Middle Triassic (246 - 216 Ma), a result in fairly close agreement with the paleobiological study of Cuny & Benton (1999), who describe a shark radiation in the Upper Triassic. Further shark diversification occurred around the end-Jurassic (145 Ma) extinctions, a time when the crown of most shark orders originated (Table 1, Fig. A3-S1). The crown of most orders originated during the Jurassic (e.g., Squatiniformes, Squaliformes, Orectolobiformes, Lamniformes, Carcharhiniformes), while the crown age of most families date to the Early Cretaceous (e.g., Hexanchidae, the bulk of Squatinidae, Dalatiidae, Somniosidae + Oxynotidae, Centrophoridae, Squalidae, Etmopteridae, Triakidae, and Carcharhinidae), supporting evidence from the fossil record (Underwood 2006; Guinot *et al.* 2012). In spite of these old ages, a number of very young radiations can be observed on the timetree, such as Heterodontiformes (Middle Eocene; 47 Ma) and the Orectolobidae, which date to the Late Oligocene (25 Ma). While our results suggest a much earlier shark stem age than that inferred from the fossil record (e.g. Cuny 1998), the timing of appearance and diversification of the ordinal lineages corroborates the paleontological data currently available, which point to a Triassic origin followed by a radiation of all major lineages during the Jurassic and Cretaceous (Maisey *et al.* 2004; Underwood 2006; Kriwet *et al.* 2009; Guinot *et al.* 2012).

Our results indicate a split between sharks and batoids during the Devonian age (364 Ma), which is congruent with the ~381 Ma of Heinicke *et al.* (2009). Similar results are obtained for the origin of the crown sharks, with an end Carboniferous age inferred by our analysis (~300

Ma), which is younger than the ~350 Ma of Heinicke *et al.* (2009). Our results suggest older ages for lower level clades. For example, our ages support a Cenomanian origin (~ 97 Ma) for the etmopterids, versus a late Paleocene/Early Eocene (48 - 56 Ma) divergence recovered by Straube *et al.* (2010). We believe this discrepancy may be explained by the limited number of non-etmopterid calibrations used in that study, and also the highly constrained fossil calibration ages, which may have prevented the authors from estimating more accurate lineage ages. Similarly, our use of a relaxed molecular clock with a large number of fossil calibrations and sequence from multiple genes most likely underlies the much older dates we obtained compared with Corrigan & Beheregaray (2009) who did not use fossils, but assumed a strict molecular clock in their analysis of sequence from the mitochondrial control region.

Habitat-mediated diversification in sharks

The habitat DIVERSITREE results did not support our hypothesis of elevated speciation rates in shelf environments. A pattern of high speciation rates in onshore (i.e. shelf) habitats compared to offshore habitats has been well described based on fossil evidence (e.g. Jablonski 2005; Kiessling *et al.* 2010); however, we could not accept a model where speciation rates were habitat-dependent for lineages occupying shelf, deepwater, and pelagic environments. Previous studies have been primarily based on the rich invertebrate fossil record; taxonomic groups that tend to be more sedentary and are overall more limited in mobility compared to fishes. Fundamental differences in the biology and ecology of the different taxonomic groups could account for the lack of an onshore-offshore biodiversity gradient signal in sharks, which may be less subject than benthic invertebrates to the mechanisms leading to differential speciation rates

among broad habitat types. Further research is warranted to determine the specific causal factors leading to the breakdown of the onshore-offshore pattern in sharks.

We find that diversification of major shark clades followed novel habitat colonization, and early success in offshore environments (i.e. deepwater) may have contributed to the breakdown of the biodiversity gradient and habitat-dependent speciation rates. Our results suggest that habitat was a major axis of divergence in early shark lineages through the lower Jurassic (300 - 179 Ma). The MRCA to all sharks diverged into two lineages: one deepwater lineage that led to the Squalimorpha, and a shelf lineage that led to the Galeomorpha. Our ancestral state reconstruction analysis supports the Klug & Kriwet (2010) hypothesis that squaliform sharks were prevalent in deepwater habitats through the middle Cretaceous. Most squaliform diversity, however, did not radiate until after major deepwater anoxic events occurred ~120 and ~93 Ma (e.g. Arthur *et al.* 1988; Menegatti *et al.* 1998). Subsequent novel habitat invasion is evident among the main shark clades, especially within the galeomorphs where major radiations into all three habitat types (shelf, deepwater, and pelagic) occurred. This included a lamniform transition to the pelagic realm ~ 140 Ma; most extant pelagic sharks, therefore, are of an ancient lineage. This is in contrast to the timing of diversification of other large-bodied pelagic fishes, such as tunas and billfishes, which radiated much later in the Miocene (Santini *et al.* 2013a; Santini & Sorenson 2013). Another galeomorph novel habitat transition included a scyliorhinid invasion of deepwater that originated approximately 136 Ma (105-147 HPD), with most clade radiations occurring between 98 - 43 Ma. The timing of carcharhinid deepwater radiations suggest that this novel deepwater invasion may have been opportunistic during

recovery from the oceanic anoxic event 2 (OAE 2; ~93 Ma) that greatly affected deepwater species diversity (e.g. Arthur *et al.* 1988).

Following invasion of deepwaters, speciation may have been spurred by subsequent ecological partitioning and morphological or behavioral evolution. Depth zonation occurs in marine habitats, with recurring boundaries on continental slopes (e.g. Rex 1977; Stefanescu *et al.* 1993; Cartes & Carrassón 2004) that partition deep-sea faunal assemblages. Deep sea sharks have been shown to partition habitats by depth (Stefanescu *et al.* 1993; Cartes & Carrassón 2004), which may be driven by interspecific competition (Rex 1977; Gage & Tyler 1991). Previous studies have compared zonation rates among various trophic levels and suggest that higher zonation rates (habitat partitioning by depth) occur in predators (Rex 1977; Gage & Tyler 1991; Cartes & Carrasson 2004). Strict depth partitioning among top predators could provide ecological opportunity for speciation to occur, thus providing a mechanism to explain our pattern of similar speciation rates in shelf and deepwater habitats in sharks, but not in lower trophic level invertebrate fossil groups. Successful radiations in deepwater habitats may have been driven by morphological novelty as well. For example, within the Squaliformes, the etmopterids (as well as dalatiids) evolved photophores and bioluminescence in response to the deep sea environment (Klug & Kriwet 2010; Straube *et al.* 2010). Variation in the patterns and location of etmopterid photophores suggest that bioluminescence functions as camouflage (Claes & Mallefet 2008) or intraspecific communication that subsequently drove speciation in several lineages (e.g. Reif 1985; Claes & Mallefet 2009; Straube *et al.* 2010; Davis *et al.* 2014).

The role of coral reefs in carcharhinid diversification

Carcharhinid shark diversification is strongly influenced by coral reefs, supporting our hypothesis that reef-associated shark lineages experience increased rates of cladogenesis compared to other shelf habitats. Based on our DIVERSITREE analyses, the carcharhinids initially appear to have undergone a slow-down in speciation (all onshore, non-reef habitats estimated at ≤ 0.027 lineages My^{-1}). Transitions onto reefs, however, elevated the cladogenesis rate to 0.046 lineages My^{-1}, a rate similar to the shelf rate (0.048 lineages My^{-1}) we estimated across the entire shark tree using the broad habitat categories (deepwater, shelf, pelagic). Our finding of reef-association accelerating lineage diversification rates is congruent with previous studies concerning other taxonomic groups based on the fossil record (Kiessling & Aberhan 2007; Renema *et al.* 2008; Kiessling *et al.* 2010) and molecular trees (e.g. Alfaro *et al.* 2007; Bellwood *et al.* 2010; Dornburg *et al.* 2011; Price *et al.* 2011; Frédérich *et al.* 2013; Santini *et al.* 2013), demonstrating that reefs have a profound effect on species richness across a wide variety of trophic levels and ecological niches. Despite their vagility, carcharhinid sharks may be affected by many of the same factors that affect diversification in other reef- associated groups, including high productivity, resource diversity (Fraser & Currie 1996), and habitat complexity (e.g. Gratwicke & Speight 2005) that provide opportunities for complex species interactions and niche partitioning. These in turn may lead to ecomorphological specialization and diversification opportunities (Bellwood & Wainwright 2002). Like many reef invertebrates and small teleost fishes (Roberts *et al.* 2002), at least some reef-associated shark species have restricted range sizes (e.g. Papastamatiou *et al.* 2009; Papastamatiou *et al.* 2010; Bond *et al.* 2012). This high site-fidelity may have lowered dispersal potential in these largely motile fishes, allowing a

greater effect of extrinsic factors such as continental drift, sea level changes, or climatic shifts on their evolution.

Scleractinian reef diversification occurred in the Late Eocene and early Miocene (Wood 1999; Budd 2000) and it appears that this radiation has been paralleled in many associated organismal groups (e.g. LaJeunesse 2005; Renema *et al.* 2008; Cowman & Bellwood 2011; Williams & Duda 2008; Cowman *et al.* 2009; Bellwood *et al.* 2010; Claremont *et al.* 2011), suggesting that reefs may have played a major role in driving reef-associated clade diversification as scleractinian corals came to dominate shallow marine environments. Fish faunas resembling modern assemblages were present on reefs at least 50 Ma (Bellwood 1996). Reef-associated carcharhinid diversification primarily began ~45 Ma; contemporaneous with the origination of many other reef fish groups (e.g. tetraodontiforms: Alfaro *et al.* 2007, Santini *et al.* 2013; pomacentrids: Frédérich *et al.* 2013, Cowman & Bellwood 2011; labrids, chaetodontids, apogonids: Cowman & Bellwood 2011; acanthurids: Sorenson *et al.* 2013). The timing in reef-association suggests that carcharhinids may have evolved reef preference in response to food availability in the new habitats; however, at the present time it is not clear what may have facilitated carcharhinid diversification.

Our maximum likelihood ancestral state reconstruction suggested multiple independent invasions of reef ecosystems by carcharhinid sharks during the past 80 million years. The vast majority of these habitat shifts occurred within Carcharhinidae between the Early Eocene (~55-50 Ma) and the Late Oligocene (30-24 Ma). This was a period when scleractinian reefs became abundant in tropical, shallow water environments, which had been largely dominated by rudist bivalve reefs towards the latter part of the Cretaceous before their extinction at the K-Pg

limit (Wood 1999; Bellwood & Wainwright 2002). Coral reefs underwent a decline at the end of the Eocene, and rapid carcharhinid diversification coincided with subsequent massive reef recovery in the Oligocene.

CONCLUSIONS

Our study, based on the largest shark molecular timetree ever assembled, suggests that habitat association and survival to mass extinctions have played an important role in driving shark evolutionary patterns. We reject the hypothesis that lineages occupying shelf habitats speciate at higher rates compared to offshore lineages (e.g. pelagic and deepwater environments), and therefore our data do not support the longstanding onshore-offshore biodiversity pattern described in lineages strongly associated to the benthos. We do however find evidence that scleractinian reefs, which have long been thought to be important sources of biodiversity, have contributed significantly to carcharhiniform species richness. This finding indicates that habitat transitions onto reefs influence species diversity across multiple trophic levels. Two major shark lineages originated towards the end of the Carboniferous and began diversifying mostly after the end-Permian mass extinctions along very different ecological trajectories; the squalimorphs into deepwater and the galeomorphs into shelf habitats, but with some lineages diversifying into offshore environments. Most shark orders originated and began diversifying during the Late Jurassic/Early Cretaceous, supporting previous paleontological research and our prediction that recovery following mass extinctions has also been important in the evolutionary history of sharks.

Table 1: Inferred divergence times for major shark timetree nodes. Mean age and 95% highest posterior density (HPD) are provided for this study. We provide Heinicke *et al.* (2009) crown ages and node confidence intervals (CI) where available for comparison.

	This study		Heinicke et al. (2009)	
Group	Crown age (Ma)	HPD	Crown age (Ma)	CI
Neoselachii	364	319-402	393	431-354
sharks	300	263-338	350	392-309
Galeomorphii	274	239-310	318	359-279
Squalimorphii	238	201-276	327	372-283
Hexanchiformes	130	80-179	236	295-183
Pristiophoriformes	73	37-116		
Squatiniformes	155	151-163		
Squaliformes	163	137-190	170	218-128
Heterodontiformes	48	20-80		
Orectolobiformes	166	126-208	237	287-186
Lamniformes	162	137-189	185	224-148
Carcharhiniformes	179	165-199	226	261-195
Carcharhinidae-Galeocerdo	80	65-95		
Etmopteridae	97	77-121		
Orectolobidae	25	13-40		

Figure 1: Shark ancestral habitat preferences. Results are based on stochastic mapping of 1000 simulations across the timetree and summarized at each node. Shark species are coded as shelf (blue), deepwater (red), and pelagic (green).

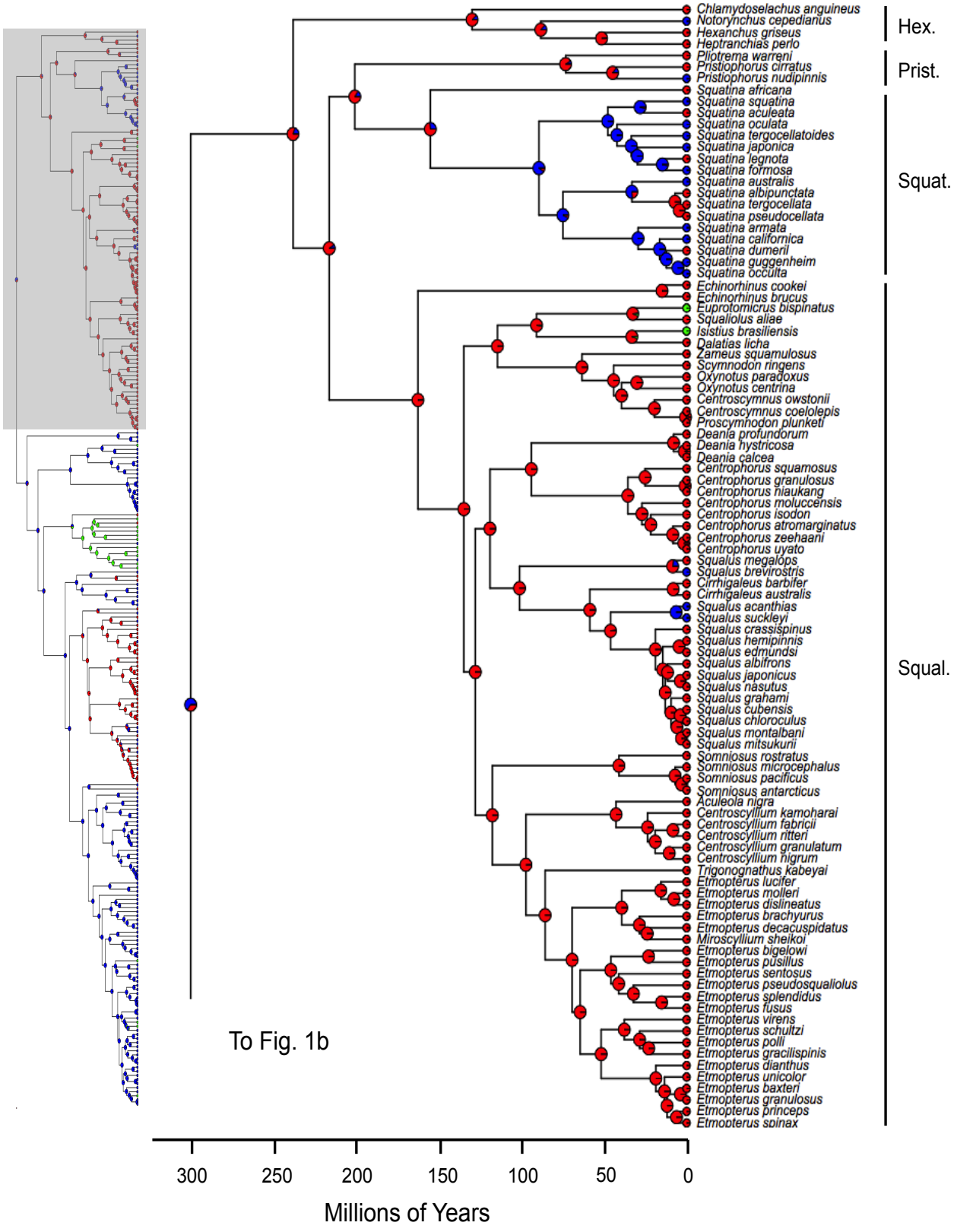
Chlamydoselachus anguineus
Notorynchus cepedianus
Hexanchus griseus
Heptranchias perlo
Pliotrema warreni
Pristiophorus cirratus
Pristiophorus nudipinnis
Squatina africana
Squatina squatina
Squatina aculeata
Squatina oculata
Squatina tergocellatoides
Squatina japonica
Squatina legnota
Squatina formosa
Squatina australis
Squatina albipunctata
Squatina tergocellata
Squatina pseudocellata
Squatina armata
Squatina californica
Squatina dumeril
Squatina guggenheim
Squatina occulta
Echinorhinus cookei
Echinorhinus brucus
Euprotomicrus bispinatus
Squaliolus aliae
Isistius brasiliensis
Dalatias licha
Zameus squamulosus
Scymnodon ringens
Oxynotus paradoxus
Oxynotus centrina
Centroscymnus owstonii
Centroscymnus coelolepis
Proscymnodon plunketi
Deania profundorum
Deania hystricosa
Deania calcea
Centrophorus squamosus
Centrophorus granulosus
Centrophorus hiaukang
Centrophorus moluccensis
Centrophorus isodon
Centrophorus atromarginatus
Centrophorus zeehaani
Centrophorus uyato
Squalus megalops
Squalus brevirostris
Cirrhigaleus barbifer
Cirrhigaleus australis
Squalus acanthias
Squalus suckleyi
Squalus crassispinus
Squalus hemipinnis
Squalus edmundsi
Squalus albifrons
Squalus japonicus
Squalus nasutus
Squalus grahami
Squalus cubensis
Squalus chloroculus
Squalus montalbani
Squalus mitsukurii
Somniosus rostratus
Somniosus microcephalus
Somniosus pacificus
Somniosus antarcticus
Aculeola nigra
Centroscyllium kamoharai
Centroscyllium fabricii
Centroscyllium ritteri
Centroscyllium granulatum
Centroscyllium nigrum
Trigonognathus kabeyai
Etmopterus lucifer
Etmopterus molleri
Etmopterus dislineatus
Etmopterus brachyurus
Etmopterus decacuspidatus
Miroscyllium sheikoi
Etmopterus bigelowi
Etmopterus pusillus
Etmopterus sentosus
Etmopterus pseudosqualiolus
Etmopterus splendidus
Etmopterus fusus
Etmopterus virens
Etmopterus schultzi
Etmopterus polli
Etmopterus gracilispinis
Etmopterus dianthus
Etmopterus unicolor
Etmopterus baxteri
Etmopterus granulosus
Etmopterus princeps
Etmopterus spinax
Hex.
Prist.
Squat.
Squal.
To Fig. 1b
300
250
200
150
100
50
0
Millions of Years

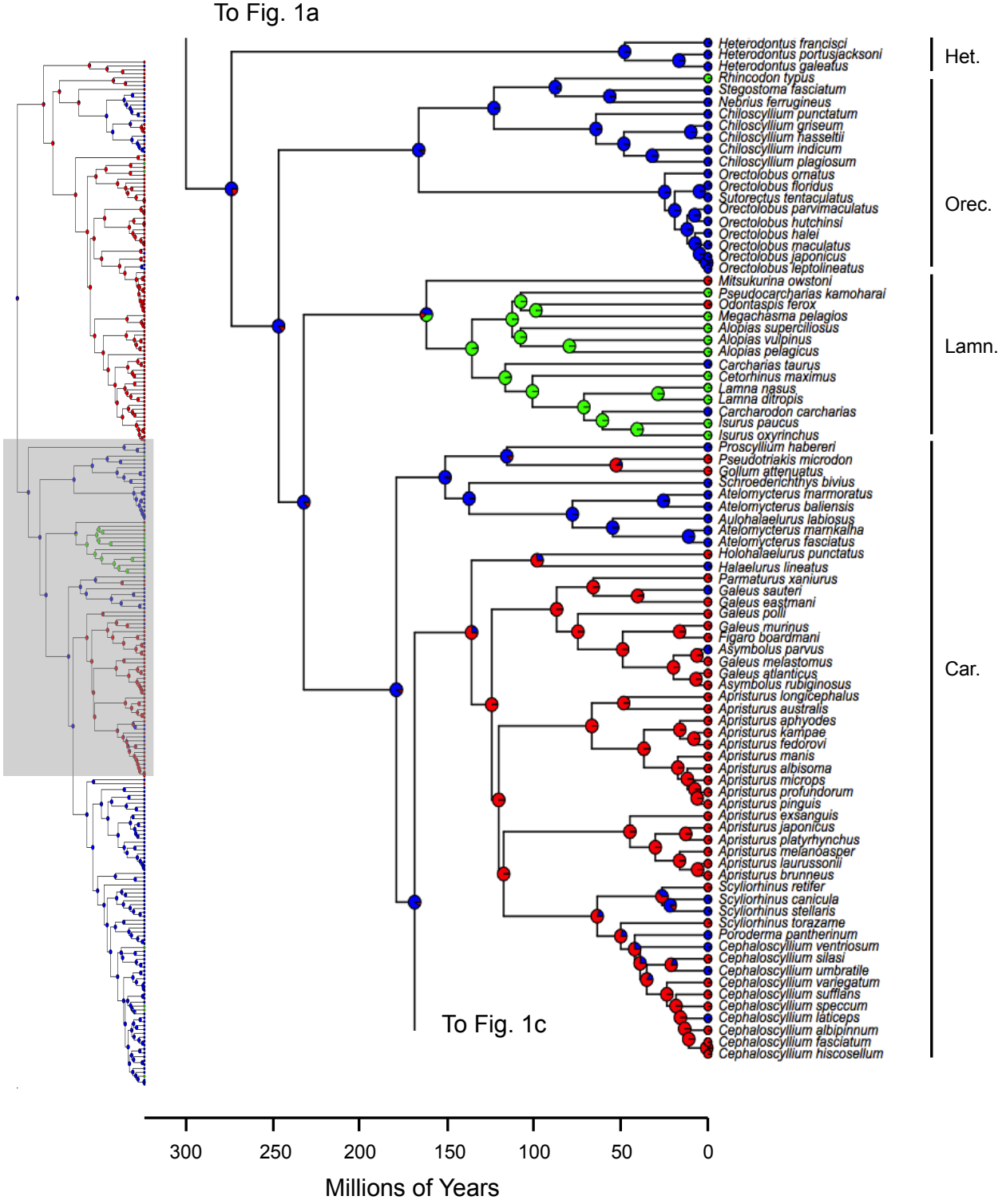
To Fig. 1a
Heterodontus francisci
Heterodontus portusjacksoni
Heterodontus galeatus
Rhincodon typus
Stegostoma fasciatum
Nebrius ferrugineus
Chiloscyllium punctatum
Chiloscyllium griseum
Chiloscyllium hasseltii
Chiloscyllium indicum
Chiloscyllium plagiosum
Orectolobus ornatus
Orectolobus floridus
Sutorectus tentaculatus
Orectolobus parvimaculatus
Orectolobus hutchinsi
Orectolobus halei
Orectolobus maculatus
Orectolobus japonicus
Orectolobus leptolineatus
Mitsukurina owstoni
Pseudocarcharias kamoharai
Odontaspis ferox
Megachasma pelagios
Alopias superciliosus
Alopias vulpinus
Alopias pelagicus
Carcharias taurus
Cetorhinus maximus
Lamna nasus
Lamna ditropis
Carcharodon carcharias
Isurus paucus
Isurus oxyrinchus
Proscyllium habereri
Pseudotriakis microdon
Gollum attenuatus
Schroederichthys bivius
Atelomycterus marmoratus
Atelomycterus baliensis
Aulohalaelurus labiosus
Atelomycterus marnkalha
Atelomycterus fasciatus
Holohalaelurus punctatus
Halaelurus lineatus
Parmaturus xaniurus
Galeus sauteri
Galeus eastmani
Galeus polli
Galeus murinus
Figaro boardmani
Asymbolus parvus
Galeus melastomus
Galeus atlanticus
Asymbolus rubiginosus
Apristurus longicephalus
Apristurus australis
Apristurus aphyodes
Apristurus kampae
Apristurus fedorovi
Apristurus manis
Apristurus albisoma
Apristurus microps
Apristurus profundorum
Apristurus pinguis
Apristurus exsanguis
Apristurus japonicus
Apristurus platyrhynchus
Apristurus melanoasper
Apristurus laurussonii
Apristurus brunneus
Scyliorhinus retifer
Scyliorhinus canicula
Scyliorhinus stellaris
Scyliorhinus torazame
Poroderma pantherinum
Cephaloscyllium ventriosum
Cephaloscyllium silasi
Cephaloscyllium umbratile
Cephaloscyllium variegatum
Cephaloscyllium sufflans
Cephaloscyllium speccum
Cephaloscyllium laticeps
Cephaloscyllium albipinnum
Cephaloscyllium fasciatum
Cephaloscyllium hiscosellum
Het.
Orec.
Lamn.
Car.
To Fig. 1c
300
250
200
150
100
50
0
Millions of Years

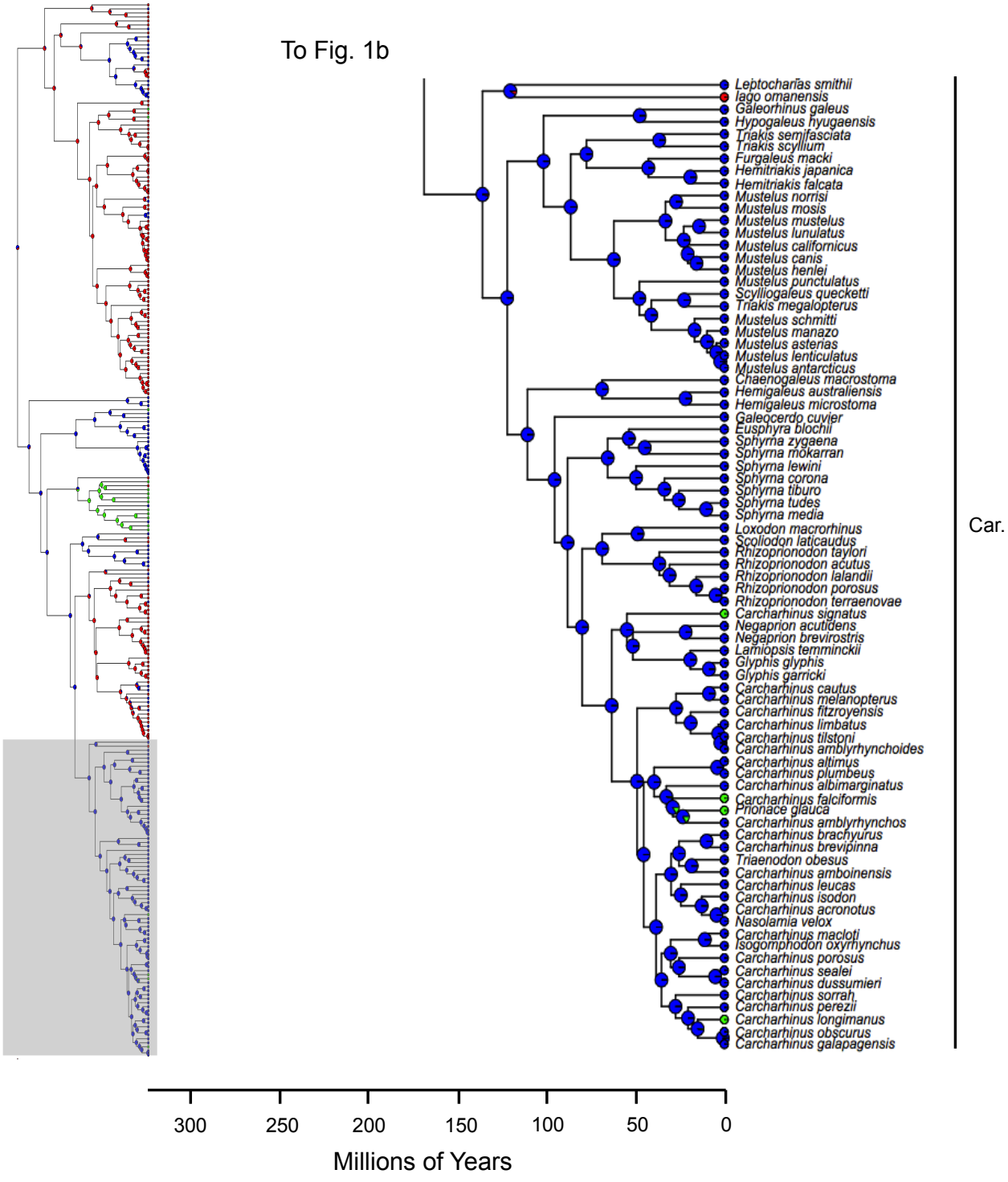
To Fig. 1b
Leptocharias smithii
Iago omanensis
Galeorhinus galeus
Hypogaleus hyugaensis
Triakis semifasciata
Triakis scyllium
Furgaleus macki
Hemitriakis japanica
Hemitriakis falcata
Mustelus norrisi
Mustelus mosis
Mustelus mustelus
Mustelus lunulatus
Mustelus californicus
Mustelus canis
Mustelus henlei
Mustelus punctulatus
Scylliogaleus quecketti
Triakis megalopterus
Mustelus schmitti
Mustelus manazo
Mustelus asterias
Mustelus lenticulatus
Mustelus antarcticus
Chaenogaleus macrostoma
Hemigaleus australiensis
Hemigaleus microstoma
Galeocerdo cuvier
Eusphyra blochii
Sphyrna zygaena
Sphyrna mokarran
Sphyrna lewini
Sphyrna corona
Sphyrna tiburo
Sphyrna tudes
Sphyrna media
Loxodon macrorhinus
Scoliodon laticaudus
Rhizoprionodon taylori
Rhizoprionodon acutus
Rhizoprionodon lalandii
Rhizoprionodon porosus
Rhizoprionodon terraenovae
Carcharhinus signatus
Negaprion acutidens
Negaprion brevirostris
Lamiopsis temminckii
Glyphis glyphis
Glyphis garricki
Carcharhinus cautus
Carcharhinus melanopterus
Carcharhinus fitzroyensis
Carcharhinus limbatus
Carcharhinus tilstoni
Carcharhinus amblyrhynchoides
Carcharhinus altimus
Carcharhinus plumbeus
Carcharhinus albimarginatus
Carcharhinus falciformis
Prionace glauca
Carcharhinus amblyrhynchos
Carcharhinus brachyurus
Carcharhinus brevipinna
Triaenodon obesus
Carcharhinus amboinensis
Carcharhinus leucas
Carcharhinus isodon
Carcharhinus acronotus
Nasolamia velox
Carcharhinus macloti
Isogomphodon oxyrhynchus
Carcharhinus porosus
Carcharhinus sealei
Carcharhinus dussumieri
Carcharhinus sorrah
Carcharhinus perezii
Carcharhinus longimanus
Carcharhinus obscurus
Carcharhinus galapagensis
Car.
300
250
200
150
100
50
0
Millions of Years

Figure 2: Maximum likelihood carcharhinid ancestral state reconstruction of shelf habitats. Species are coded as brackish, shelf, reef-associated, and coastal-pelagic. Black circles represent nodes with > 0.95 posterior probability support from the BEAST analysis.

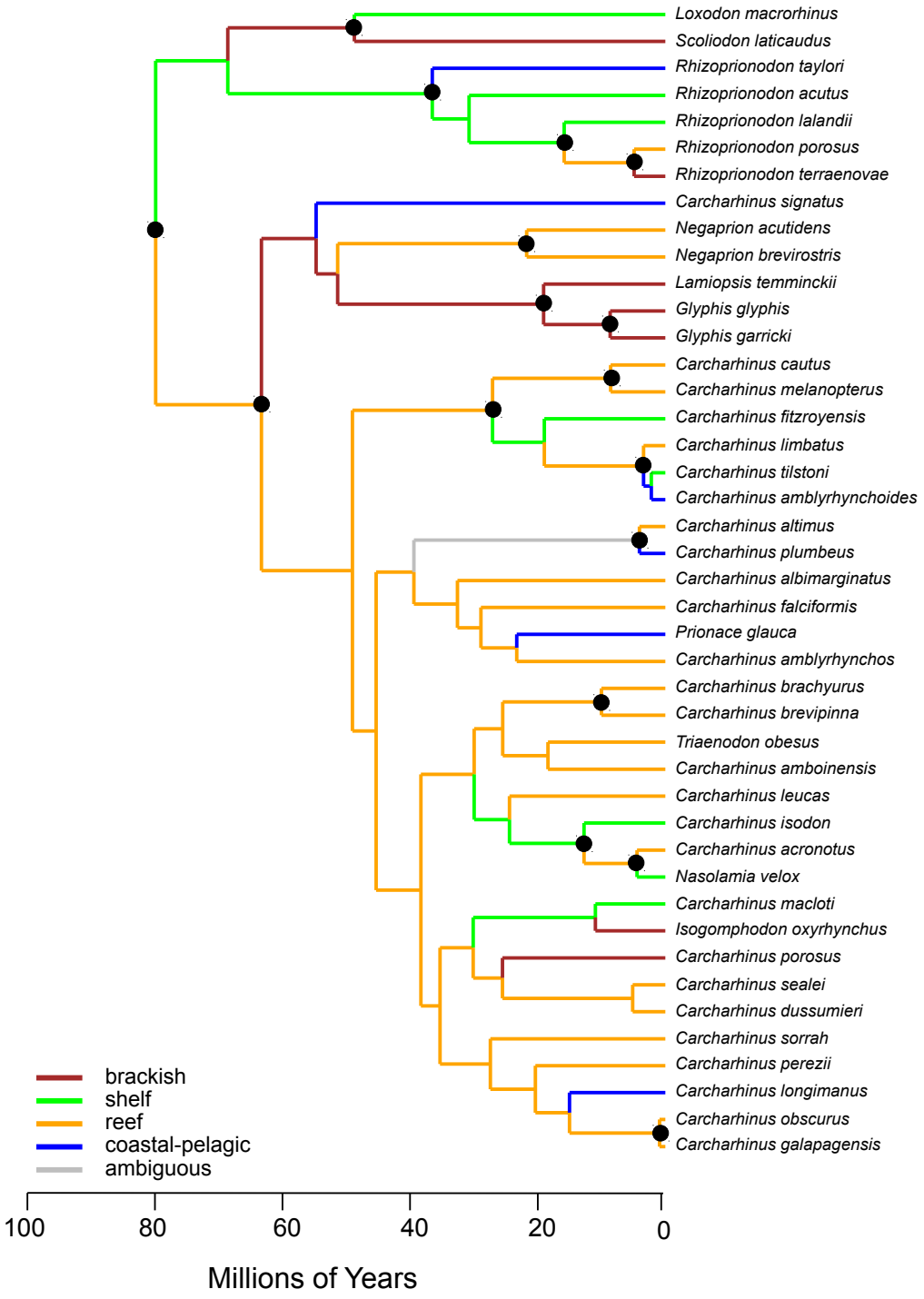

APPENDIX 3

Table A3-S1: Molecular data collected from GenBank for this study. Available sequence data were obtained for four mitochondrial and one nuclear gene. Two batoids and two chimaera were selected as outgroups.

	Taxon name	***COI***	***Cytb***	***NADH2***	***Rag1***	***16S***
Ingroup taxa						
	Carcharhinus acronotus	FJ519036	DQ422070	DQ422101		FJ598678
	Carcharhinus albimarginatus	FJ519191				
	Carcharhinus altimus	EU398589				AY830722
	Carcharhinus amblyrhynchoides	EF609307				
	Carcharhinus amblyrhynchos	FJ519197				AY462148
	Carcharhinus amboinensis	DQ885075				
	Carcharhinus brachyurus	FJ519057				
	Carcharhinus brevipinna	FJ519062				AY462149
	Carcharhinus cautus	EU398607				
	Carcharhinus dussumieri	EU398608				
	Carcharhinus falciformis	EU398613				FJ598676
	Carcharhinus fitzroyensis	EU398615				
	Carcharhinus galapagensis	JQ654714				
	Carcharhinus isodon	FJ519096				AY830729
	Carcharhinus leucas	FJ519001			U62645	FJ598692
	Carcharhinus limbatus	DQ884980				FJ598682
	Carcharhinus longimanus	FJ518920	AY973054			AY820736
	Carcharhinus macloti	EF609312				
	Carcharhinus melanopterus	EF609313				AY462150
	Carcharhinus obscurus	DQ108291				AY830738
	Carcharhinus perezii	FJ519137				FJ598673
	Carcharhinus plumbeus	EU398639	L08032	U91421		AY462151
	Carcharhinus porosus	FJ519157	L08033	U91420		FJ598684
	Carcharhinus sealei	EU398640				

	Taxon name	*COI*	*Cytb*	*NADH2*	*Rag1*	*16S*
	Carcharhinus signatus	FJ519159				AY830744
	Carcharhinus sorrah	DQ108292				
	Carcharhinus tilstoni	DQ108283				
	Galeocerdo cuvier	FJ519625	DQ422074	DQ422105		FJ598694
	Glyphis garricki	EU398794				
	Glyphis glyphis	EU818708				
	Isogomphodon oxyrhynchus					FJ598693
	Lamiopsis temminckii	EU398901				
	Loxodon macrorhinus	HQ171680				
	Nasolamia velox	FJ519181				
	Negaprion acutidens	EU398939				AY462153
	Negaprion brevirostris	FJ519227		U91418	AY949031	AY830756
	Prionace glauca	JQ654713	EU427559	DQ422102		AY820737
	Rhizoprionodon acutus	DQ108276				
	Rhizoprionodon lalandii	FJ519255				
	Rhizoprionodon porosus	FJ519264				
	Rhizoprionodon taylori	EU399001				
	Rhizoprionodon terraenovae	FJ519274				AY830764
	Scoliodon laticaudus	JQ693102				
	Triaenodon obesus	FJ519600				
	Chaenogaleus macrostoma		DQ422076	DQ422107		
	Hemigaleus australiensis	EU398812				
	Hemigaleus microstoma	EU398820	DQ422075	DQ422106		
	Leptocharias smithii		DQ422077	DQ422108		
	Proscyllium habereri				AY462184	AY462183
	Gollum attenuatus		DQ422079	DQ422110		
	Pseudotriakis microdon	EU148299	DQ422078	DQ422109	AY462185	AY049049
	Apristurus albisoma					AY462154
	Apristurus aphyodes					AF358916
	Apristurus australis	EU398554				
	Apristurus brunneus	GU440228				EU099509
	Apristurus exsanguis					AY049048

	Taxon name	*COI*	*Cytb*	*NADH2*	*Rag1*	*16S*
	Apristurus fedorovi					AY462155
	Apristurus japonicus					AY462156
	Apristurus kampae	FJ519548				EU099515
	Apristurus laurussonii					AF329376
	Apristurus longicephalus	GU130672			AY462159	AY462158
	Apristurus manis	FJ519552			AY462160	AF329375
	Apristurus melanoasper				AY462161	AF329374
	Apristurus microps					AF382947
	Apristurus pinguis	EU398547				
	Apristurus platyrhynchus	EU398531				
	Apristurus profundorum	FJ519554				
	Asymbolus parvus	EU398565				
	Asymbolus rubiginosus	EU398566				
	Atelomycterus baliensis	EU398569				
	Atelomycterus fasciatus	EU398570				
	Atelomycterus marmoratus	EU398572				
	Atelomycterus marnkalha	EU398575				
	Aulohalaelurus labiosus	EU398578				
	Cephaloscyllium albipinnum	EU398670				
	Cephaloscyllium fasciatum	EU398669				
	Cephaloscyllium hiscosellum	EU398669				
	Cephaloscyllium laticeps	DQ108322				
	Cephaloscyllium pictum	EU398673				
	Cephaloscyllium silasi	HM467791				HM467792
	Cephaloscyllium speccum	EU398675				
	Cephaloscyllium sufflans	HM909795				
	Cephaloscyllium umbratile					AY462170
	Cephaloscyllium variegatum	EU398672				
	Cephaloscyllium ventriosum	GU440268				
	Cephalurus sp				AY462172	AY462171
	Galeus atlanticus			DQ902846		
	Galeus boardmani	EU398789				
	Galeus eastmani					AY462173
	Galeus melastomus			DQ902840	AF329372	

	Taxon name	*COI*	*Cytb*	*NADH2*	*Rag1*	*16S*
	Galeus murinus				AY462174	AF329373
	Galeus polli	HQ945985				
	Galeus sauteri					AY462175
	Halaelurus lineatus	GU805054				
	Holohalaelurus punctatus	GU804939				
	Parmaturus xaniurus	FJ519576				AY958658
	Poroderma pantherinum		DQ422081	DQ422112		
	Schroederichthys bivius	EU074582				
	Scyliorhinus canicula	Y16067	Y16067		AY462179	Y16067
	Scyliorhinus retifer	FJ519584				
	Scyliorhinus stellaris	JN641247			AY462180	AF327706
	Scyliorhinus torazame	EU339365			AY462182	AY462181
	Eusphyra blochii	EU398784	DQ422073	DQ422104		
	Sphyrna corona			GU385349		
	Sphyrna lewini	DQ885127	L08041	U91422		AY958661
	Sphyrna media			GU385348		
	Sphyrna mokarran	EU399017	DQ422072	DQ422103		FJ598665
	Sphyrna tiburo	FJ519284		U91423		FJ598661
	Sphyrna tudes	FJ519524				FJ598662
	Sphyrna zygaena	EU399018				AY830772
	Furgaleus macki	DQ108316	DQ422084	DQ422115		
	Galeorhinus galeus	DQ108308	DQ422087	DQ422118		AY462186
	Hemitriakis falcata	EU398828				
	Hemitriakis japanica		DQ422082	DQ422113		
	Hypogaleus hyugaensis		DQ422088	DQ422119		
	Iago omanensis		DQ422083	DQ422114		
	Mustelus antarcticus	DQ108313				EU848452
	Mustelus asterias	FM164478	DQ422092	DQ422123	AY462188	AY049050
	Mustelus californicus	FJ519211	DQ422093	DQ422124		AY958675
	Mustelus canis	FJ519213	DQ422098	DQ422129		AY830754

	Taxon name	*COI*	*Cytb*	*NADH2*	*Rag1*	*16S*
	Mustelus henlei	FJ519222	DQ422094	DQ422125		EU099503
	Mustelus intermedius		DQ422100	DQ422131		
	Mustelus lenticulatus	DQ108307				
	Mustelus lunulatus	GU125716				HQ010108
	Mustelus manazo	AB015962	AB015962	DQ422130		AB015962
	Mustelus mosis	EU541308	DQ422096	DQ422127		
	Mustelus mustelus	JN641215	DQ422097	DQ422128		AY462189
	Mustelus norrisi		DQ422095	DQ422126		AY830755
	Mustelus punctulatus		AF183926			
	Mustelus schmitti	EU074486	DQ422091	DQ422122		
	Scylliogaleus quecketti	GU805060	DQ422090	DQ422121		
	Triakis megalopterus		DQ422089	DQ422120		
	Triakis scyllium		DQ422086	DQ422117	AY462191	AY462190
	Triakis semifasciata	FJ519290	DQ422085	DQ422116		AY958599
	Heterodontus francisci	FJ519566	AJ310141	AJ310141	JN184089	AJ310141
	Heterodontus galeatus	EU398829				
	Heterodontus portusjacksoni	EU398834				EU848461
	Chlamydoselachus anguineus		D50022			
	Heptranchias perlo	EU869818				AY147888
	Hexanchus griseus	EU398837	DQ132493			AY147887
	Hexanchus vitulus					AY830716
	Notorynchus cepedianus	EU074507	M91186			
	Notorynchus maculatus	HQ010053				AY958614
	Alopias pelagicus	EU398518	U91441	U91431	AF135473	EU099475
	Alopias superciliosus	GU440214	U91443	U91433	AF135481	
	Alopias vulpinus	FJ518987	U91442	U91432		AY147892
	Cetorhinus maximus	FJ519302	U91439	U91429	AF135476	AY462146
	Carcharodon carcharias	DQ108328	DQ082914	U91426	AF135482	AY836586
	Isurus oxyrinchus	EU398893	L08036	U91424	AF135480	AY147894
	Isurus paucus	EU398900	L08037	U91425		AY147895
	Lamna ditropis	FJ519022	U91438	U91428	AF135478	

	Taxon name	*COI*	*Cytb*	*NADH2*	*Rag1*	*16S*
	Lamna nasus	FJ519725	L08038	U91427		AY830753
	Megachasma pelagios	EU398905	U91440	U91430	AF135483	HQ010097
	Mitsukurina owstoni	EU528659	EU528659	EU528659	AF135477	EU528659
	Carcharias taurus	FJ519786	U91447	U91437	AF135475	AY830759
	Odontaspis ferox	FJ519236	U91445	U91435	AY462145	AY462144
	Pseudocarcharias kamoharai	FJ519578	U91446	U91436	AF135479	
	Nebrius ferrugineus	FJ519572				
	Chiloscyllium griseum	FJ583140				
	Chiloscyllium hasseltii	EU398678				
	Chiloscyllium indicum	EU398680				
	Chiloscyllium plagiosum	EU398696	EU363748	FJ853422		JX162601
	Chiloscyllium punctatum	FJ583142				
	Orectolobus cf japonicus	EU398961				
	Orectolobus floridus	EU398963				
	Orectolobus halei	EU398942				EU848471
	Orectolobus hutchinsi	EU398948				
	Orectolobus leptolineatus	EU398962				
	Orectolobus maculatus	EU398953				EU848431
	Orectolobus ornatus	DQ108323				
	Orectolobus parvimaculatus	DQ108331				
	Sutorectus tentaculatus	EU399054				
	Rhincodon typus	EU398993	AM265573			AY496446
	Stegostoma fasciatum	HQ171777				HM239663
	Pliotrema warreni	GU805041				
	Pristiophorus cirratus	EU398981				
	Pristiophorus nudipinnis	DQ108205				AY147885
	Squatina aculeata	FN431671				FN431790
	Squatina africana	FN431673				FN431792
	Squatina albipunctata	EU399043				FN431809
	Squatina armata	FN431694				FN431814
	Squatina australis	DQ108203				
	Squatina californica	FJ519596				FN431849
	Squatina dumeril	FJ519598				FN431857

	Taxon name	*COI*	*Cytb*	*NADH2*	*Rag1*	*16S*
	Squatina formosa	EU399040				FN431860
	Squatina guggenheim	FN431747				FN431867
	Squatina japonica	FN431750				FN431869
	Squatina legnota	EU399042				FN431870
	Squatina occulta	FN431752				FN431871
	Squatina oculata	FN431754				FN431873
	Squatina pseudocellata	EU399045				FN431876
	Squatina squatina	FN431762				AY462192
	Squatina tergocellata	DQ108196				FN431882
	Squatina tergocellatoides	FN431766				FN431885
	Centrophorus atromarginatus	EU398647				
	Centrophorus granulosus	EU003893				AY147884
	Centrophorus isodon	EU398654				
	Centrophorus moluccensis	DQ108227				
	Centrophorus niaukang	DQ108228				
	Centrophorus squamosus	DQ108230			GU130774	GU130628
	Centrophorus zeehaani	EU398659				
	Deania calcea	DQ108223			GU130772	GU130626
	Deania hystricosa	EU148140				
	Deania profundorum					HM239666
	Centrophorus uyato	EU398658				
	Dalatias licha	DQ108221			GU130749	GU130603
	Euprotomicrus bispinatus	DQ521013	DQ082909			AY835658
	Isistius brasiliensis					GU130817
	Squaliolus aliae	GU130675			GU130748	GU130602
	Echinorhinus brucus	HM467790			GU130818	HM239653
	Echinorhinus cookei	DQ521002	M91185			
	Aculeola nigra	GU130678			GU130751	GU130631
	Centroscyllium fabricii	FJ519561			GU130780	
	Centroscyllium granulatum	GU130708			GU130781	GU130635
	Centroscyllium kamohari					HM231289
	Centroscyllium nigrum	GU130705			GU130778	GU130632
	Centroscyllium ritteri	GU130706			GU130779	GU130633

	Taxon name	*COI*	*Cytb*	*NADH2*	*Rag1*	*16S*
	Etmopterus baxteri	DQ108216			GU130810	GU130668
	Etmopterus bigelowi	GU130723			GU130763	GU130650
	Etmopterus brachyurus	GU130716			GU130789	HM231288
	Etmoptedecacuspidatus	GU130684				
	Etmopterus dianthus	GU130693			GU130766	GU130620
	Etmopterus dislineatus	GU130681			GU130754	GU130608
	Etmopterus fusus	GU130687			GU130760	GU130614
	Etmopterus gracilispinis	FJ519564			GU130797	GU130651
	Etmopterus granulosus	GU130737			GU130809	GU130665
	Etmopterus lucifer				GU130756	GU130638
	Etmopterus molleri	GU130710			GU130783	GU130642
	Etmopterus polli	GU130742			GU130815	GU130669
	Etmopterus princeps	FJ519565			GU130800	GU130654
	Etmopterus pseudosqualiolus	GU130686			GU130759	GU130613
	Etmopterus pusillus	EU869809			GU130762	GU130649
	Etmopterus schultzi	GU130719			GU130792	GU130646
	Etmopterus sentosus	GU130720			GU130793	GU130647
	Etmopterus sheikoi	GU130680			GU130782	GU130636
	Etmopterus spinax	GU130725			GU130764	GU130653
	Etmopterus splendidus					HM231283
	Etmopterus unicolor	GU130739			GU130814	GU130666
	Etmopterus virens	GU130743			GU130816	GU130670
	Trigonognathus kabeyai	GU130702			GU130775	GU130629
	Oxynotus centrina	JF834320				
	Oxynotus paradoxus	GU130674			GU130747	GU130601
	Centroscymnus coelolepis	DQ108219				
	Centroscymnus owstoni	EU003886			GU130768	GU130622
	Centroscymnus plunketi	GU130696				GU130623
	Centroselachus crepidater	GU130694			GU130767	GU130621
	Scymnodon ringens	GU130697			GU130770	GU130624
	Somniosus antarcticus		EF090963			
	Somniosus microcephalus	GU130677	EF090949		GU130750	GU130604

	Taxon name	*COI*	*Cytb*	*NADH2*	*Rag1*	*16S*
	Somniosus pacificus	FJ165366	EF090962			AY835659
	Somniosus rostratus					AY462193
	Zameus squamulosus	DQ108217				
	Cirrhigaleus australis	DQ108220				
	Cirrhigaleus barbifer	EU398719				
	Squalus acanthias	EF539278	Y18134	Y18134		EF119335
	Squalus albifrons	DQ108256				
	Squalus brevirostris	EF539297				
	Squalus chloroculus	DQ108261				
	Squalus crassispinus	DQ108248				
	Squalus cubensis	FJ519595				
	Squalus edmundsi	EF539305				
	Squalus grahami	DQ108236				
	Squalus hemipinnis	EF539308				
	Squalus japonicus	EF539314	D50026			
	Squalus megalops	EU399029			GU130771	GU130625
	Squalus mitsukurii	EU074610				AF288198
	Squalus montalbani	DQ108274				
	Squalus nasutus	DQ108250				
	Squalus suckleyi	FJ379933				
Outgroup taxa						
	Callorhinchus callorynchus	EU074378				
	Chimaera monstrosa	AJ310140	AJ310140	AJ310140		
	Manta birostris	EU398902				JN184248
	Amblyraja radiata	AF106038	AF106038	AF106038		

Table A3-S2: Fossil calibration points used for timetree inference.

Calibration point	**Fossil - minimum age**	**Age (Ma)**	**References**	**Fossil - soft upper bound**	**Age (Ma)**	**References**	**Prior (offset; mean)**
MRCA of Chimaeriformes and Neoselachii	oldest chimaeroid	374	Capetta 1993	Burgess Shale stem chordates	505		374; 13.7
MRCA of Batoids and sharks	fossil Synechodontiformes	204	Underwood 2006	oldest chimaeroid	374	Capetta 1993	204; 57
MCRA of Squalimorpha	Hexanchidae s.l.	190	Underwood 2006	fossil Synechodontiformes	204	Underwood 2006	190; 20.4
MRCA of Squatiniformes	*Squatina* sp.	151	Underwood 2006	fossil Synechodontiformes	204	Underwood 2006	151; 17.7
MRCA of Squaliformes	*Protosqualus*	130	Klug & Kriwet 2010	*Squatina* sp.	151	Underwood 2006	130; 7
MRCA of Etmopteridae	*Etmopterus*	48.6	Klug & Kriwet 2010	*Protosqualus*	130	Klug & Kriwet 2010	48.6; 27.2
MRCA of Centrophoridae	*Centrophorus*	89	Klug & Kriwet 2010	*Protosqualus*	130	Klug & Kriwet 2010	89; 13.7
MRCA of Squalidae	*Squalus*	98	Klug & Kriwet 2010	*Protosqualus*	130	Klug & Kriwet 2010	98; 10.7
MRCA of Lamniformes minus *Mitsukurina*	*Carcharias* sp.	125	Underwood 2006	unnamed Hemiscyllidae	176	Underwood 2006	125; 17
MRCA of *Carcharodon* + *Isurus*	fossil *Carcharodon*	56	Purdy 1996	*Carcharias* sp.	125	Underwood 2006	56; 23
MRCA of *Megachasmidae* + *Odontaspis*	*Megachasma pelagios*	95	Shimada 2007	*Carcharias* sp.	125	Underwood 2006	95; 10
MRCA of Carcharhiniformes	*Paleoscyllium tenuidens*	165	Underwood 2006	unnamed Hemiscyllidae	176	Underwood 2006	165; 8.5
MRCA of Triakidae + Carcharhinidae + Sphyrnidae + Leptochariidae + Hemigaleidae	*Paratriakis*	130	Maisey 2004, Underwood 2006	*Paleoscyllium tenuidens*	165	Underwood 2006	130; 11.7
MRCA of Carcharhinidae + Sphyrnidae	*Abdounia africana*	59	Maisey 2004	*Paratriakis*	130	Maisey 2004, Underwood 2006	59; 10.1

Table A3-S3: Monophyly constraints used for timetree inference.

Monophyly constraints (no fossil calibration)	
1	Alopiidae
2	*Somnniosus*
3	Orectolobidae + *Sutorectus*
4	Selachii
5	*Lamna*
6	Heterodontidae
7	Hemigaleidae (*Chanogaleus macrostoma* + *Hemigaleus australiensis* + *H. microstoma*)
8	Orectolobiformes
9	Pristiophoriformes
10	Echinorhinidae
11	Dalatiidae
12	Sphyrnidae
13	Lamniformes
14	Hexanchiformes
15	Hexanchiformes
16	*Squatina armata* + *S. californica* + *S. dumeril* + *S. guggenheim* + *S. occulta*
17	*Squatina californica* + *S. dumeril* + *S. guggenheim* + *S. occulta*
18	*Squatina australis* + *S. albipunctata S. pseudocellata* + *S. tergocellata*
19	*Squatina oculata* + *S. aculeata* + *S. squatina* + *S. japonica* + *S. tergocellatoides* + *S. legnota* + *S. formosa*
20	Lamnidae
21	Rhincodontidae + Ginglystomatidae + Stegostomidae
22	Orectolobiformes - Orectolobidae
23	Hexanchidae
24	*Squaliolus aliae* + *Euprotomicrus bispinatus*
25	*Isistius brasiliensis* + *Dalatias licha*
26	*Deania*
27	*Isurus*
28	*Poroderma panterhinum* + *Scyliorhinus retifer* + *S. stellaris* + *S. canicula* + *S. torazame* + *Cephaloscyllium*
29	*Apristurus exsanguis* + *A. japonicus* + *A. platyrhynchus* + *A. melanoasper* + *A. laurussoni* + *A. brunneus*
30	*Apristurus australis* + *A. longicephalus* + *A. aphyodes* + *A. kampae* + *A. fedorovi* + *A. profundorum* + *A. pinguis* + *A. manis* + *A. microps* + *A. albisoma*
31	*Atelomycterus* + *Aulohalaelurus labiosus*
32	*Negaprion*
33	*Carcharhinus tilstoni* + *C. limbatus* + *C. amblyrhynchoides* + *C. fitzroyensis* + *C. melanopterus* + *C. cautus*

Table A3-S4: Taxa and habitat preference data used for habitat stochastic mapping. Taxa were scored as shelf, deepwater (occurrence at depths > 200 m), and pelagic.

Taxon name	**Habitat**
Chlamydoselachus anguineus	deepwater
Notorynchus cepedianus	shelf
Hexanchus griseus	deepwater
Heptranchias perlo	deepwater
Pliotrema warreni	deepwater
Pristiophorus cirratus	deepwater
Pristiophorus nudipinnis	shelf
Squatina africana	deepwater
Squatina squatina	shelf
Squatina aculeata	deepwater
Squatina oculata	shelf
Squatina tergocellatoides	shelf
Squatina japonica	shelf
Squatina legnota	deepwater
Squatina formosa	shelf
Squatina australis	shelf
Squatina albipunctata	deepwater
Squatina tergocellata	deepwater
Squatina pseudocellata	deepwater
Squatina armata	shelf
Squatina californica	shelf
Squatina dumeril	deepwater
Squatina guggenheim	shelf
Squatina occulta	shelf
Echinorhinus brucus	deepwater
Echinorhinus cookei	deepwater
Euprotomicrus bispinatus	pelagic
Squaliolus aliae	deepwater
Isistius brasiliensis	pelagic
Dalatias licha	deepwater
Zameus squamulosus	deepwater
Scymnodon ringens	deepwater
Oxynotus paradoxus	deepwater

Taxon name	Habitat
Oxynotus centrina	deepwater
Centroscymnus owstonii	deepwater
Centroscymnus coelolepis	deepwater
Centroscymnus plunketi	deepwater
Deania profundorum	deepwater
Deania hystricosa	deepwater
Deania calcea	deepwater
Centrophorus squamosus	deepwater
Centrophorus granulosus	deepwater
Centrophorus niaukang	deepwater
Centrophorus moluccensis	deepwater
Centrophorus isodon	deepwater
Centrophorus atromarginatus	deepwater
Centrophorus zeehaani	deepwater
Centrophorus uyato	deepwater
Squalus megalops	deepwater
Squalus brevirostris	shelf
Cirrhigaleus australis	deepwater
Cirrhigaleus barbifer	deepwater
Squalus acanthias	shelf
Squalus suckleyi	shelf
Squalus crassispinus	deepwater
Squalus hemipinnis	deepwater
Squalus edmundsi	deepwater
Squalus albifrons	deepwater
Squalus japonicus	deepwater
Squalus nasutus	deepwater
Squalus grahami	deepwater
Squalus cubensis	deepwater
Squalus chloroculus	deepwater
Squalus montalbani	deepwater
Squalus mitsukurii	deepwater
Somniosus rostratus	deepwater
Somniosus microcephalus	deepwater
Somniosus pacificus	deepwater
Somniosus antarcticus	deepwater
Aculeola nigra	deepwater
Centroscyllium kamoharai	deepwater
Centroscyllium fabricii	deepwater

Taxon name	Habitat
Centroscyllium ritteri	deepwater
Centroscyllium granulatum	deepwater
Centroscyllium nigrum	deepwater
Trigonognathus kabeyai	deepwater
Etmopterus lucifer	deepwater
Etmopterus molleri	deepwater
Etmopterus dislineatus	deepwater
Etmopterus brachyurus	deepwater
Etmopterus decacuspidatus	deepwater
Miroscyllium sheikoi	deepwater
Etmopterus bigelowi	deepwater
Etmopterus pusillus	deepwater
Etmopterus sentosus	deepwater
Etmopterus pseudosqualiolus	deepwater
Etmopterus splendidus	deepwater
Etmopterus fusus	deepwater
Etmopterus virens	deepwater
Etmopterus schultzi	deepwater
Etmopterus polli	deepwater
Etmopterus gracilispinis	deepwater
Etmopterus dianthus	deepwater
Etmopterus unicolor	deepwater
Etmopterus baxteri	deepwater
Etmopterus granulosus	deepwater
Etmopterus princeps	deepwater
Etmopterus spinax	deepwater
Heterodontus francisci	shelf
Heterodontus portusjacksoni	shelf
Heterodontus galeatus	shelf
Rhincodon typus	pelagic
Stegostoma fasciatum	shelf
Nebrius ferrugineus	shelf
Chiloscyllium punctatum	shelf
Chiloscyllium griseum	shelf
Chiloscyllium hasseltii	shelf
Chiloscyllium indicum	shelf
Chiloscyllium plagiosum	shelf
Orectolobus ornatus	shelf
Orectolobus floridus	shelf

Taxon name	Habitat
Sutorectus tentaculatus	shelf
Orectolobus parvimaculatus	shelf
Orectolobus hutchinsi	shelf
Orectolobus halei	shelf
Orectolobus maculatus	shelf
Orectolobus japonicus	shelf
Orectolobus leptolineatus	shelf
Mitsukurina owstoni	deepwater
Pseudocarcharias kamoharai	pelagic
Odontaspis ferox	deepwater
Megachasma pelagios	pelagic
Alopias pelagicus	pelagic
Alopias superciliosus	pelagic
Alopias vulpinus	pelagic
Carcharias taurus	shelf
Cetorhinus maximus	pelagic
Lamna ditropis	pelagic
Lamna nasus	pelagic
Carcharodon carcharias	shelf
Isurus oxyrinchus	pelagic
Isurus paucus	pelagic
Proscyllium habereri	shelf
Pseudotriakis microdon	deepwater
Gollum attenuatus	deepwater
Schroederichthys bivius	shelf
Atelomycterus marmoratus	shelf
Atelomycterus baliensis	shelf
Aulohalaelurus labiosus	shelf
Atelomycterus marnkalha	shelf
Atelomycterus fasciatus	shelf
Holohalaelurus punctatus	deepwater
Halaelurus lineatus	shelf
Parmaturus xaniurus	deepwater
Galeus sauteri	shelf
Galeus eastmani	deepwater
Galeus polli	deepwater
Galeus murinus	deepwater
Figaro boardmani	deepwater
Asymbolus parvus	shelf

Taxon name	Habitat
Galeus melastomus	deepwater
Galeus atlanticus	deepwater
Asymbolus rubiginosus	deepwater
Apristurus longicephalus	deepwater
Apristurus australis	deepwater
Apristurus aphyodes	deepwater
Apristurus kampae	deepwater
Apristurus fedorovi	deepwater
Apristurus manis	deepwater
Apristurus albisoma	deepwater
Apristurus microps	deepwater
Apristurus profundorum	deepwater
Apristurus pinguis	deepwater
Apristurus exsanguis	deepwater
Apristurus japonicus	deepwater
Apristurus platyrhynchus	deepwater
Apristurus melanoasper	deepwater
Apristurus laurussonii	deepwater
Apristurus brunneus	deepwater
Scyliorhinus retifer	deepwater
Scyliorhinus canicula	shelf
Scyliorhinus stellaris	shelf
Scyliorhinus torazame	deepwater
Poroderma pantherinum	shelf
Cephaloscyllium ventriosum	shelf
Cephaloscyllium silasi	deepwater
Cephaloscyllium umbratile	shelf
Cephaloscyllium variegatum	deepwater
Cephaloscyllium sufflans	deepwater
Cephaloscyllium speccum	deepwater
Cephaloscyllium laticeps	shelf
Cephaloscyllium albipinnum	deepwater
Cephaloscyllium fasciatum	deepwater
Cephaloscyllium hiscosellum	deepwater
Leptocharias smithii	shelf
Iago omanensis	deepwater
Galeorhinus galeus	shelf
Hypogaleus hyugaensis	shelf
Triakis semifasciata	shelf

Taxon name	Habitat
Triakis scyllium	shelf
Furgaleus macki	shelf
Hemitriakis japanica	shelf
Hemitriakis falcata	shelf
Mustelus norrisi	shelf
Mustelus mosis	shelf
Mustelus mustelus	shelf
Mustelus lunulatus	shelf
Mustelus californicus	shelf
Mustelus canis	shelf
Mustelus henlei	shelf
Mustelus punctulatus	shelf
Scylliogaleus quecketti	shelf
Triakis megalopterus	shelf
Mustelus schmitti	shelf
Mustelus manazo	shelf
Mustelus asterias	shelf
Mustelus lenticulatus	shelf
Mustelus antarcticus	shelf
Chaenogaleus macrostoma	shelf
Hemigaleus australiensis	shelf
Hemigaleus microstoma	shelf
Galeocerdo cuvier	shelf
Eusphyra blochii	shelf
Sphyrna zygaena	shelf
Sphyrna mokarran	shelf
Sphyrna lewini	shelf
Sphyrna corona	shelf
Sphyrna tiburo	shelf
Sphyrna tudes	shelf
Sphyrna media	shelf
Loxodon macrorhinus	shelf
Scoliodon laticaudus	shelf
Rhizoprionodon taylori	shelf
Rhizoprionodon acutus	shelf
Rhizoprionodon lalandii	shelf
Rhizoprionodon porosus	shelf
Rhizoprionodon terraenovae	shelf
Carcharhinus signatus	pelagic

Taxon name	Habitat
Negaprion acutidens	shelf
Negaprion brevirostris	shelf
Lamiopsis temminckii	shelf
Glyphis garricki	shelf
Glyphis glyphis	shelf
Carcharhinus cautus	shelf
Carcharhinus melanopterus	shelf
Carcharhinus fitzroyensis	shelf
Carcharhinus limbatus	shelf
Carcharhinus tilstoni	shelf
Carcharhinus amblyrhynchoides	shelf
Carcharhinus altimus	shelf
Carcharhinus plumbeus	shelf
Carcharhinus albimarginatus	shelf
Carcharhinus falciformis	pelagic
Prionace glauca	pelagic
Carcharhinus amblyrhynchos	shelf
Carcharhinus brachyurus	shelf
Carcharhinus brevipinna	shelf
Triaenodon obesus	shelf
Carcharhinus amboinensis	shelf
Carcharhinus leucas	shelf
Carcharhinus isodon	shelf
Carcharhinus acronotus	shelf
Nasolamia velox	shelf
Carcharhinus macloti	shelf
Isogomphodon oxyrhynchus	shelf
Carcharhinus porosus	shelf
Carcharhinus sealei	shelf
Carcharhinus dussumieri	shelf
Carcharhinus sorrah	shelf
Carcharhinus perezii	shelf
Carcharhinus longimanus	pelagic
Carcharhinus obscurus	shelf
Carcharhinus galapagensis	shelf

Table A3-S5: Carcharhinid taxa and habitat preference data used for the ancestral state reconstruction. Taxa were scored as brackish, shelf, reef-associated, or coastal-pelagic.

Taxon name	Habitat
Carcharhinus acronotus	reef
Carcharhinus albimarginatus	reef
Carcharhinus altimus	reef
Carcharhinus amblyrhynchoides	coastal-pelagic
Carcharhinus amblyrhynchos	reef
Carcharhinus amboinensis	reef
Carcharhinus brachyurus	reef
Carcharhinus brevipinna	reef
Carcharhinus cautus	reef
Carcharhinus dussumieri	reef
Carcharhinus falciformis	reef
Carcharhinus fitzroyensis	shelf
Carcharhinus galapagensis	reef
Carcharhinus isodon	shelf
Carcharhinus leucas	reef
Carcharhinus limbatus	reef
Carcharhinus longimanus	coastal-pelagic
Carcharhinus macloti	shelf
Carcharhinus melanopterus	reef
Carcharhinus obscurus	reef
Carcharhinus perezii	reef
Carcharhinus plumbeus	coastal-pelagic
Carcharhinus porosus	brackish
Carcharhinus sealei	reef
Carcharhinus signatus	coastal-pelagic
Carcharhinus sorrah	reef
Carcharhinus tilstoni	shelf
Glyphis garricki	brackish
Glyphis glyphis	brackish
Isogomphodon oxyrhynchus	brackish
Lamiopsis temminckii	brackish
Loxodon macrorhinus	shelf
Nasolamia velox	shelf
Negaprion acutidens	reef
Negaprion brevirostris	reef
Prionace glauca	coastal-pelagic
Rhizoprionodon acutus	shelf
Rhizoprionodon lalandii	shelf
Rhizoprionodon porosus	reef
Rhizoprionodon taylori	coastal-pelagic
Rhizoprionodon terraenovae	brackish
Scoliodon laticaudus	brackish
Triaenodon obesus	reef

Figure A3-S1: RAxML tree topology based on concatenated gene sequences. Nodes with ≥ 90% bootstrap support (bsp) are indicated in black, nodes between 65 and 90% bsp are indicated in gray, and bsp < 65% are indicated in white.

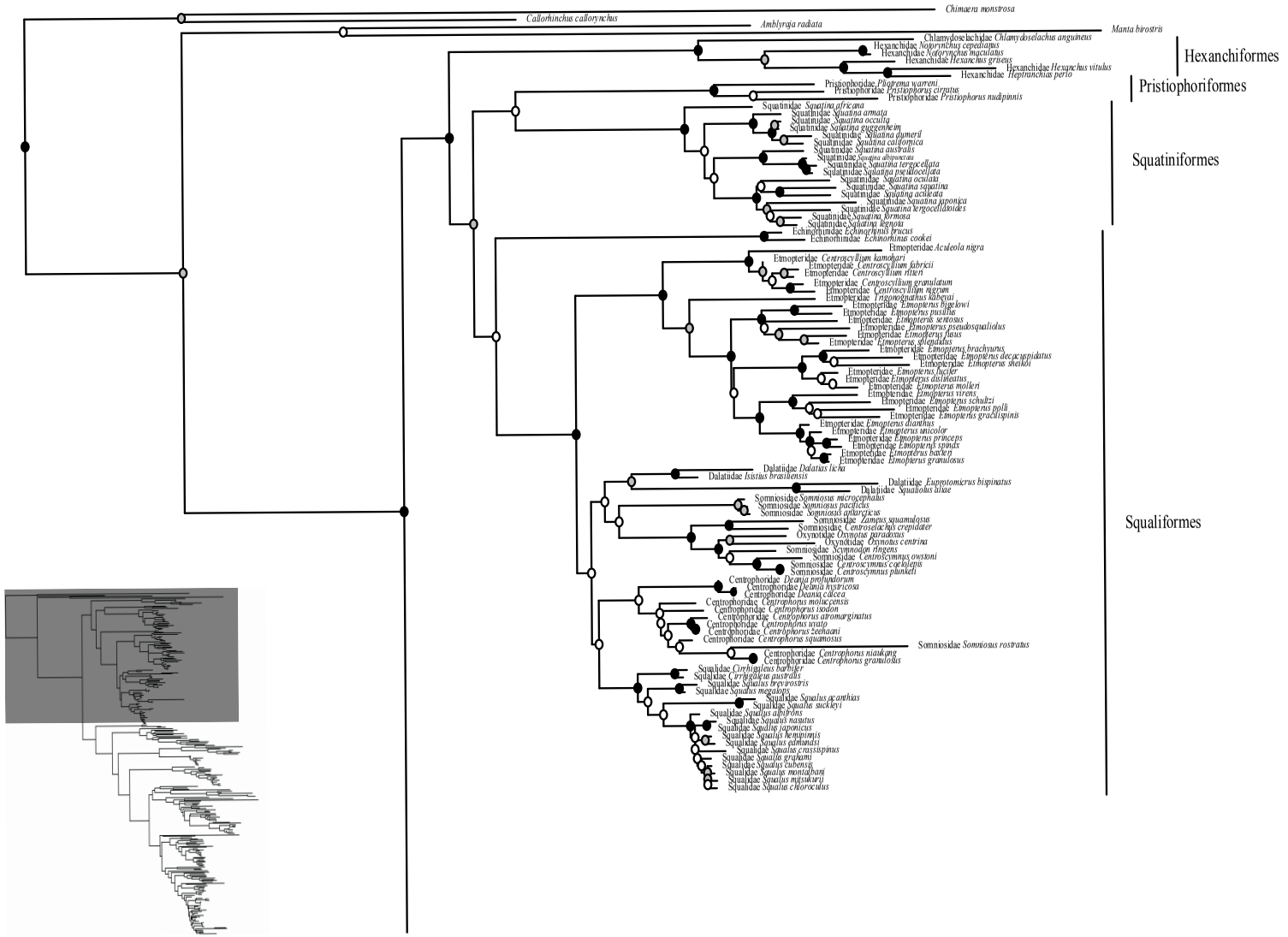

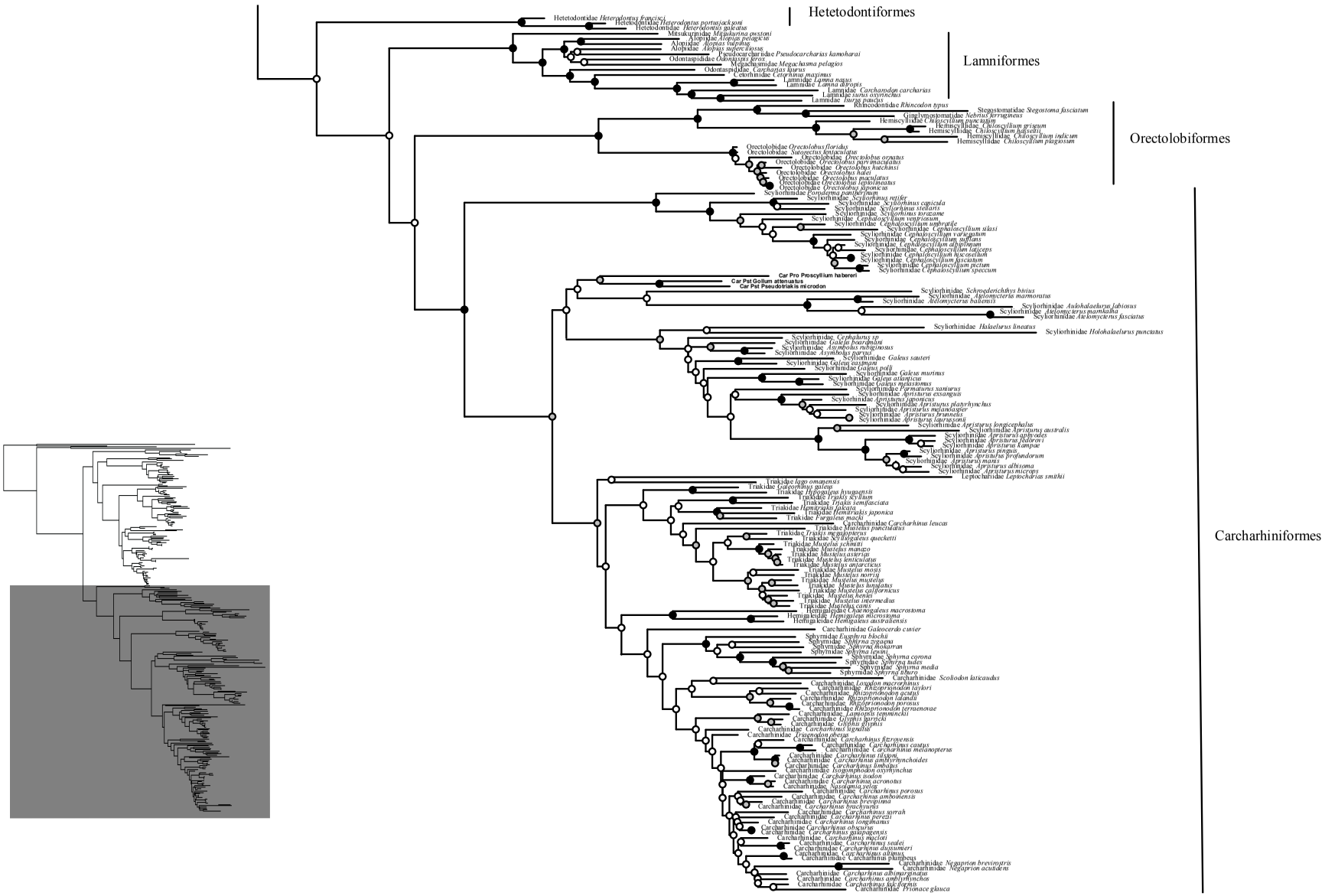
Hetetodontiformes
Lamniformes
Orectolobiformes
Carcharhiniformes
Hetetodontidae Heterodontus francisci
Hetetodontidae Heterodontus portusjacksoni
Hetetodontidae Heterodontus galeatus
Mitsukurinidae Mitsukurina owstoni
Alopiidae Alopias pelagicus
Alopiidae Alopias vulpinus
Alopiidae Alopias superciliosus
Pseudocarchariidae Pseudocarcharias kamoharai
Odontaspididae Odontaspis ferox
Megachasmidae Megachasma pelagios
Odontaspididae Carcharias taurus
Cetorhinidae Cetorhinus maximus
Lamnidae Lamna nasus
Lamnidae Lamna ditropis
Lamnidae Carcharodon carcharias
Lamnidae Isurus oxyrinchus
Lamnidae Isurus paucus
Rhincodontidae Rhincodon typus
Stegostomatidae Stegostoma fasciatum
Ginglymostomatidae Nebrius ferrugineus
Hemiscyllidae Chiloscyllium punctatum
Hemiscyllidae Chiloscyllium griseum
Hemiscyllidae Chiloscyllium hasselti
Hemiscyllidae Chiloscyllium indicum
Hemiscyllidae Chiloscyllium plagiosum
Orectolobidae Orectolobus floridus
Orectolobidae Sutorectus tentaculatus
Orectolobidae Orectolobus ornatus
Orectolobidae Orectolobus parvimaculatus
Orectolobidae Orectolobus hutchinsi
Orectolobidae Orectolobus halei
Orectolobidae Orectolobus maculatus
Orectolobidae Orectolobus leptolineatus
Orectolobidae Orectolobus japonicus
Scyliorhinidae Poroderma pantherinum
Scyliorhinidae Scyliorhinus retifer
Scyliorhinidae Scyliorhinus capicola
Scyliorhinidae Scyliorhinus stellaris
Scyliorhinidae Scyliorhinus torazame
Scyliorhinidae Cephaloscyllium ventriosum
Scyliorhinidae Cephaloscyllium umbratile
Scyliorhinidae Cephaloscyllium silasi
Scyliorhinidae Cephaloscyllium variegatum
Scyliorhinidae Cephaloscyllium suffluns
Scyliorhinidae Cephaloscyllium albipinnum
Scyliorhinidae Cephaloscyllium laticeps
Scyliorhinidae Cephaloscyllium hiscosellum
Scyliorhinidae Cephaloscyllium fasciatum
Scyliorhinidae Cephaloscyllium pictum
Scyliorhinidae Cephaloscyllium speccum
Car Pro Proscyllium habereri
Car Pst Gollum attenuatus
Car Pst Pseudotriakis microdon
Scyliorhinidae Schroederichthys bivius
Scyliorhinidae Apristurus marmoratus
Scyliorhinidae Atelomycterus baliensis
Scyliorhinidae Aulohalaelurus labiosus
Scyliorhinidae Atelomycterus marmakha
Scyliorhinidae Atelomycterus fasciatus
Scyliorhinidae Halaelurus lineatus
Scyliorhinidae Holohalaelurus punctatus
Scyliorhinidae Cephalurus sp
Scyliorhinidae Galeus boardmani
Scyliorhinidae Asymbolus rubiginosus
Scyliorhinidae Asymbolus parvus
Scyliorhinidae Galeus sauteri
Scyliorhinidae Galeus eastmani
Scyliorhinidae Galeus polli
Scyliorhinidae Galeus murinus
Scyliorhinidae Galeus atlanticus
Scyliorhinidae Galeus melastomus
Scyliorhinidae Parmaturus xaniurus
Scyliorhinidae Apristurus exasperatus
Scyliorhinidae Apristurus japonicus
Scyliorhinidae Apristurus platyrhynchus
Scyliorhinidae Apristurus melanoasper
Scyliorhinidae Apristurus laurussoni
Scyliorhinidae Apristurus longicephalus
Scyliorhinidae Apristurus australis
Scyliorhinidae Apristurus aphyodes
Scyliorhinidae Apristurus fedorovi
Scyliorhinidae Apristurus kampae
Scyliorhinidae Apristurus pinguis
Scyliorhinidae Apristurus profundorum
Scyliorhinidae Apristurus manis
Scyliorhinidae Apristurus albisoma
Scyliorhinidae Apristurus microps
Leptocharias smithii
Triakidae Iago omanensis
Triakidae Galeorhinus galeus
Triakidae Hypogaleus hyugaensis
Triakidae Triakis scyllium
Triakidae Triakis semifasciata
Triakidae Hemitriakis falcata
Triakidae Hemitriakis japonica
Triakidae Furgaleus macki
Carcharhinidae Carcharhinus leucas
Triakidae Mustelus punctulatus
Triakidae Triakis megalopterus
Triakidae Scylliogaleus quecketti
Triakidae Mustelus schmitti
Triakidae Mustelus manazo
Triakidae Mustelus asterias
Triakidae Mustelus lenticulatus
Triakidae Mustelus antarcticus
Triakidae Mustelus lenticulatus
Triakidae Mustelus canis
Triakidae Mustelus mustelus
Triakidae Mustelus lunulatus
Triakidae Mustelus californicus
Triakidae Mustelus henlei
Triakidae Mustelus intermedius
Triakidae Mustelus canis
Hemigaleidae Chaenogaleus macrostoma
Hemigaleidae Hemigaleus microstoma
Hemigaleidae Hemigaleus australiensis
Carcharhinidae Galeocerdo cuvier
Sphyrnidae Eusphyra blochii
Sphyrnidae Sphyrna zygaena
Sphyrnidae Sphyrna tiburo
Sphyrnidae Sphyrna lewini
Sphyrnidae Sphyrna corona
Sphyrnidae Sphyrna tudes
Sphyrnidae Sphyrna media
Sphyrnidae Sphyrna mokarran
Carcharhinidae Scoliodon laticaudus
Carcharhinidae Loxodon macrorhinus
Carcharhinidae Rhizoprionodon taylori
Carcharhinidae Rhizoprionodon acutus
Carcharhinidae Rhizoprionodon porosus
Carcharhinidae Rhizoprionodon ternatensis
Carcharhinidae Lamiopsis temminckii
Carcharhinidae Glyphis sp
Carcharhinidae Glyphis glyphis
Carcharhinidae Carcharhinus signatus
Carcharhinidae Triaenodon obesus
Carcharhinidae Carcharhinus fitzroyensis
Carcharhinidae Carcharhinus cautus
Carcharhinidae Carcharhinus melanopterus
Carcharhinidae Carcharhinus sp
Carcharhinidae Carcharhinus amblyrhynchoides
Carcharhinidae Carcharhinus limbatus
Carcharhinidae Isogomphodon oxyrhynchus
Carcharhinidae Carcharhinus isodon
Carcharhinidae Carcharhinus acronotus
Carcharhinidae Negaprion acutidens
Carcharhinidae Carcharhinus porosus
Carcharhinidae Carcharhinus amboinensis
Carcharhinidae Carcharhinus brevipinna
Carcharhinidae Carcharhinus brachyurus
Carcharhinidae Carcharhinus sorrah
Carcharhinidae Carcharhinus perezi
Carcharhinidae Carcharhinus longimanus
Carcharhinidae Carcharhinus obscurus
Carcharhinidae Carcharhinus galapagensis
Carcharhinidae Carcharhinus leucas
Carcharhinidae Carcharhinus dussumieri
Carcharhinidae Carcharhinus albimarginatus
Carcharhinidae Carcharhinus amblyrhynchos
Carcharhinidae Carcharhinus falciformis
Carcharhinidae Prionace glauca

Figure A3-S2: Bayesian timetree inferred using BEAST and concatenated gene sequences with individual partitions. Black circles indicate monophyly constraints and black circles with numbers indicate shark fossil calibration points. Calibration point numbers refer to Table S2 fossils. Outgroups and associated fossil calibrations not shown.

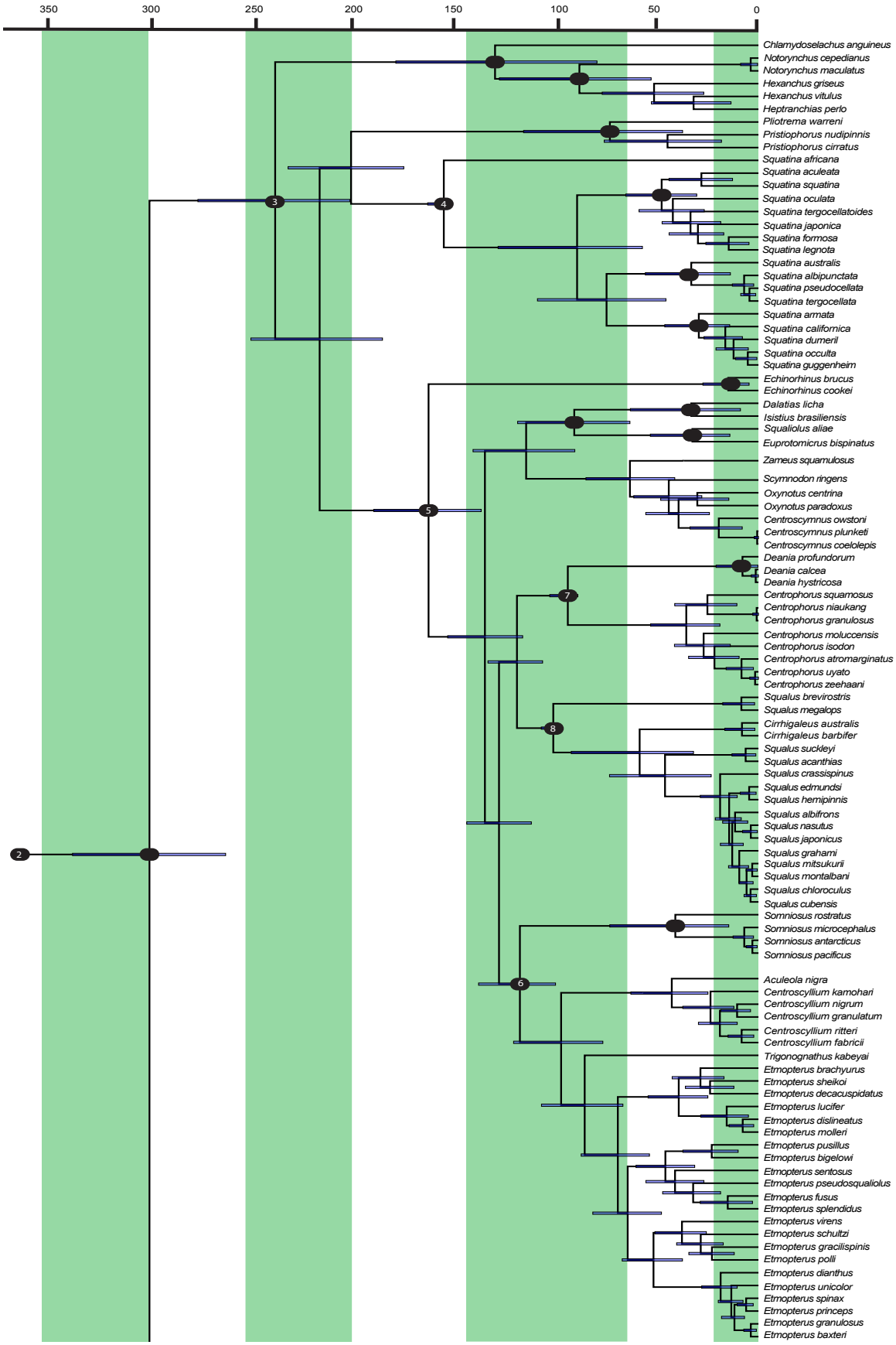
350
300
250
200
150
100
50
0
2
3
4
5
6
7
8
Chlamydoselachus anguineus
Notorynchus cepedianus
Notorynchus maculatus
Hexanchus griseus
Hexanchus vitulus
Heptranchias perlo
Pliotrema warreni
Pristiophorus nudipinnis
Pristiophorus cirratus
Squatina africana
Squatina aculeata
Squatina squatina
Squatina oculata
Squatina tergocellatoides
Squatina japonica
Squatina formosa
Squatina legnota
Squatina australis
Squatina albipunctata
Squatina pseudocellata
Squatina tergocellata
Squatina armata
Squatina californica
Squatina dumeril
Squatina occulta
Squatina guggenheim
Echinorhinus brucus
Echinorhinus cookei
Dalatias licha
Isistius brasiliensis
Squaliolus aliae
Euprotomicrus bispinatus
Zameus squamulosus
Scymnodon ringens
Oxynotus centrina
Oxynotus paradoxus
Centroscymnus owstoni
Centroscymnus plunketi
Centroscymnus coelolepis
Deania profundorum
Deania calcea
Deania hystricosa
Centrophorus squamosus
Centrophorus niaukang
Centrophorus granulosus
Centrophorus moluccensis
Centrophorus isodon
Centrophorus atromarginatus
Centrophorus uyato
Centrophorus zeehaani
Squalus brevirostris
Squalus megalops
Cirrhigaleus australis
Cirrhigaleus barbifer
Squalus suckleyi
Squalus acanthias
Squalus crassispinus
Squalus edmundsi
Squalus hemipinnis
Squalus albifrons
Squalus nasutus
Squalus japonicus
Squalus grahami
Squalus mitsukurii
Squalus montalbani
Squalus chloroculus
Squalus cubensis
Somniosus rostratus
Somniosus microcephalus
Somniosus antarcticus
Somniosus pacificus
Aculeola nigra
Centroscyllium kamohari
Centroscyllium nigrum
Centroscyllium granulatum
Centroscyllium ritteri
Centroscyllium fabricii
Trigonognathus kabeyai
Etmopterus brachyurus
Etmopterus sheikoi
Etmopterus decacuspidatus
Etmopterus lucifer
Etmopterus dislineatus
Etmopterus molleri
Etmopterus pusillus
Etmopterus bigelowi
Etmopterus sentosus
Etmopterus pseudosqualiolus
Etmopterus fusus
Etmopterus splendidus
Etmopterus virens
Etmopterus schultzi
Etmopterus gracilispinis
Etmopterus polli
Etmopterus dianthus
Etmopterus unicolor
Etmopterus spinax
Etmopterus princeps
Etmopterus granulosus
Etmopterus baxteri

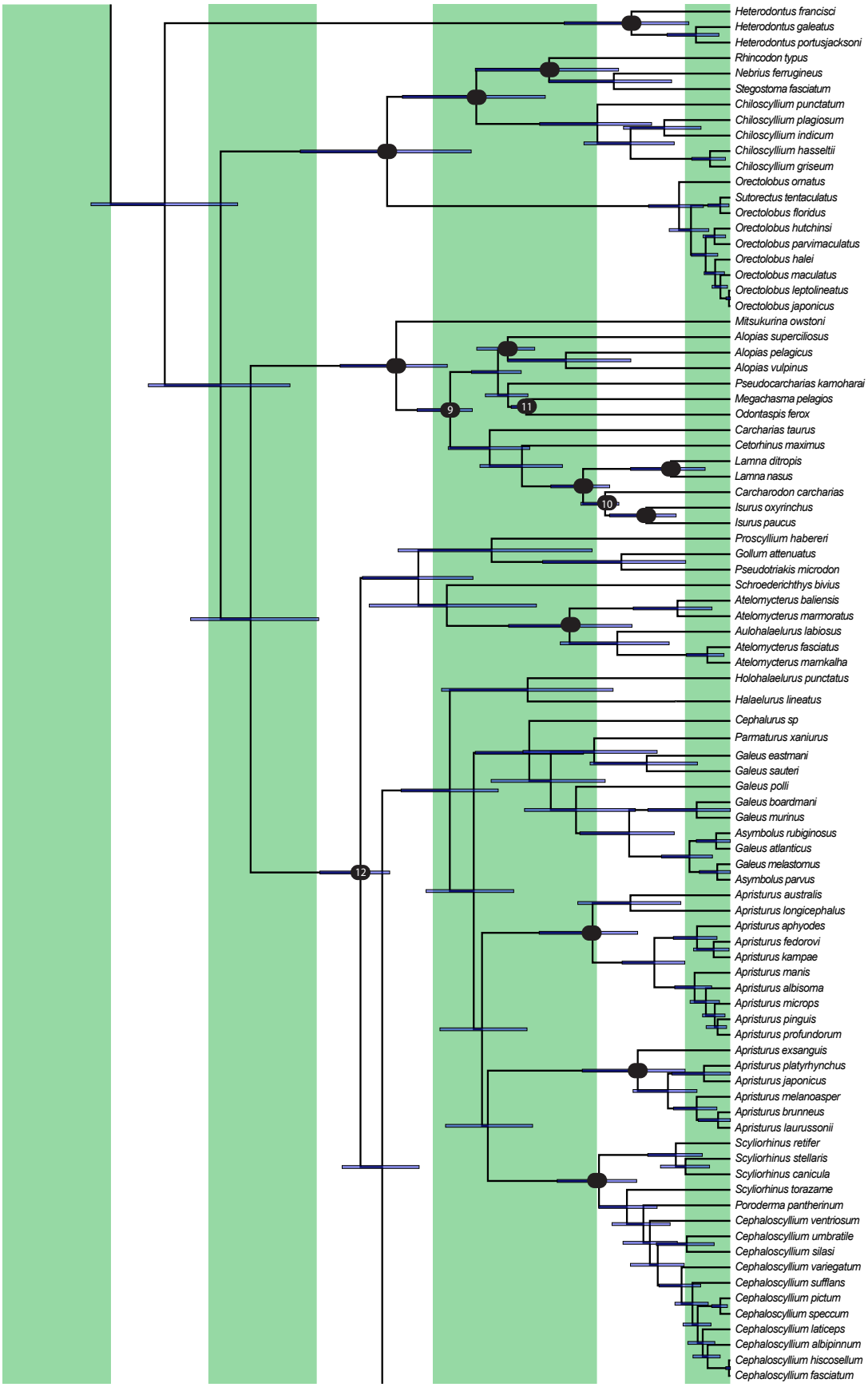
Heterodontus francisci
Heterodontus galeatus
Heterodontus portusjacksoni
Rhincodon typus
Nebrius ferrugineus
Stegostoma fasciatum
Chiloscyllium punctatum
Chiloscyllium plagiosum
Chiloscyllium indicum
Chiloscyllium hasseltii
Chiloscyllium griseum
Orectolobus ornatus
Sutorectus tentaculatus
Orectolobus floridus
Orectolobus hutchinsi
Orectolobus parvimaculatus
Orectolobus halei
Orectolobus maculatus
Orectolobus leptolineatus
Orectolobus japonicus
Mitsukurina owstoni
Alopias superciliosus
Alopias pelagicus
Alopias vulpinus
Pseudocarcharias kamoharai
Megachasma pelagios
Odontaspis ferox
Carcharias taurus
Cetorhinus maximus
Lamna ditropis
Lamna nasus
Carcharodon carcharias
Isurus oxyrinchus
Isurus paucus
Proscyllium habereri
Gollum attenuatus
Pseudotriakis microdon
Schroederichthys bivius
Atelomycterus baliensis
Atelomycterus marmoratus
Aulohalaelurus labiosus
Atelomycterus fasciatus
Atelomycterus marnkalha
Holohalaelurus punctatus
Halaelurus lineatus
Cephalurus sp
Parmaturus xaniurus
Galeus eastmani
Galeus sauteri
Galeus polli
Galeus boardmani
Galeus murinus
Asymbolus rubiginosus
Galeus atlanticus
Galeus melastomus
Asymbolus parvus
Apristurus australis
Apristurus longicephalus
Apristurus aphyodes
Apristurus fedorovi
Apristurus kampae
Apristurus manis
Apristurus albisoma
Apristurus microps
Apristurus pinguis
Apristurus profundorum
Apristurus exsanguis
Apristurus platyrhynchus
Apristurus japonicus
Apristurus melanoasper
Apristurus brunneus
Apristurus laurussonii
Scyliorhinus retifer
Scyliorhinus stellaris
Scyliorhinus canicula
Scyliorhinus torazame
Poroderma pantherinum
Cephaloscyllium ventriosum
Cephaloscyllium umbratile
Cephaloscyllium silasi
Cephaloscyllium variegatum
Cephaloscyllium sufflans
Cephaloscyllium pictum
Cephaloscyllium speccum
Cephaloscyllium laticeps
Cephaloscyllium albipinnum
Cephaloscyllium hiscosellum
Cephaloscyllium fasciatum
9
10
11
12

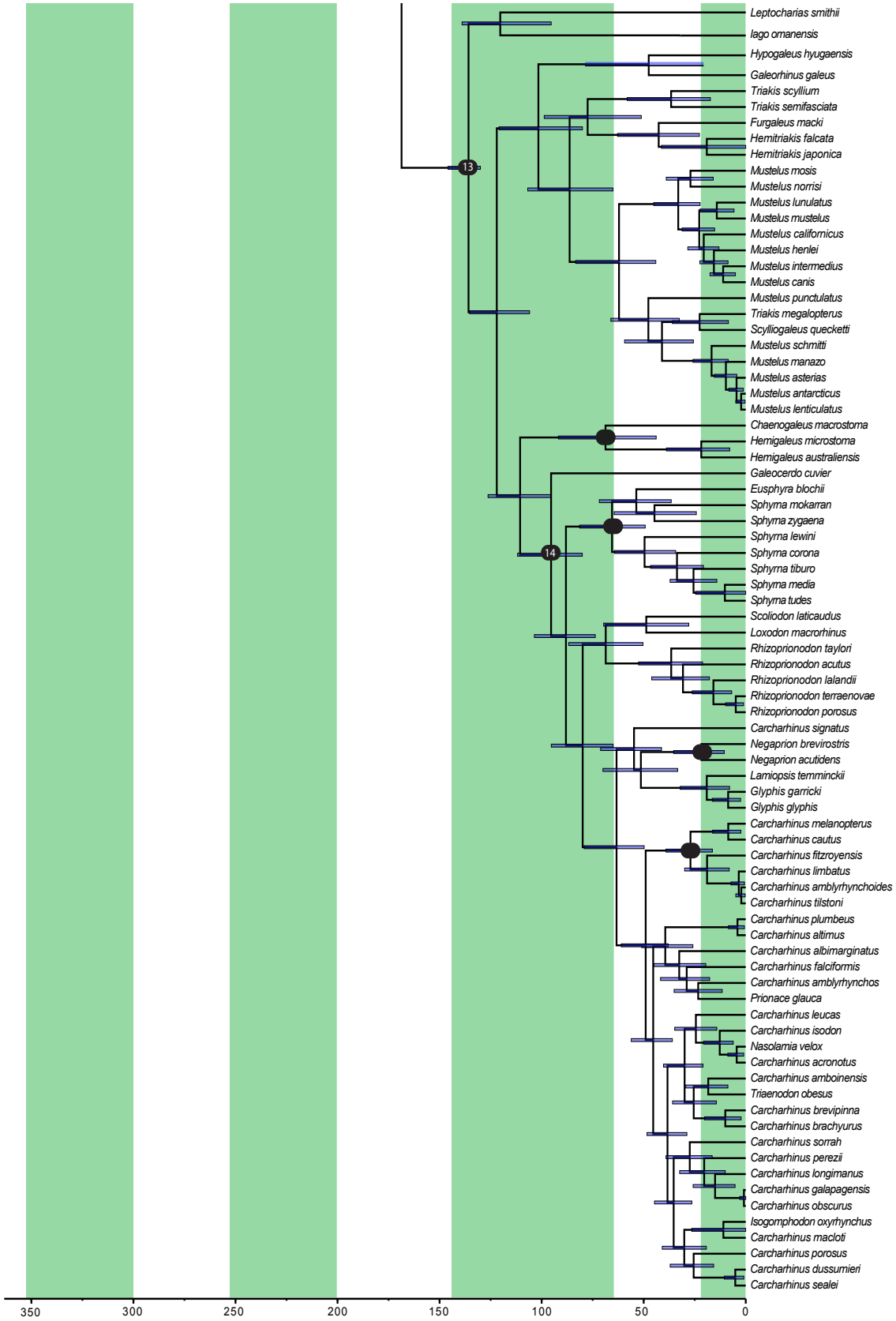
Leptocharias smithii
Iago omanensis
Hypogaleus hyugaensis
Galeorhinus galeus
Triakis scyllium
Triakis semifasciata
Furgaleus macki
Hemitriakis falcata
Hemitriakis japonica
Mustelus mosis
Mustelus norrisi
Mustelus lunulatus
Mustelus mustelus
Mustelus californicus
Mustelus henlei
Mustelus intermedius
Mustelus canis
Mustelus punctulatus
Triakis megalopterus
Scylliogaleus quecketti
Mustelus schmitti
Mustelus manazo
Mustelus asterias
Mustelus antarcticus
Mustelus lenticulatus
Chaenogaleus macrostoma
Hemigaleus microstoma
Hemigaleus australiensis
Galeocerdo cuvier
Eusphyra blochii
Sphyrna mokarran
Sphyrna zygaena
Sphyrna lewini
Sphyrna corona
Sphyrna tiburo
Sphyrna media
Sphyrna tudes
Scoliodon laticaudus
Loxodon macrorhinus
Rhizoprionodon taylori
Rhizoprionodon acutus
Rhizoprionodon lalandii
Rhizoprionodon terraenovae
Rhizoprionodon porosus
Carcharhinus signatus
Negaprion brevirostris
Negaprion acutidens
Lamiopsis temminckii
Glyphis garricki
Glyphis glyphis
Carcharhinus melanopterus
Carcharhinus cautus
Carcharhinus fitzroyensis
Carcharhinus limbatus
Carcharhinus amblyrhynchoides
Carcharhinus tilstoni
Carcharhinus plumbeus
Carcharhinus altimus
Carcharhinus albimarginatus
Carcharhinus falciformis
Carcharhinus amblyrhynchos
Prionace glauca
Carcharhinus leucas
Carcharhinus isodon
Nasolamia velox
Carcharhinus acronotus
Carcharhinus amboinensis
Triaenodon obesus
Carcharhinus brevipinna
Carcharhinus brachyurus
Carcharhinus sorrah
Carcharhinus perezii
Carcharhinus longimanus
Carcharhinus galapagensis
Carcharhinus obscurus
Isogomphodon oxyrhynchus
Carcharhinus macloti
Carcharhinus porosus
Carcharhinus dussumieri
Carcharhinus sealei
13
14
350
300
250
200
150
100
50
0
Millions of years

LITERATURE CITED

Aberhan, M., Kiessling, W. & Fürsich, F.T. 2006. Testing the role of biological interactions in the evolution of mid-Mesozoic marine benthic ecosystems. *Paleobiology* **32:** 259-277.

Alfaro, M.E., Santini, F. & Brock, C.D. 2007. Do reefs drive diversification in marine teleosts? Evidence from the pufferfish and their allies (Order Tetraodontiformes). *Evolution* **61:** 2104-2126.

Allen, A.P., Gillooly, J.F., Savage, V.M. & Brown, J.H. 2006. Kinetic effects of temperature on rates of genetic divergence and speciation. *P. Natl. Acad. Sci. USA* **103:** 9130-9135.

Arthur, M.A., Dean, W.E. & Pratt, L.M. 1988. Geochemical and climatic effects of increased marine organic carbon burial at the Cenomanian/Turonian boundary. *Nature* **335:** 714-717.

Bascompte, J., Melian, C.J. & Sala, E. 2005. Interaction strength combinations and the overfishing of a marine food web. *P. Natl. Acad. Sci. USA* **102:** 5443-5447.

Bellwood, D.R. 1996. The Eocene fishes of Monte Bolca: the earliest coral reef fish assemblage. *Coral Reefs* **15:** 11-19.

Bellwood, D.R. & Wainwright, P.C. 2002. The history and biogeography of fishes on coral reefs. In: Coral Reef Fishes: Dynamics and Diversity in a Complex Ecosystem (P.F. Sale, ed). Academic Press, San Diego, California.

Bellwood, D.R., Klanten, S., Cowman, P.F., Pratchett, M.S., Konow, N. & Van Herwerden, L. 2010. Evolutionary history of the butterflyfishes (f: Chaetodontidae) and the rise of coral feeding fishes. *J. Evol. Biol.* **23:** 335-349.

Bond, M.E., Babcock, E.A., Pikitch, E.K., Abercrombie, D.L., Lamb, N.F. & Chapman, D.D.

2012. Reef sharks exhibit site-fidelity and higher relative abundance in marine reserved on the Mesoamerican Barrier Reef. *Plos One* **7:** e32983.

Budd, A.F. 2000. Diversity and extinction in the Cenozoic history of Caribbean reefs. *Coral Reefs* **19:** 25-35.

Cartes, J.E. 1994. Influence of depth and seasonality in the diet of the deep-water shrimp *Aristeus antennatus* along the slope (between 400 and 2300 m). *Mar. Biol.* **120:** 639-648.

Cartes, J.E. & Carrassón, M. 2004. Influence of trophic variables on the depth-range distributions and zonation rates of deep-sea megafauna: the case of the Western Mediterranean assemblages. *Deep Sea Res. Pt. I* **51:** 263-279.

Claes, J.M. & Mallefet, J. 2008. Early development of bioluminescence suggest camouflage by counter-illumination in the velvet belly lantern *shark Etmopterus spinax* (Squaloidea: Etmopteridae). *J. Fish Biol.* **73:** 1337-1350.

Claes, J.M. & Mallefet, J. 2009. Ontogeny of photophore pattern in the velvet belly lantern shark, *Etmopterus spinax. Zoology* **112:** 433-441.

Claremont, M., Reid, D.G. & Williams, S.T. 2011. Evolution of corallivory in the gastropod genus *Drupella. Coral Reefs* **30:** 977-990.

Corrigan, S. & Beheregaray, L.B. 2009. A recent shark radiation: Molecular phylogeny, biogeography and speciation of wobbegong sharks (family: Orectolobidae). *Mol. Phylogenet. Evol.* **52:** 205-216.

Cowman, P.F. & Bellwood, D.R. 2011. Coral reefs as drivers of cladogenesis: expanding coral reefs, cryptic extinction events, and the development of biodiversity hotspots. *J. Evol. Biol.* **24:** 2543-2562.

Cowman, P.F., Bellwood, D.R. & van Herwerden, L. 2009. Dating the evolutionary origins of wrasse lineages (Labridae) and the rise of trophic novelty on coral reefs. *Mol. Phylogenet. Evol.* **52:** 621-631.

Cuny, G. 1998. Primitive neoselachian sharks: a survey. *Oryctos* **1:** 3-21.

Cuny, G. & Benton, M.J. 1999. Early radiation of the neoselachian sharks in Western Europe. *Geobios* **32:** 193-204.

Davies, T.J., Savolainen, V., Chase, M.W., Moat, J. & Barraclough, T.G. 2004. Environmental energy and evolutionary rates in flowering plants. *P. R. Soc. B-Biol. Sci.* **22:** 2195-2200.

Davis, M.P., Holcroft, N.I., Wiley, E.O., Sparks, J.S. & Smith, W.L. 2014. Species-specific bioluminescence facilitates speciation in the deep sea. Mar. Biol. doi: 10.1007/00227-014-2406-x.

Dornburg, A., Sidlauskas, B., Santini, F., Sorenson, L., Near, T.J. & Alfaro, M.E. 2011. The influence of an innovative locomotor strategy on the phenotypic diversification of triggerfish (Family: Balistidae). *Evolution* **65:** 1912-1926.

Drummond, A.J. & Rambaut, A. 2007. BEAST: Bayesian evolutionary analysis by sampling trees. *BMC Evol. Biol.* **7:** 214-221.

Edgar, R.C. 2004. MUSCLE: multiple sequence alignment with high accuracy and high throughput. *Nucleic Acids Res.* **32:** 1792-1797.

Fitzjohn, R.G. 2012. DIVERSITREE: comparative phylogenetic analyses of diversification in R. *Methods Ecol. Evol.* **3:** 1084-1092.

Fraser, R.H. & Currie, D.J. 1996. The species richness-energy hypothesis in a system where historical factors are thought to prevail: coral reefs. *Am. Nat.* **148:** 138-159.

Frédérich, B., Sorenson, L., Santini, F., Slater, G.J. & Alfaro, M.E. 2013. Iterative ecological radiation and convergence during the evolutionary history of damselfishes (Pomacentridae). *Am. Nat.* **181:** 94-113.

Friedlander, A.M. & DeMartini, E.E. 2002. Contrasts in density, size, and biomass of reef fishes between the northwestern and the main Hawaiian islands: the effects of fishing down apex predators. *Mar. Ecol. Prog. Ser.* **230:** 253-264.

Froese, R. & Pauly, D. 2012. FishBase. (www.fishbase.org).

Gage, J.D. & Tyler, P.A. 1991. Deep Sea Biology: A Natural History of Organisms at the Deep-Sea Floor. Cambridge University Press, Cambridge.

Gratwicke, B. & Speight, M.R. 2005. The relationship between fish species richness, abundance and habitat complexity in a range of shallow tropical marine habitats. *J. Fish Biol.* **66:** 650-667.

Guinot G., Adnet, S. & Cappetta, H. 2012. An analytical approach for estimating fossil record and diversification events in sharks, skates and rays. *Plos One* **7:** e44632.

Harmon, L., Weir, J.T., Brock, C.D., Glor, R.E. & Challenger, W. 2008. GEIGER: investigating evolutionary radiations. *Bioinformatics* **24:** 129-131.

Heinicke, M.P., Naylor, G.J.P. & Hedges, S.B. 2009. Cartilaginous fishes (Chondrichthyes). In: *The Timetree of Life* (S.B. Hedges & S. Kumar, eds), pp. 320-327. Oxford Univ. Press, Oxford.

Hoffman, A.A. & Hercus, M.J. 2000. Environmental stress as an evolutionary force. *BioScience* **50:** 217-226.

Jablonski, D. 2005. Evolutionary innovations in the fossil record: the intersection of ecology,

development, and macroevolution. *J. Exp. Zool. Part B* **304B:** 504-519.

Kiessling, W. & Aberhan, M. 2007. Environmental determinants of marine benthic biodiversity dynamics through Triassic-Jurassic time. *Paleobiology* **33:** 414-434.

Kiessling, W., Simpson, C. & Foote, M. 2010. Reefs as cradles of evolution and sources of biodiversity in the Phanerozoic. *Science* **327:** 196-198.

Klug, S. & Kriwet, J. 2010. Timing of deep-sea adaptation in dogfish sharks: insights from a supertree of extinct and extant taxa. *Zool. Scr.* **39:** 331-342.

Kriwet, J., Kiessling, W. & Klug, S. 2009. Diversification trajectories and evolutionary life-history traits in early sharks and batoids. *P. Roy. Soc. Lond. B Bio.* **276:** 945-951.

LaJeunesse, T.C. 2005. "Species" radiations of symbiotic dinoflagellates in the Atlantic and Indo-Pacific since the Miocene-Pliocene transition. *Mol. Biol. Evol.* **22:** 570-581.

Leighton, L.R. 1999. Possible latitudinal predation gradient in middle Paleozoic oceans. *Geology* **27:** 47-50.

Li, C., Matthes-Rosana, K.A., Garcia, M. & Naylor, G.J.P. 2012. Phylogenetics of Chondrichthyes and the problem of rooting phylogenies with distant outgroups. *Mol. Phylogenet. Evol.* **63:** 365-373.

Lingo, M.E. & Szedlmayer, S.T. 2006. The influence of habitat complexity on reef fish communities in the northeastern Gulf of Mexico. *Environ. Biol. Fish.* **76:** 71-80.

Maddison, W.P., Midford, P.E. & Otto, S.P. 2007. Estimating a binary character's effect on speciation and extinction. *Syst. Biol.* **56:** 701-710.

Maisey, J.G., Naylor, G.J.P & Ward, D.J. 2004. Mesozoic elasmobranchs, neoselachian phylogeny and the rise of modern elasmobranch diversity. In: *Mesozoic Fishes 3-*

Systematics, Paleoenvironments and Biodiversity (G. Arratia & A. Tintori, eds), pp. 17-56. Verlag Dr. Friedrich Pfeil, Munich, Germany.

Menegatti, A.P., Weissert, H.R., Brown, S., Tyson, R.V., Farrimond, P., Strasser, A. *et al.* 1998. High-resolution δ13C stratigraphy through the early Aptian "Livello Selli" of the Alpine Tethys. *Paleoceanography* **13:** 530-545.

Naylor, G.J.P., Ryburn, J.A., Fedrigo, O. & Lopez, J.A. 2005. Phylogenetic relationships among the major lineages of modern elasmobranchs. In: *Reproductive Biology and Phylogeny, vol. 3* (W.C. Hamlett & B.G.M. Jamieson, eds). Science Publishers Inc., Enfield, New Hampshire.

Nevo, E. 2001. Evolution of genome-phenome diversity under environmental stress. *P. Natl. Acad. Sci. USA* **98:** 6233-6240.

Papastamatiou, Y.P., Lowe, C.G., Caselle, J.E. & Friedlander, A.M. 2009. Scale-dependent effects of habitat movements and path structure of reef sharks at a predator-dominated atoll. *Ecology* **90:** 996-1008.

Papastamatiou, Y.P., Friedlander, A.M., Caselle, J.E. & Lowe, C.G. 2010. Long-term movement patterns and trophic ecology of blacktip reef sharks (Carcharhinus *melanopterus)* at Palmyra Atoll. *J. Exp. Mar. Biol. Ecol.* **386:** 94-102.

Price, S.A., Holzman, R., Near, T.J. & Wainwright, P.C. 2011. Coral reefs promote the evolution of morphological diversity and ecological novelty in labrid fishes. *Ecol. Lett.* **14:** 462-469.

Posada, D. 2008. jModelTest: Phylogenetic model averaging. *Mol. Biol. Evol.* **25:** 1253-1256.

R Core Team. (2012). R: A language and environment for statistical computing. R Foundation for

Statistical Computing, Vienna, Austria.

Rabosky, D.L. 2009. Extinction rates should not be estimated from molecular phylogenies. *Evolution* **64:** 1816-1824.

Reif, W.-E. 1985. Functions of scales and photophores in Mesopelagic luminescent sharks. *Acta Zool.* **66:** 111-118.

Renema, W., Bellwood, D., Braga, J., Bromfield, K., Hall, R., Johnson, K. *et al.* 2008. Hopping hotspots: global shifts in marine biodiversity. *Science* **321:** 654-657.

Revell, L.J. 2012. phytools: an R package for phylogenetic comparative biology (and other things). *Methods Ecol. Evol.* **3:** 217-223.

Rex, M.A. 1977. Zonation in deep-sea gastropods: the importance of biological interactions to rates of zonation. In: *Biology of Benthic Organisms (B.F.* Keenan, P.O. Ceidign & P.J.S. Boaden, eds), pp. 521-529. 11th European Symposium on Marine Biology, Galway.

Roberts, C.M., McClean, C.J., Veron, J.E.N., Hawkins, J.P., Allen, G.R., McAllister, D.E. *et al.* 2002. Marine biodiversity hotspots and conservation priorities for tropical reefs. *Science* **295:** 1280-1284.

Sanderson, M.J., Boss, D., Duhong, C., Cranston, K.A. & Wehe, A. 2008. The PhyLoTA Browser: Processing GenBank for molecular phylogenetics research. *Syst. Biol.* **57:** 335-346.

Santini, F. & Sorenson, L. 2013. First molecular timetree of billfishes (Istiophoriformes: Acanthomorpha) shows a Late Miocene radiation of marlins and allies. *Ital. J. Zool.* **80:** 481-489.

Santini, F., Carnevale, G. & Sorenson, L. 2013a. First molecular scombrid timetree

(Percomorpha: Scombridae) shows recent radiation of tunas following invasion of pelagic habitat. *Ital. J. Zool.* **80:** 210-221.

Santini, F., Sorenson, L., Marcroft, T., Dornburg, A. & Alfaro, M.E. 2013b. A multilocus molecular phylogeny of boxfishes (Aracanidae, Ostraciidae: Tetraodontiformes). *Mol. Phylogenet. Evol.* **66:** 153-160.

Schluter, D., Price, T., Mooers, A.Ø. & Ludwig, D. 1997. Likelihood of ancestor states in adaptive radiation. *Evolution* **51:** 1699-1711.

Sepkoski, J.J., Jr. 1982. Mass extinctions in the Phanerozoic oceans: a review. In: *Geological Implications of Impacts of Large Asteroids and Comets on the Earth* (Silver, L.T. & P.H. Schultz, eds), pp. 283-289. Geological Society of America Special Paper 190.

Sorenson, L., Santini, F., Carnevale, G. & Alfaro, M.E. 2013. A multi-locus timetree of surgeonfishes (Acanthuridae, Percomorpha), with revised family taxonomy. *Mol. Phylogenet. Evol.* **68:** 150-160.

Stamatakis, A. 2006. RAxML-VI-HPC: maximum likelihood-based phylogenetic analysis with thousands of taxa and mixed models. *Bioinformatics* **22:** 2688-2690.

Stefanescu, C., Lloris, D. & Rucabado, J. 1993. Deep-sea fish assemblages in the Catalan Sea (western Mediterranean) below a depth of 1000 m. *Deep-Sea Res. I* **40:** 695-707.

Straube, N., Iglesias, S.P., Sellos, D.Y., Kriwet, J., Schliewen, U.K. 2010. Molecular phylogeny and node time estimation of bioluminescent lantern sharks (Elasmobranchii: Etmopteridae). *Mol. Phylogenet. Evol.* **56:** 905-917.

Tainaka, K.-I., Itoh, Y., Yoshimura, J., Asami, T. 2006. A geographical model of high species diversity. *Popul. Ecol.* **48:** 113-119.

Tamura, K., Peterson, D., Peterson, N., Stecher, G., Nei, M. & Kumar, S. 2011. MEGA5: Molecular evolutionary genetics analysis using maximum likelihood, evolutionary distance, and maximum parsimony methods. *Mol. Biol. Evol.* **28:** 2731-2739.

Underwood, C.J. 2006. Diversification of the Neoselachii (Chondrichthyes) during the Jurassic and Cretaceous. *Paleobiology* **32:** 215-235.

Vélez-Zuazo, X. & Agnarsson, I. 2011. Shark tales: A molecular species-level phylogeny of sharks (Selachimorpha, Chondrichthyes). *Mol. Phylogenet. Evol.* **58:** 207-217.

Williams, S.T. & Duda, T.F. 2008. Did tectonic activity stimulate Oligo-Miocene speciation in the Indo-West Pacific? *Evolution* **62:** 1618-1634.

Wood, R. 1999. Reef Evolution. Oxford Univ. Press, Oxford, U. K.

Yang, Z. 2006. Computational molecular evolution. Oxford Univ. Press, Oxford, U.K.